UC Santa Cruz
UC Santa Cruz Electronic Theses and Dissertations

Title

Allosteric and inhibitory investigations of human 15- Lipoxygenases

Permalink

https://escholarship.org/uc/item/38j7h7xz

Author

Joshi, Netra

Publication Date

2013

Peer reviewed|Thesis/dissertation

UNIVERSITY OF CALIFORNIA

SANTA CRUZ

ALLOSTERIC AND INHIBITORY INVESTIGATIONS OF HUMAN 15-LIPOXYGENASES

A dissertation submitted in partial satisfaction
of the requirements for the degree of

DOCTOR OF PHILOSOPHY

in

CHEMISTRY

by

NETRA SUBHASH JOSHI

June 2013

The Dissertation of Netra Subhash Joshi is approved:

\---
Professor Theodore R. Holman

\---
Professor Glenn Millhauser (Chair)

\---
Professor Pradip Mascharak

\---
Tyrus Miller
Vice Provost and Dean of Graduate Studies

Table of Contents

List of Figures

Chapter 1

Chapter 2

Chapter 3

Chapter 4

List of Tables

Chapter 3

Chapter 4

Abstract

ALLOSTERIC AND INHIBITORY INVESTIGATIONS OF 15- HUMAN LIPOXYGENASES

by

Netra S. Joshi

This dissertation focuses on two isoforms of 15-human lipoxygenase, reticulocyte 15-LOX-1 and epithelial 15-LOX-2, that differ considerably in their tissue expression, reaction specificity, auto-inactivation and response to the allosteric effectors. These 15-LOX isoforms exert their function in the cells by reacting with a variety of endogenous fatty acid substrates and producing hydroperoxy products, which regulate the inflammatory process in the cells. These 15-LOX products can participate in opposing roles in human diseases, and their ratios are known to regulate cell-cell adhesion processes in cells, playing a vital role in inflammation, cancer and thrombosis. Therefore, understanding the factors that affect the substrate specificity of these two LOX isozymes is critical to comprehend their exact role in human diseases. Furthermore, 15-LOX-1 has been recently implicated in stroke related damage via hydroperoxidation of fatty acid containing membranes and its ability to degrade mitochondrial membrane when triggered by reactive oxygen species. Studies indicate the potential of 15-LOX-1 inhibitors as neuroprotectors against stroke related damage. However drug discovery for stroke therapeutics is a long, tedious process with high chance of failure and presents a constant search for potent, selective inhibitors

This dissertation investigates the discovery of a novel chemotype for 15-LOX-1 inhibitors. It describes in detail the initial screening, characterization and optimization of potent and selective inhibitors of 15-LOX-1. The results of the *in-vivo* and *in-vitro* studies demonstrate the potential of this chemotype as a stroke therapeutic. Finally, the factors that regulate the substrate specificity of human epithelial 15-LOX-2 are also investigated here. The findings demonstrate that both pH and LOX products alter the kinetic parameters of C_{20} and C_{18} fatty acid substrates differentially, with both pH and LOX products activating the C_{20} kinetics but both inhibit C_{18} kinetics, resulting into a significant increase in the C_{20}/C_{18} substrate specificity ratio. These alterations in the product ratio may present important consequences in human disease progression due to the distinct biological effects of these products.

Acknowledgments

I would like to take this opportunity to thank with gratitude my research advisor, Prof. Ted Holman for giving me a valuable opportunity to work in his lab. You have always been a very patient, understanding and helpful mentor. I remember the second quarter when I had a severe neck injury and I was not even sure if I could continue my studies here at UC Santa Cruz. I can't thank you enough for taking it easy on me that time and helping me pursue my dream of doing a Ph.D. Your guidance, approachable and friendly nature, made it easier for me to continue my studies and I will always be indebted to you. I would also like to thank my thesis reading committee, Prof. Glenn Millhauser (Chair) and Prof. Pradip Mascharak, for their patience, and timely review of my Ph.D. progress. I learnt a lot from both of your classes during the first year and that enhanced my interest further in this field.

I now want to extend my thanks to all the past and current Holman Lab members I worked with and whose support made my lab work experience enjoyable. Thank you for your efforts to accommodate my restricted schedule in the lab; it made my life easier. I am especially thankful to Dr. Aaron Wecksler, Dr. Eric Hoobler, Brian Jameson and a dear colleague of 5 years, Late Ken Ikei for their support. I also want to convey my thanks to my two undergraduates- Quang Tran and Max Stefan. Working with you both helped me to develop my mentoring skills. Qiangli Zhang aka Li, from Mass spectrometry facility is another person in the department whom I am thankful to for patiently helping me schedule, run and analyze my samples on LTQ.

The text of this document includes permitted reprints of the following previously published material:

Yigitkanli K, Pekcec A, Karatas H, Pallast S, Mandeville E, Joshi N, Smirnova N, Gazaryan I, Ratan RR, Witztum JL, Montaner J, Holman TR, Lo EH, van Leyen K., Inhibition of 12/15-lipoxygenase as therapeutic strategy to treat stroke, Ann Neurol. **2013** Jan;73(1):129-35.

The co-author, Theodore R. Holman, listed in this publication directed and supervised the research which forms the basis for this dissertation.

<center>**Chapter 1**</center>

<center>**Introduction**</center>

1.1 Lipoxygenase

Lipoxygenase (LOX) represents an important superfamily of non-heme iron containing enzymes which catalyze the stereo-specific peroxidation of polyunsaturated fatty acids (PUFAs) containing at least one 1,4-cis, cis -pentadiene moiety.[1-3] They are widely found in plants, animals and fungi and mainly serve their function by synthesizing biologically active compounds from various endogenous PUFAs, which in turn trigger cellular response via signaling cascades.[1, 2, 4] In plants, they serve the role in the physiological processes involved in growth and development, wound response, synthesis of regulatory molecules and senescence.[5, 6] In mammals, the signaling cascades initiated by LOX products are implicated in regulation of inflammatory and hyper-proliferative diseases.[7]

1.2 Types of lipoxygenase

Higher plants contain multiple lipoxygenase isoforms with at least thirteen identified in soybean and twenty in rice.[1, 2] Six homologues are characterized in humans, while in mice there are seven known genes that express lipoxygenase proteins.[2] The conventional nomenclature for animal lipoxygenase is based on their positional specificity with arachidonic acid (AA).[2, 4] In humans, the LOX isoforms are leukocyte 5-LOX, platelet 12-(S)-LOX, epidermis 12-(R)-LOX, reticulocyte 15-LOX-1, epithelial 15-LOX-2 and epidermal eLOX-3. This type of nomenclature is not ideal since these enzymes show quite different positional specificities with

substrates other than AA, a 20 carbon fatty acid. These oxidation specificities of LOX come from their ability to bind the substrates with their methyl tail end first, thus inserting oxygen at the ω-6 position of the fatty acid substrates.[1] Hence, 15-LOX generates 15-HPETE from AA, the C_{20} fatty acid substrate and generates 13-HPODE from LA, the C_{18} fatty acid substrate.

Also, evolutionarily related LOX isoforms often exhibit distinct reaction specificities in contrast to those sharing a low degree of phylogenetic relatedness. For example, the soybean enzyme, sLOX-1 that oxygenates AA (20-carbon fatty acid) at position 15 shares only 25% sequence identity to any mammalian 15-LOX; whereas two human 15-LOX isoforms share only 35% sequence identity with each other.[1] By contrast, human epithelial 15-LOX-2 shares 78% sequence identity with murine 8-LOX, with no overlap in their positional specificity.[8]

1.3 Lipoxygenase structure

1.3.1   General structural characteristics

The complete crystal structures of a number of LOX proteins from plants and animals are now available,[9-14] including human 5-lipoxygenase (5-LOX).[15] Lipoxygenase proteins constitute a single polypeptide chain which folds into a two-domain structure **[Figure 1.1]**, a small N-terminal beta barrel domain and a larger mostly alpha helical catalytic domain containing a single non-heme iron.[2] Lipoxygenase have a molecular mass of between 75 and 80kDa in animals, whereas in plants they are relatively larger, with a molecular mass of ~ 94-104kDa.[1] Due to the non-heme nature of the iron they appear virtually colorless. In lower organisms,

LOX exist as fusion proteins where the LOX domain is linked to another catalytic domain responsible for the secondary metabolism of hydro-peroxy fatty acids.[16-20]

1.3.2 N-terminal domain

Based on all the available structures of LOX to the date, the N-terminal domain has been seen primarily made up of anti-parallel beta strands. The beta barrel domain is smaller in animals than that of in the plants, however, their overall structure is very similar. In sLOX-1, the first 146 amino acids constitute the N-terminal domain.[10] On the other hand, only 120 N-terminal amino acids form the beta barrel domain in human 5-LOX[15] and in rabbit reticulocyte 15-LOX, this number of amino acids is further reduced to 110.[21] Still, the high degree of conservation of the two domains structure in lipoxygenase suggests a functional role for this N-terminal domain.

Its overall structure resembles that of the C2 domain of pancreatic lipases, therefore it is also known as polycystin / lipoxygenase / alpha-toxin (PLAT) domain.[22] Although located in the cytosol, LOXs need to access their membrane sequestered or micelle bound substrates. The presence of this domain allows the LOX proteins to access and catalyze lipid peroxidation in complex biological structures via direct di-oxygenation of phospholipids and cholesterol esters of bio-membranes and plasma lipoproteins.[2, 4] Truncation studies of various lipoxygenase including plant and human have also indicated that this domain is not required for catalytic activity but is responsible for membrane binding and substrate acquisition.[23-27]

1.3.3 C- terminal catalytic domain

The catalytic domain of all LOX isoforms known to the date primarily consists of alpha helices and harbors one catalytically active non- heme iron atom per molecule of LOX. In all the isoforms, the iron is octahedrically coordinated by side chains of five amino acids and a hydroxide ligand. [1, 2]

In case of sLOX-1 and coral 8-LOX, the iron protein ligands are three His, the c-terminal Ile and one Asn residue.[10, 14] The Asn is relatively distant from the central iron (3°A apart) and hence its ligation is rather weak.[28] However these coordination forces are then stabilized by second sphere hydrogen bond interactions. This sixth Asn ligand in the first coordination sphere of non-heme iron is of great interest since it varies from one isozyme to another and mutational studies show that it influences the catalytic efficiency of the LOX isozymes. [29-31]

In the rabbit reticulocyte 15-LOX-1, apart from three conserved His residues and C-terminal Ile, the Asn is replaced by another His.[21] Sequence alignment studies also show similar His replacement of Asn in human 15-LOX-1 and a Ser placed in human 15-LOX-2. Interestingly, 12-LOX contains the Asn residue as seen in sLOX-1 and is known for its increased catalytic efficiency as compared to 15-LOX isozymes.[32] The recently crystallized human 5-LOX shows the active site with a conserved constellation of five invariant residues- three His, Asn and C-terminal Ile.[15]

1.4 Lipoxygenase reaction mechanism

LOX catalyze the bimolecular reaction between endogenous unsaturated fatty acid and molecular oxygen. **[Figure 1.2]** The currently accepted reaction mechanism

of LOX is based on extensive kinetic investigation of soybean LOX-1 (sLOX-1) with linoleic acid (LA),[33-36] 15-LOX-1 with linoleic acid (LA) and 15-LOX-2 with arachidonic acid (AA) as a substrate.[37-40] Upon isolation, the non-heme iron in LOX is found in the resting state ($Fe^{2+}-OH_2$) and requires oxidation to the active state ($Fe^{3+}-OH$). This is achieved by one equivalent of hydroperoxy product, available from the auto-oxidation of the substrates in small amounts. The LOX reaction is thought to begin with a diffusion controlled encounter of the substrate with the enzyme. Upon substrate binding, solvent dependent multiple H-bonding rearrangements take place leading to a conformation change to position the substrate in close vicinity to the iron. After proper positioning of the substrate, stereo-selective hydrogen abstraction takes place (via proton coupled electron transfer), with the hydrogen atom being abstracted by the ligated hydroxide and the resulting electron reducing the non-heme ferric iron (Fe^{3+}) to its ferrous form (Fe^{2+}). Kinetic isotope effect studies have shown that this hydrogen abstraction takes place via quantum mechanical tunneling.[34] The newly formed radical undergoes a radical rearrangement and the electron gets delocalized either in the direction of methyl end of the fatty acid (+2 rearrangement) or in the carboxylate group direction (-2 rearrangement).

Lipoxygenase is a unique enzyme in a sense that the catalysis occurs via substrate activation instead of oxygen activation seen in most dioxygenases.[34] Oxygen kinetic experiments have shown that oxygen insertion occurs only after hydrogen abstraction. Molecular oxygen doesn't bind or react with lipoxygenase, but rather traps the activated enzyme-substrate complex.[35] Oxygen insertion occurs antarafacially

5

(opposite direction of the plane determined by the double bond system) from hydrogen abstraction.[41] The resulting hydroperoxide radical is subsequently reduced by another proton coupled electron transfer event, thus reducing the radical to the corresponding anion and the ferrous iron gets converted to the active ferric form again. This is followed by another hydrogen bonding rearrangement reaction, resulting into the protonation of the peroxide anion followed by product release. The catalytic mechanism of LOX involves many microscopic steps and the rate-limiting nature of the various steps varies among isozymes and for each substrate.[42] For 15-LOX, the rate limiting contributions to the catalysis at low temperature are from diffusion, hydrogen bond rearrangement and hydrogen abstraction. At high temperature, hydrogen abstraction is the only rate limiting step.

1.5 Lipoxygenase substrates

Various endogenously available poly-unsaturated fatty acids serve as LOX substrates **[Figure 1.3]**, which are found integrated into the cellular membranes at the sn-2 position of glycero-phospholipids. [43-45]

In most cells, the concentration of free fatty acids is limited and thus these LOX substrates have to be liberated from cellular stores by lipid hydrolyzing enzymes.[46] Cytoplasmic phospholipase A_2 ($cPLA_2$) is the calcium dependent, cytosolic lipid hydrolyzing enzyme, which within minutes of intracellular calcium release or protein phosphorylation gets translocated from the cytosol to the nuclear / endoplasmic reticulum membrane, facilitating its proximity to its membrane incorporated fatty acid substrates.[47, 48]

6

LOX substrates differ in their carbon chain length and number/ position of unsaturation points. These substrates can be divided into two distinct categories (omega – 3 (ω-3) and omega – 6 (ω-6)), which are named according to the location of their first unsaturation from the methyl end of the fatty acid. The LOX substrates discussed in this dissertation are divided into two main classes, C_{18} fatty acids and C_{20} fatty acids, based on their carbon chain length. Linoleic acid (LA), an ω-6, 18:2 fatty acid and alpha linolenic acid (ALA), an ω-3, 18:3 are the essential fatty acids and therefore must be supplied through diet.[44] The rest of the LOX substrates can be either ingested or metabolically synthesized, using these essential fatty acid precursors by a series of elongase and desaturase enzymes.[49, 50]

1.6 Significance of lipoxygenase in human diseases

Identification of LOX isozymes and their biological role has been ongoing for the past number of years. According to the conventional view, the biological role of the LOX was thought to be through the generation of eicosanoids in the arachidonic acid cascade.[51-54] However, recently it was discovered that the ability of the LOX proteins to modify the lipoproteins and bio-membranes also contributes towards their significance in human diseases.[55-57]

1.6.1   5-LOX

5-LOX is a soluble monomeric enzyme composed of 673 amino acids with a molecular mass of about 78kDa. The expression of 5-LOX is restricted to the cells derived from bone marrow such as granulocytes, monocytes/ macrophages, mast cells, dendritic cells and B-lymphocytes.[47] 5-LOX has been unequivocally linked to

7

human diseases due to its ability to form leukotrienes,[7, 58] the potent bioactive molecules known as mediators of inflammation and are responsible for various inflammatory diseases such as Asthma,[59-61] Chronic Obstructive Pulmonary Disease (COPD),[62] rhinitis,[63] atherosclerosis[58, 64, 65] and arthritis.[66, 67] However, LTA_4, the first intermediate in making pro-inflammatory leukotrienes, is also the first intermediate in the biosynthesis of lipoxins, the anti-inflammatory molecules.[7, 68] Thus, 5-LOX is responsible for both pro- and anti-inflammatory responses in the human body, which complicates their targeting in human disease. The recently analyzed 2.4°A crystal structure of human 5-LOX opens up the possibilities in terms of designing 5-LOX specific inhibitors to treat various human diseases.[15]

1.6.2   12-LOX

There are two 12-LOX isozymes in humans based on their stereo-specificity of the products and the expression pattern- platelet and epidermis. Human platelet 12-LOX is a 663 amino acid containing polypeptide with a molecular mass of 75 KDa.[69-71] It is primarily expressed in platelets and their precursors, megakaryocytes, as well as in keratinocytes in the germinal layer.[47] It is involved in platelet aggregation, the major component in blood clot formation.[72] Recently, it was shown that 12-HETE, the 12-LOX product of arachidonic acid (AA), shows pro-thrombotic properties, whereas 12-HETrE, the 12-LOX product of dihomo gamma linoleic acid (DGLA) is known to show anti-thrombotic effects.[73] Experimental evidence suggests a link between 12-LOX activation of platelets and cardiovascular related links in human diseases, such as diabetes[74, 75] and hypertension.[76, 77] Also, the product of platelet 12-

LOX, 12-HPETE is found abundantly in psoriatic lesions and later on its role in the pathogenesis of psoriasis was confirmed.[78, 79] In addition, numerous studies have indicated the role of human platelet 12-LOX in different cancers, such as pancreatic[80] and breast.[81] 12-LOX mRNA was found to have increased expression in cancerous tissues as compared to non-cancerous cell lines.[82] This is further confirmed by experimental evidence where inhibitors of 12-LOX inhibited growth of cancerous cell lines.[83, 84]

Human epidermis 12-(R)-LOX is a 701 amino acid containing protein that shares 86% sequence identity with a mouse ortholog.[85-87] It is the first LOX found in humans that introduces molecular oxygen in the opposite stereo configuration than all other human LOX isozymes. It is expressed in skin and hair follicles. It shows a very weak activity with AA and is also capable of oxygenation at omega-9 position of poly-unsaturated fatty acids. It plays a vital role in epidermal function and 12-(R)-LOX knock out mice were shown to have skin drying out hours after birth resulting in neonatal mortality.[88] The null mutations in the gene ALOX12B that encodes 12-(R)-LOX give rise to strikingly scaly skin phenotype characterized as autosomal recessive congenital ichthyosis.[89] It has been proposed that the product of 12-(R)-LOX from lipid substrate linoleoyl- ω-hydroxyceramide present in stratum corneum undergoes some downstream modifications and allows formation of a lipid-protein scaffold that maintains the epidermal permeability barrier.[90]

1.6.3   15-LOX

15-LOX is widely known to exert opposing effects in human inflammatory diseases via formation of bio-active lipid mediators. The pro-inflammatory leukotrienes and anti-inflammatory resolvins, protectins and lipoxins are formed sequentially during the acute inflammation.[7] [**Figure 1.4**] The pro-inflammatory leukotrienes are secreted only during acute inflammation, following the appearance of polymorphonuclear neutrophils (PMN), while lipoxins and resolvins are produced during the resolution phase of inflammation.[51] 15-LOX is expressed as two isozymes in humans, reticulocyte 15-LOX-1 and epithelial 15-LOX-2, which show opposite expression pattern in prostate cancer tissues.[91-94] Their biochemical properties, such as substrate specificity, and the biological roles in human diseases are discussed in further detail in the following sections.

1.7 Human reticulocyte 15-lipoxygenase-1 (15-LOX-1)

1.7.1   Physical properties of 15-LOX-1

Reticulocyte 15-LOX-1 is a single polypeptide chain with a molecular mass of about 75kDa.[4] It is expressed primarily in reticulocytes, but is also found in eosinophils, airway respiratory epithelial cells, macrophages and colon cells.[1] It possesses broad substrate specificity and reacts effectively with many polyenoic fatty acids [**Figure 1.3**]. In addition, ester lipids (phospho-lipids, cholesterol esters, mono-, di- and tri-acyl glycerols) containing fatty acids and more complex lipid protein assembly, such as bio-membranes and lipo-proteins, are also the substrates of this enzyme.[4] The flexible active site gives 15-LOX-1 its dual positional specificity, generating approximately 90% 15-(S)-HpETE and approximately 10% 12-(S)-

HPETE from arachidonic acid (AA). The enzyme undergoes suicidal inactivation following progressive substrate turnovers, however the mechanism underlying this process in currently unknown.[95] Interestingly, 15-LOX-1 shares very low sequence homology (35%) with epithelial 15-lipoxygenase -2 (15-LOX-2), which produces 15-HpETE primarily, but it shares a high homology with mouse leukocyte 12 lipoxygenase (ml -12-LOX) (78%), which produces 12-HpETE primarily.[47] These two orthologs also react with ester lipids and produce mixtures of 12-HpETE and 15-HpETE and thus are both referred to as 12/15-LOX in the literature.

1.7.2 Biological role of 15-LOX-1

15-LOX-1 exerts its function in the cells via two major pathways- i) by production of eicosanoids and other bioactive lipid mediators, such as leukotrienes, lipoxins, resolvins and protectins,[7, 52] ii) by directly reacting with membrane ester lipids, thus altering the structural characteristics of the cells.[56, 57, 96]

15-LOX-1 is implicated in several human diseases such as atherosclerosis,[97] prostate and colon cancers,[98-100] stroke,[101, 102] arthritis[67, 103] and asthma.[104, 105] It also plays a regulatory role in cell differentiation of erythrocytes, macrophages and cornea.[106, 107] In prostate cancer tissue, the higher expression of 15-LOX has been shown to positively correlate with the virulence of the tumor;[93, 98] whereas the down regulation of 15-LOX-1 is found to be pro-tumorigenic in colon cancer.[100] The substrate specificity of 15-LOX-1 is also thought to play a significant role when it comes to human diseases.[94] 13-(S)-HPODE, a product of 15-LOX-1 and linoleic acid (LA) activates the MAP Kinase pathway leading to cell proliferation and

11

differentiation. On the contrary, 15-(S)-HPETE, a product of 15-LOX-1 with arachidonic acid (AA) down-regulates the MAP Kinase pathway thus preventing cell growth. Both of these products play important role in tumorigenesis.

15-LOX-1 is also known to be involved in erythrocyte maturation, where it helps carry out the programmed membrane degradation of the mitochondria and nucleus, while keeping the cellular membrane intact.[57] 15-LOX-1 is also involved in a variety of other human diseases, such as atherosclerosis, prostate and colon cancer and inflammation,(*vide supra*) but their detailed analysis is beyond the scope of this dissertation. The following section, however, does explain in detail the role of 15-LOX-1 in stroke, which forms the basis of Chapters 2 and 3 of this dissertation.

1.7.3 Role of 15-LOX-1 in Ischemic stroke

Stroke happens when there is a sudden interruption of the blood supply to the brain.[108] There are two types of injuries that can lead to stroke, i) Ischemia – 67% of stroke cases occur due to ischemia which is lack of blood flow to the brain due to the blockage of the blood vessel by either a thrombus or embolus. ii) Hemorrhage –33% of stroke cases are due to the hemorrhage in the brain following the rupture of the blood vessels.[109] Reperfusion is when the normal blood flow returns to the brain after the initial stroke. During the stroke, due to the lack of glucose and oxygen, the brain neuronal cells begin to die rapidly. However, the reperfusion seems equally damaging to the brain without any preventative measures.[110]

Three major biochemical pathways are currently known that cause the damage to the brain cells following stroke and reperfusion. They are excito-toxicity, oxidative

stress and apoptosis.[111, 112] All the three pathways are interlinked and are shown in **Figure 1.5**. Following stroke, there is an acute shortage of oxygen and glucose to the cells exhausting the cells energy resources since the ATP levels begin to drop. ATP dependent ionic gradient pumps fail leading to rise in the intracellular Ca^{2+}.[113]

This increase in Ca^{2+} causes glutamate release that further activates the NMDA receptor, causing more influx of Ca^{2+} ions into the cells and causes glutathione depletion, by blocking the cysteine intake receptor on the plasma membrane.[114] Glutathione normally regulates the concentration of reactive oxygen species (ROS), as well as the reduction of the hydroperoxide products from LOX and COX since glutathione is the reducing agent for glutathione peroxidase.[115, 116] Glutathione depletion increases ROS in the cells causing oxidative stress. Influx of Ca^{2+} in the cells also activates various synthases, lipases and proteases, resulting in generation of NO and peroxynitrite.[117, 118] As a consequence of NO synthase activation, protein degradation is increased due to proteases and fatty acids are released from the membrane, due to activation of cytosolic phospholipase A_2 ($cPLA_2$).[113]

The lack of ATP causes mitochondrial function failure and the escaped electrons, from the electron transport chain, react with the burst of oxygen upon reperfusion, further amplifying the oxidative stress via ROS.[119] These ROS attack cell membrane lipids, cellular proteins, and nucleic acids and they also trigger 15-LOX-1 activation, creating havoc in the cells.[120, 121] 15-LOX-1 reacts with the abundant supply of free fatty acids, released by the activated cPLA2, forming pro-

13

inflammatory molecules, such as leukotrienes, and starting the inflammatory response cascade.[122, 123]

Recent studies have shown that 15-LOX-1 attacks the neuronal mitochondria membrane by oligomerizing and integrating into the membrane forming large hydrophilic pores and thus disintegrating the membranes.[56, 124] As a result, the luminal proteins from the intra-cellular region are easy accessed by the extracellular proteases, causing their degradation. The cytochrome c, the mitochondrial inner membrane protein, subsequently gets translocated to the cytosol and signals various apoptosis inducing proteins, such as caspases, leading to neuronal cell death.[125]

Moreover, 15-LOX-1 products, such as 13-(S)-HODE and 12-(S)-HETE activate the p38 MAPK cascade,[126] which leads to downstream p53 activation, causing programmed cell death. ROS generated from mitochondria are also capable of triggering p53 activation.[127, 128]

Taken together, 15-LOX-1 contributes to the stroke related damage via i) formation of leukotrienes that lead the cells towards apoptosis, inflammatory response cascade and amplification of oxidative stress ii) attacking the mitochondrial membranes by inducing pore formation causing release of luminal proteins, which induce membrane degradation and apoptosis. This role of 15-LOX-1 in oxidative stress induces neuronal cell death following stroke and reperfusion and has been directly observed in various in-vitro and in-vivo experimental studies.[102, 129, 130]

1.7.4 Inhibition studies of 15-LOX-1

The primary goal of developing 15-LOX-1 inhibitor therapeutics would be to prevent stroke related damage in brain cells. In fact, recent studies were carried out and experimental evidence indicated that 15-LOX-1 inhibitors showed neuro-protection against stroke related damage in the in-vitro studies (HT22 mouse hippocampus neuronal cell line), as well as neuro-protection from mouse middle cerebral artery occlusion (MCAO) induced stroke damage, when the drug is administered 4-6 hours post ischemic stroke.[101, 131] These results suggest that 15-LOX-1 inhibitors are excellent candidates for preventing stroke related neuronal cell damage.

However, the drug discovery process to find effective drugs for stroke therapy is long, tedious and requires extensive in-vitro and in-vivo trials, which face a high chance of failure due to many reasons.[132] Hence there is a constant need for new 15-LOX-1 inhibitors that are not only potent but also selective against other LOX isozymes in the body.

Drug discovery for human 15-LOX-1 is somewhat restricted due to the lack of crystal structure. However, there is a crystal structure for rabbit reticulocyte 15-LOX-1, with an inhibitor bound, and it shares a high degree of sequence identity (81%) to human 15-LOX-1.[13] Hence, many drug discovery studies for human 15-LOX-1 are based on the structure of rabbit reticulocyte 15-LOX-1.

The approach used by the Holman lab and their collaborators in search of a therapeutic drug target for stroke involves initial screening of a huge chemical library consisting thousands of compounds. The screening is performed via either virtual

method (docking the compounds on the homology model of the human 15-LOX-1 structure) or a high-throughput screen, using a colorimetric assay that involves the detection of the peroxide enzyme product. Structure-activity relationship (SAR) analysis is done on potent inhibitors, with structural modifications being made to improve their potency and solubility. Potent "hits" are then analyzed in detail using various techniques, such as IC_{50} analysis (for accurate determination of the potency), selectivity studies against other human LOX isozymes (to confirm the specificity towards 15-LOX-1), redox nature determination and inhibition kinetics (to determine the nature of inhibition).

Currently there are very few 15-LOX-1 potent inhibitors that are selective over the other LOX isozymes, such as 5-LOX, 12-LOX and 15-LOX-2, as well as selective over the cyclooxygenases, COX-1 and COX-2. Because these enzymes coexist in human body and mutually influence / interact with each other, discovering enzyme specific inhibitors is the key step towards a successful therapeutic for a particular disease.

Frequently during the process of discovering new drug targets, potent inhibitors are found to be redox in nature. These redox inhibitors function by reducing the active site ferric iron to its inactive ferrous form and can be recycled by the cells' antioxidant system in some cases. However, these compounds are poor therapeutics as they can hit multiple off target enzymes. To determine the nature of the inhibition, steady state inhibition kinetics are performed which classify the inhibitors into competitive (most desirable in the industry), uncompetitive and mixed-type

inhibitors, which yields two equilibrium constants K_{ic}, describing the dissociation of the inhibitor from the active site and K_{iu}, describing the secondary site. A competitive inhibitor binds only to the active site of the free enzyme, an un-competitive inhibitor binds only to the enzyme-substrate complex and a mixed type inhibitor is capable of binding both the free enzyme as well as enzyme-substrate complex. If the K_{ic} and the K_{iu} for mixed-type inhibiton are the same, then this inhibition is called non-competitive inhibition, which rarely occurs in biological systems. Non-redox, potent and selective compounds found from the screening and the characterization studies are further evaluated for their efficacy in the in-vitro (HT22 Mouse hippocampus neuronal cell line) and in-vivo mouse models (middle cerebral artery occlusion-induced stroke model).

1.8 Human epithelial 15-lipoxygenase-2 (15-LOX-2)

1.8.1 Characteristics of 15-LOX-2

Epithelial 15-LOX-2 is a 676 amino acid containing single polypeptide chain, with a molecular mass of about 76KDa.[133, 134] In humans, it is primarily expressed in prostate tissue, as well as in skin, lung and cornea tissue.[91] It shares only 35% sequence identity with 15-LOX-1 but, is highly homologous to murine 8-LOX (78% sequence identity), which has no overlap of to its positional specificities.[2] This information indicates that sequence homology in general does not explain LOX substrate specificity but rather specific residues in the active site. 15-LOX-2 differs from 15-LOX-1 catalytically in that it exclusively oxygenates at carbon 15 of AA (>99%), compared to 90% for 15-1, and it reacts poorly with linoleic acid (LA), while

15-LOX-1 reacts equally well with AA and LA. Unlike 15-LOX-1, 15-LOX-2 converts almost all of its substrates completely into the products with no suicidal inactivation yet reported.

1.8.2 Biological role of 15-LOX-2

The biological role of 15-LOX-2 has been difficult to decipher due to its disparate expression in various human tissues. However, in human prostate glands, 15-LOX-2 was found in benign prostate epithelial cells with a reduced expression in prostate adenocarcinoma.[91, 92] This led to the finding that 15-LOX-2 acts as a negative cell cycle regulator. 15-HPETE, the product of 15-LOX-2 with arachidonic acid (AA) is known to down-regulate the MAP kinase pathway responsible for cell growth and differentiation.[135] This functional role of 15-LOX-2 as a tumor suppressor in prostate cancer was further confirmed by in vitro studies of prostate cancer cell lines (PCa), where enforced expression of 15-LOX-2 induced cell cycle arrest and senescence-like phenotypes.[91] The in-vivo studies on mouse models showed that the induced expression of 15-LOX-2 inhibited tumor development.[136, 137] Most of experimental studies have focused on only the 15-LOX-2 substrates, arachidonic acid (AA) and linoleic acid (LA),[38] however, it is known that a broad range of 15-LOX-2 substrates are in human tissue, and their 15-LOX-2 products can play confounding roles in different human diseases.[94] These facts justify the need for the investigation into the substrate specificity of 15-LOX-2 and its kinetics with various fatty acid substrates.

1.8.3 Allosteric regulation of 15-LOX-2 via alteration of its substrate specificity

In cells, almost all of the chemical reactions are catalyzed by enzymes and require regulation to maintain the integrity of the biological system. On the protein level, the regulation is achieved via i) pH/ionic strength changes ii) post translational modification such as phosphorylation, biotiynlation, glycosylation, etc. and iii) allostery where binding of the effector molecule to enzyme alters its activity. Allosteric effector binding usually results in conformational changes and/or association/dissociation of proteins/multimers.[138]

Recently, our lab demonstrated the presence of allosteric sites in the 15-LOX human isozymes via kinetic studies.[38, 39] It was also shown that LOX products themselves act as allosteric effectors and change the substrate specificities of these isozymes. In addition to the differences between the 15-LOX isozymes (*vide supra*), they also respond differently to allosteric effector molecules. The LA product, 13-(S)-HODE, increases the substrate specificity ratio $(k_{cat}/K_M)^{AA}/(k_{cat}/K_M)^{LA}$ for 15-LOX-1 whereas 13-(S)-HODE decreases the $(k_{cat}/K_M)^{AA}/(k_{cat}/K_M)^{LA}$ for 15-LOX-2. The magnitude of these substrate specificity changes was over four fold, which is comparable in magnitude to that observed for the allosteric regulation of ribonucleotide reductase (RNR) substrate specificity.[139-141]

These earlier findings from steady-state kinetics of 15-LOX-1 were confirmed by a novel competitive substrate capture method developed by our lab, demonstrating saturating effects on the substrate specificity ratio of AA/LA with a $K_D = 1.2 \pm 0.1$ μM for perdeuterated 13-(S)-HPODE.[38] Interestingly, the addition of 13-(S)-HPODE showed no effect on 15-LOX-2 kinetics at pH 7.5, which contradicted the change

19

between steady state kinetics and competitive substrate capture, 8.0 ±1.0 and 2.2 ±0.2 respectively This discrepancy was postulated to be due to a tight association of 13-(S)-HPODE with 15-LOX-2, thus saturating the allosteric binding site. It was also observed that the AA/LA substrate specificity ratio was pH dependent, changing from 1.4 ± 0.3 at pH 6.0 to 4.5 ± 0.5, at pH 10. The pH titration curve showed a pK_a of 7.7 ± 0.1, suggesting a charged interaction between 13-(S)-HPODE and a possible Histidine residue, whose neutral state lowered the affinity of 13-(S)-HPODE for 15-LOX-2. Docking of 13-(S)-HODE to the surface of a homology model of 15-LOX-2 led us to hypothesize the location of the allosteric site to be between the two domains of 15-LOX-2, with His627 interacting with the carboxylate group of 13-(S)-HODE.[39]

Changes in pH are known to play significant role in LOX chemistry for two main reasons. First, it alters the degree of dissociation of their substrates, unsaturated fatty acids and second, it modifies the dissociation of amino acid side chains residues, mainly histidines. For example, these structural changes induced by pH have been shown to affect the positional specificity of sLO by reversing the substrate arrangement at the active site.[142, 143]

In cells, pH alterations are usually caused by metabolic changes such as lactoacidosis and inflammation.[144, 145] Even under physiological conditions, pH gradients exist across certain types of bio-membranes such as lysosomes, mitochondria.[146] Since LOX confer their function via formation of different bioactive products, the pH induced changes with respect to their reaction specificity or product

20

profile must be biologically relevant and the pH effect seen with 15-LOX-2 warrants further investigation. `

After the initial finding of the allosteric site in 15-LOX-2, inhibition kinetics were performed in the presence of 13-(S)-HODE, which indicated that the proposed allosteric site is different from the active site.[39] Viscosity, kinetic isotope effect and solvent isotope effect studies showed that the allosteric effector, 13-HODE doesn't influence the microscopic rates of diffusion and hydrogen bond abstraction steps in the reaction mechanism, but eliminates the kinetic dependency on the hydrogen bond rearrangement. Its binding also affects the affinity towards the substrate, most likely due to structural changes in the active site of 15-LOX-2.

1.9 Scope of the dissertation

As discussed in the introduction, this dissertation focuses on the two isoforms of human 15-lipoxygenase, the reticulocyte 15-LOX-1 and the epithelial 15-LOX-2. The strong experimental evidence of the involvement of 15-LOX-1 in various human diseases and the availability of the structural information through its close homologue rabbit 15-LOX justify the tremendous efforts put in by researchers all over the world to discover its potent and selective inhibitors as potential therapeutics in different human diseases. Its inhibitor discovery will not only aid in the treatment of several human ailments, but will also provide necessary tools for the scientists in pinpointing its role and mechanism of action in particular diseases.

On the other hand, the studies performed to investigate the biological function of 15-LOX-2 are still in their infancy. Currently, there is no structural information

available for 15-LOX-2. Its low homology with 15-LOX-1 and the striking differences between their kinetics and substrate specificities indicate that the active site of 15-LOX-2 is different from that of 15-LOX-1. Moreover, the allosteric properties of 15-LOX-2 previously reported by our lab are very complex and their biological significance is difficult to interpret, as seen by the confounding roles of its AA and LA products, 15-HPETE and 13-HPODE in the human body. Hence, a comprehensive analysis of the substrate specificity of 15-LOX-2, using endogenously available substrates, is required in order to understand the role of their various products in human body, as well as the their regulation of 15-LOX-2 substrate specificity.

The chapter two in this dissertation discusses the collaborative efforts of our lab with Dr. Klaus van Leyen to test the efficacy of our 15-LOX-1 inhibitors as therapeutics for in-vivo and in-vitro stroke models. Cell culture and tissue samples, with and without 15-LOX-1 inhibitors, were generated by the Dr. Van Leyen's lab and sent to us for their LC-MS analysis. The ex vivo system demonstrated that that our 15-LOX-1 inhibitors protected neuronal HT22 cells against oxidative stress. It was also determined that 15-LOX-1 activity increased in stroke induced mouse models and 15-LOX-1 inhibitors reduced the infarct size 24 hours and 14 days post stroke, even when the doses were administered 4-6 hours post ischemia.

The chapter three is another collaborative work with Dr. Van Leyen and Dr. Maloney that emphasizes on the discovery of a novel chemotype for 15-LOX-1 inhibitors. It describes in detail the discovery, characterization and optimization of the

potent and selective inhibitors of human 15-LOX-1. The *in-vivo* and *in-vitro* studies demonstrate the potential of 15-LOX-1 inhibitors as therapeutics for stroke related damage.

In chapter four of this dissertation, the previous substrate specificity studies of 15-LOX-2 are expanded beyond the AA-LA pair by thoroughly studying its substrate preference with AA versus various PUFAs, differing in chain length and unsaturation, at different pH values with and without added LOX products. Our results demonstrate that C_{18} fatty acid and C_{20} fatty acid products alter the substrate specificity of 15-LOX-2 differently, which is suggestive of a distinct mechanism of catalysis for these two classes of LOXs substrates. In addition, pH affects substrate specificity in a similar manner, indicating a similar mechanism of action. This allosteric investigation of 15-LOX-2 via kinetic studies thus provides a detailed insight into the factors that influence the regulation of its substrate specificity and have important implications to the role of 15-LOX-2 in human tissue.

1.10 Figures

Figure 1.1 Lipoxygenase structure

Catalytic domain

Beta barrel domain
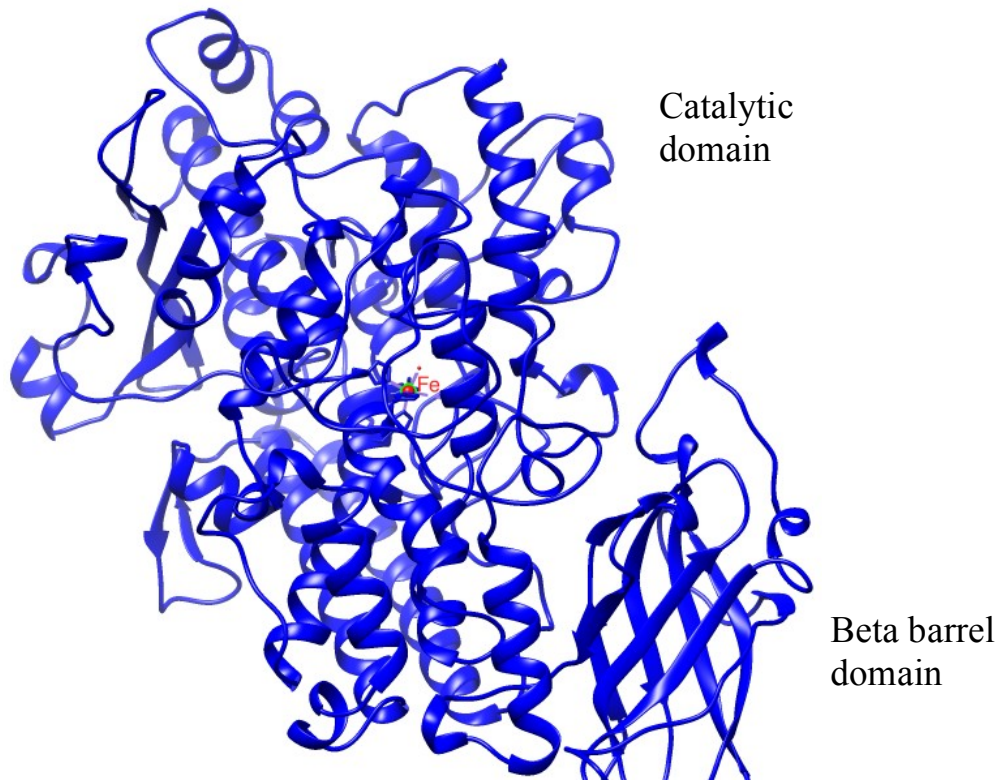
Figure 1.2

A) Proposed catalytic cycle of LOX B) Various microscopic steps involved in LOX reaction mechanism

A

H-abstraction   Radical rearrangement

Oxygen insertion
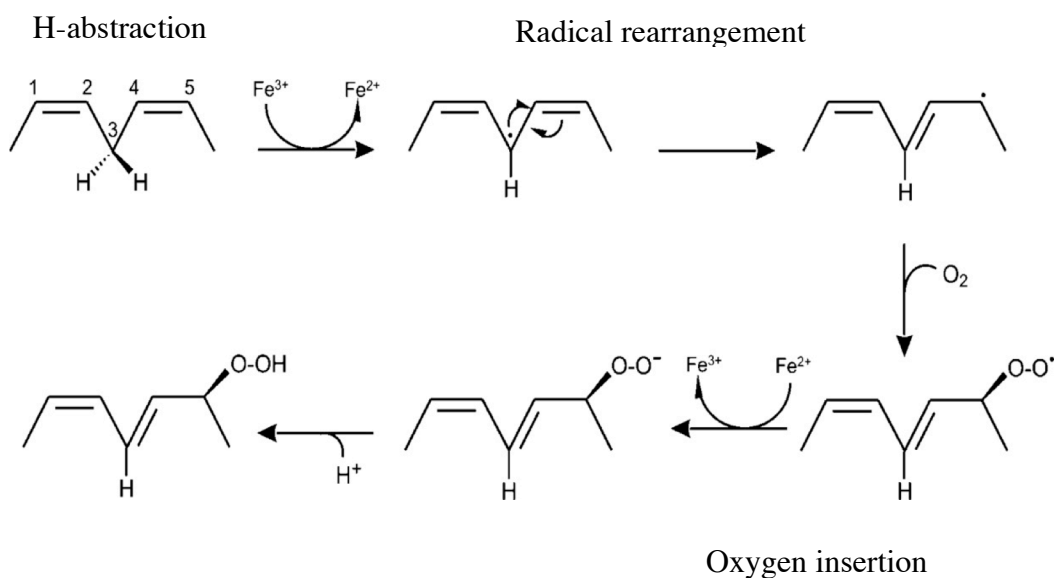
B
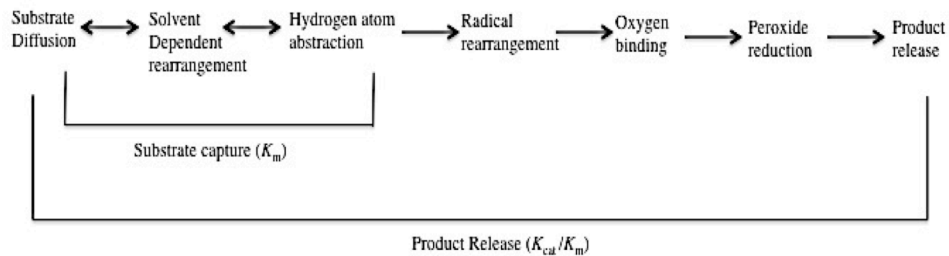
Figure 1.3 Poly-unsaturated fatty acids as LOX substrates
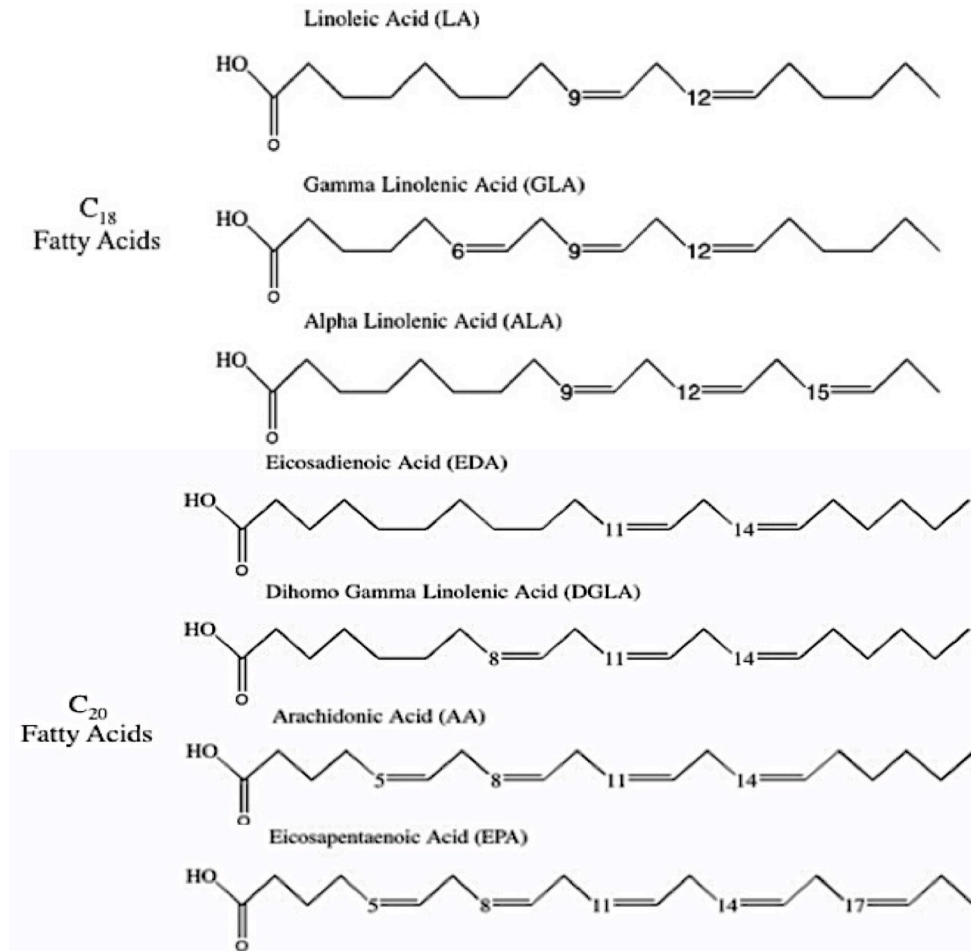
Figure 1.4 Role of 15-LOX in the formation of leukotrienes and lipoxins.

cPLA2

↓

Arachidonic Acid (AA)

15-LOX

↓

15-(S)-HPETE

5-LOX

↓

Leukotriene A_4

Epoxide hydrolase

15S Epoxy-tetraene

Lipoxin A_4

Lipoxin B_4
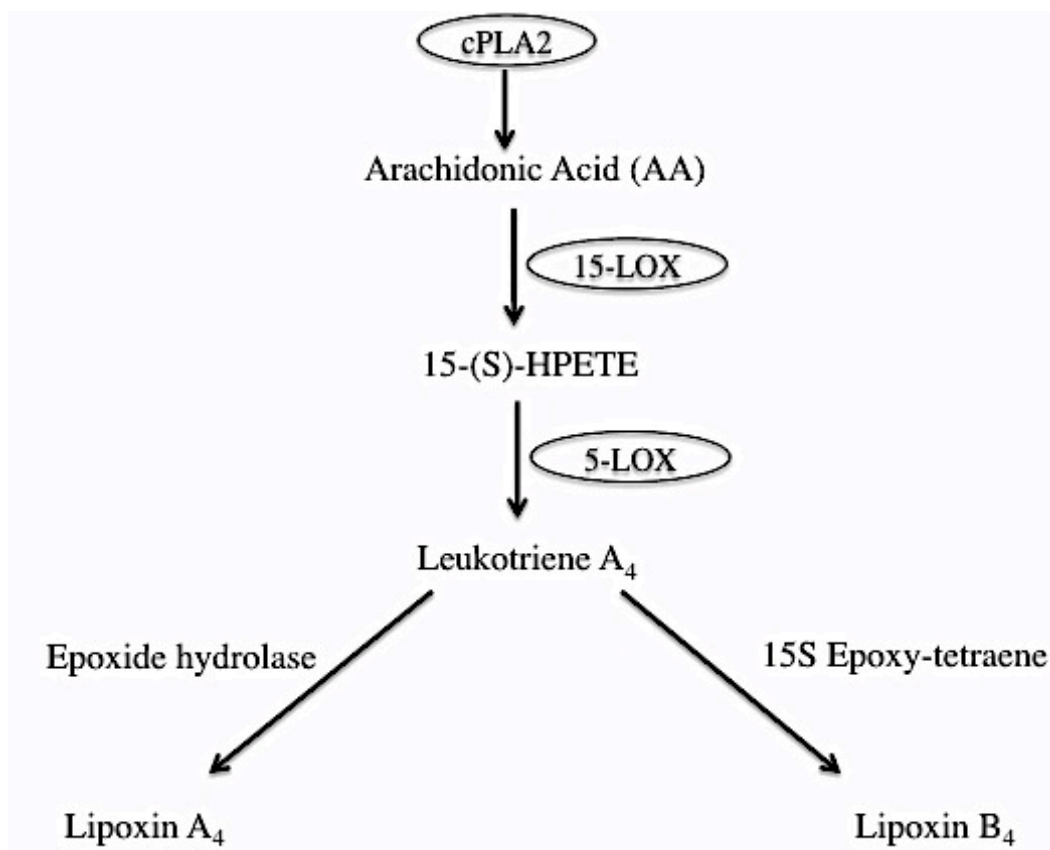
Figure 1.5 Role of 15-LOX-1 in stroke related damage.
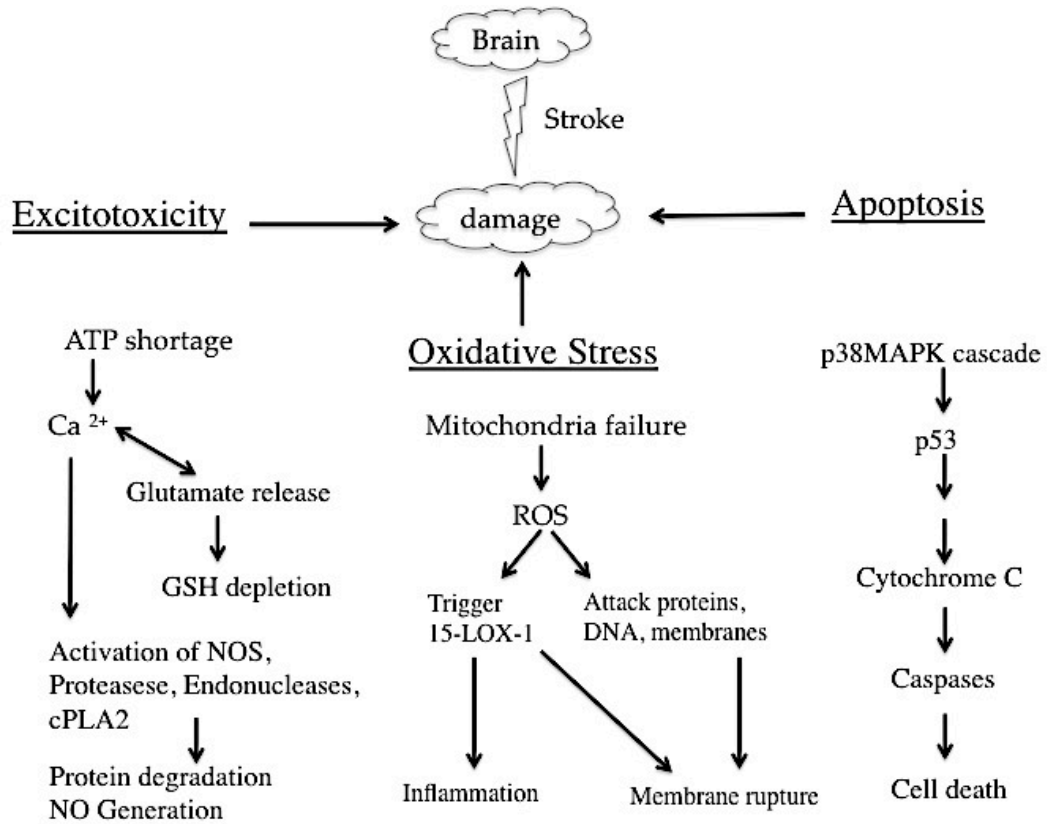
1.11 References

1. Brash, A. R. (1999) Lipoxygenases: Occurrence, Functions, Catalysis and Acquisition of Substrate, *J. Biol. Chem. 274*, 23679-23682.

2. Ivanov, I., Heydeck, D., Hofheinz, K., Roffeis, J., O'Donnell, V. B., Kuhn, H., and Walther, M. (2010) Molecular enzymology of lipoxygenases, *Arch Biochem Biophys 503*, 161-174.

3. Solomon, E. I., Zhou, J., Neese, F., and Pavel, E. G. (1997) New Insights from Spectroscopy into the structure/function relationships of lipoxygenases, *Chem. Biol. 4*, 795-808.

4. Kuhn, H., Walther, M., and Kuban, R. J. (2002) Mammalian arachidonate 15-lipoxygenases: Structure, function, and biological implications, *Prostag. oth. Lipid M. 68-69*, 263-290.

5. Siedow, J. N. (1991) Plant lipoxygenase : structure and function, *Annu. Rev. Plant Physiol. Plant Mol. Biol 42*, 145-188.

6. Grechkin, A. (1998) Recent Developments in Biochemistry of the Plant Lipoxygenase Pathway, *Prog. Lipid Res. 37*, 317-352.

7. Samuelsson, B., Dahlen, S. E., Lindgren, J. A., Rouzer, C. A., and Serhan, C. N. (1987) Leukotrienes and Lipoxins: Structures, Biosynthesis, and Biological Effects, *Science 237*, 1171-1176.

8. Jisaka, M., Kim, R. B., Boeglin, W. E., and Brash, A. R. (2000) Identification of amino acid determinants of the positional specificity of mouse 8S-lipoxygenase and human 15S-lipoxygenase-2, *The Journal of biological chemistry 275*, 1287-1293.

9. Boyington, J. C., Gaffney, B. J., and Amzel, L. M. (1997) The three-dimensional structure of soybean lipoxygenase-1: an arachidonic acid 15-lipoxygenase, *Advances in experimental medicine and biology 400A*, 133-138.

10. Minor, W., Steczko, J., Boguslaw, S., Otwinowski, Z., Bolin, J. T., Walter, R., and Axelrod, B. (1996) Crystal Structure of Soybean Lipoxygenase L-1 at 1.4 A Resolution, *Biochemistry 35*, 10687-10701.

11. Youn, B., Sellhorn, G. E., Mirchel, R. J., Gaffney, B. J., Grimes, H. D., and Kang, C. (2006) Crystal structures of vegetative soybean lipoxygenase VLX-B and VLX-D, and comparisons with seed isoforms LOX-1 and LOX-3, *Proteins 65*, 1008-1020.

12. Skrzypczak-Jankun, E., Zhou, K., and Jankun, J. (2003) Inhibition of lipoxygenase by (-)-epigallocatechin gallate: X-ray analysis at 2.1 A reveals degradation of EGCG and shows soybean LOX-3 complex with EGC instead, *International journal of molecular medicine 12*, 415-420.

13. Choi, J., Chon, J. K., Kim, S., and Shin, W. (2008) Conformational flexibility in mammalian 15S-lipoxygenase: Reinterpretation of the crystallographic data, *Proteins 70*, 1023-1032.

14. Neau, D. B., Gilbert, N. C., Bartlett, S. G., Boeglin, W., Brash, A. R., and Newcomer, M. E. (2009) The 1.85 A structure of an 8R-lipoxygenase suggests a general model for lipoxygenase product specificity, *Biochemistry 48*, 7906-7915.

15. Gilbert, N. C., Bartlett, S. G., Waight, M. T., Neau, D. B., Boeglin, W. E., Brash, A. R., and Newcomer, M. E. (2011) The structure of human 5-lipoxygenase, *Science 331*, 217-219.

16. Coffa, G., Imber, A. N., Maguire, B. C., Laxmikanthan, G., Schneider, C., Gaffney, B. J., and Brash, A. R. (2005) On the relationships of substrate orientation, hydrogen abstraction, and product stereochemistry in single and double dioxygenations by soybean lipoxygenase-1 and its Ala542Gly mutant, *The Journal of biological chemistry 280*, 38756-38766.

17. Koljak, R., Boutaud, O., Shieh, B. H., Samel, N., and Brash, A. R. (1997) Identification of a naturally occurring peroxidase-lipoxygenase fusion protein, *Science 277*, 1994-1996.

18.   Varvas, K., Jarving, I., Koljak, R., Valmsen, K., Brash, A. R., and Samel, N. (1999) Evidence of a cyclooxygenase-related prostaglandin synthesis in coral. The allene oxide pathway is not involved in prostaglandin biosynthesis, *The Journal of biological chemistry 274*, 9923-9929.

19.   Oldham, M. L., Brash, A. R., and Newcomer, M. E. (2005) The structure of coral allene oxide synthase reveals a catalase adapted for metabolism of a fatty acid hydroperoxide, *Proceedings of the National Academy of Sciences of the United States of America 102*, 297-302.

20.   Abraham, B. D., Sono, M., Boutaud, O., Shriner, A., Dawson, J. H., Brash, A. R., and Gaffney, B. J. (2001) Characterization of the coral allene oxide synthase active site with UV-visible absorption, magnetic circular dichroism, and electron paramagnetic resonance spectroscopy: evidence for tyrosinate ligation to the ferric enzyme heme iron, *Biochemistry 40*, 2251-2259.

21.   Gillmor, S. A., Villasenor, A., Fletterick, R., Sigal, E., and Browner, M. (1997) The structure of mammalian 15-lipoxygenase reveals similarity to the lipases and the determinants of substrate specificity., *Nature Struct. Biol. 4*, 1003-1009.

22.   Chahinian, H., Sias, B., and Carriere, F. (2000) The C-terminal domain of pancreatic lipase: functional and structural analogies with c2 domains, *Current protein & peptide science 1*, 91-103.

23.   Walther, M., Anton, M., Wiedmann, M., Fletterick, R., and Kuhn, H. (2002) The N-terminal domain of the reticulocyte-type 15-lipoxygenase is not essential for enzymatic activity but contains determinants for membrane binding, *J. Biol. Chem. 277*, 27360-27366.

24.   Chen, X. S., and Funk, C. D. (2001) The N-terminal "beta-barrel" domain of 5-lipoxygenase is essential for nuclear membrane translocation, *The Journal of biological chemistry 276*, 811-818.

25.   Walther, M., Hofheinz, K., Vogel, R., Roffeis, J., and Kuhn, H. The N-terminal beta-barrel domain of mammalian lipoxygenases including mouse 5-lipoxygenase is not essential for catalytic activity and membrane binding but exhibits regulatory functions, *Arch Biochem Biophys*.

26. Hammel, M., Walther, M., Prassl, R., and Kuhn, H. (2004) Structural flexibility of the N-terminal beta-barrel domain of 15-lipoxygenase-1 probed by small angle X-ray scattering. Functional consequences for activity regulation and membrane binding, *Journal of molecular biology 343*, 917-929.

27. Ivanov, I., Di Venere, A., Horn, T., Scheerer, P., Nicolai, E., Stehling, S., Richter, C., Skrzypczak-Jankun, E., Mei, G., Maccarrone, M., and Kuhn, H. Tight association of N-terminal and catalytic subunits of rabbit 12/15-lipoxygenase is important for protein stability and catalytic activity, *Biochimica et biophysica acta*.

28. Tomchick, D. R., Phan, P., Cymborowski, M., Minor, W., and Holman, T. R. (2001) Structural and functional characterization of second-coordination sphere mutants of soybean lipoxygenase-1, *Biochemistry 40*, 7509-7517.

29. Holman, T. R., Zhou, J., and Solomon, E. I. (1998) Spectroscopic and Functional Characterization of a Ligand Coordination Mutant of Soybean Lipoxygenase: First Coordination Sphere Analogue of Human 15-Lipoxygenase., *J. Am. Chem. Soc. 120*, 12564-12572.

30. Segraves, E. N., Chruszcz, M., Neidig, M. L., Ruddat, V., Zhou, J., Wecksler, A. T., Minor, W., Solomon, E. I., and Holman, T. R. (2006) Kinetic, spectroscopic, and structural investigations of the soybean lipoxygenase-1 first-coordination sphere mutant, Asn694Gly, *Biochemistry 45*, 10233-10242.

31. Neidig, M. L., Wecksler, A. T., Schenk, G., Holman, T. R., and Solomon, E. I. (2007) Kinetic and spectroscopic studies of N694C lipoxygenase: a probe of the substrate activation mechanism of a nonheme ferric enzyme, *Journal of the American Chemical Society 129*, 7531-7537.

32. Kilty, I., Logan, A., and Vickers, P. J. (1999) Differential characteristics of human 15-lipoxygenase isozymes and a novel splice variant of 15S-lipoxygenase, *Eur J Biochem 266*, 83-93.

33. Glickman, M. H., and Klinman, J. P. (1995) Nature of Rate-Limiting Steps in the Soybean Lipoxygenase-1 Reaction, *Biochemistry 34*, 14077-14092.

34. Jonsson, T., Glickman, M. H., Sun, S. J., and Klinman, J. P. (1996) Experimental Evidence for Extensive Tunneling of Hydrogen in the Lipoxygenase Reaction: Implications for Enzyme Catalysis, *J. Am. Chem. Soc. 118*, 10319-10320.

35. Glickman, M. H., and Klinman, J. P. (1996) Lipoxygenase reaction mechanism: Demonstration that hydrogen abstraction from substrate precedes dioxygen binding during catalytic turnover, *Biochemistry 35*, 12882-12892.

36. Rickert, K. W., and Klinman, J. P. (1999) Nature of Hydrogen Transfer in Soybean Lipoxygenase-1: Separation of Primary and Secondary Isotope Effects, *Biochemistry 38*, 12218-12228.

37. Lewis, E. R., Johansen, E., and Holman, T. R. (1999) Large competitive kinetic isotope effects in human 15-LO catalysis measured by a novel HPLC method., *J. Am. Chem. Soc. 121*, 1395-1396.

38. Wecksler, A. T., Kenyon, V., Deschamps, J. D., and Holman, T. R. (2008) Substrate specificity changes for human reticulocyte and epithelial 15-lipoxygenases reveal allosteric product regulation, *Biochemistry 47*, 7364-7375.

39. Wecksler, A. T., Deschamps, J. D., Kenyon, V., Garcia, N. K., van der Donk, W. A., and Holman, T. R. (2009) Kinetic and structural investigations of the allosteric site in human epithelial 15-lipoxygenase-2, *Biochemistry Manuscript in revisions*.

40. Wecksler, A. T., Jacquot, C., van der Donk, W. A., and Holman, T. R. (2009) Mechanistic Investigations of Human Reticulocyte 15- and Platelet 12-Lipoxygenases with Arachidonic Acid, *Biochemistry 48*, 6259-6267.

41. Knapp, M. J., Seebeck, F. P., and Klinman, J. P. (2001) Steric control of oxygenation regiochemistry in soybean lipoxygenase-1, *Journal of the American Chemical Society 123*, 2931-2932.

42. Tsai, S., and Klinman, J. P. (2001) Probes of hydrogen tunneling with horse liver alcohol dehydrogenase at subzero temperatures, *Biochemistry 40*, 2303-2311.

43. Yehuda, S., Rabinovitz, S., and Mostofsky, D. I. (1999) Essential fatty acids are mediators of brain biochemistry and cognitive functions, *Journal of neuroscience research 56*, 565-570.

44. Das, U. N. (2006) Essential Fatty acids - a review, *Current pharmaceutical biotechnology 7*, 467-482.

45. Das, U. N. (2006) Essential fatty acids: biochemistry, physiology and pathology, *Biotechnology journal 1*, 420-439.

46. Andreou, A., and Feussner, I. (2009) Lipoxygenases - Structure and reaction mechanism, *Phytochemistry 70*, 1504-1510.

47. Haeggstrom, J., and Funk, C. D. (2011) Lipoxygenase and Leukotriene Pathways: Biochemistry, Biology, and Roles in Disease, *Chemical Reviews ASAP*.

48. Sierra-Honigmann, M. R., Bradley, J. R., and Pober, J. S. (1996) "Cytosolic" phospholipase A2 is in the nucleus of subconfluent endothelial cells but confined to the cytoplasm of confluent endothelial cells and redistributes to the nuclear envelope and cell junctions upon histamine stimulation, *Laboratory investigation; a journal of technical methods and pathology 74*, 684-695.

49. Calder, P. C. (2001) omega 3 polyunsaturated fatty acids, inflammation and immunity, *World review of nutrition and dietetics 88*, 109-116.

50. Calder, P. C. (2001) Polyunsaturated fatty acids, inflammation, and immunity, *Lipids 36*, 1007-1024.

51. Serhan, C. N., Chiang, N., and Van Dyke, T. E. (2008) Resolving inflammation: dual anti-inflammatory and pro-resolution lipid mediators, *Nat Rev Immunol 8*, 349-361.

52. Khanapure, S. P., Garvey, D. S., Janero, D. R., and Letts, L. G. (2007) Eicosanoids in inflammation: biosynthesis, pharmacology, and therapeutic frontiers, *Curr Top Med Chem 7*, 311-340.

53.   Nie, D., Che, M., Grignon, D., Tang, K., and Honn, K. V. (2001) Role of eicosanoids in prostate cancer progression, *Cancer Metastasis Rev 20*, 195-206.

54.   Nie, D., Tang, K., Diglio, C., and Honn, K. V. (2000) Eicosanoid regulation of angiogenesis: role of endothelial arachidonate 12-lipoxygenase, *Blood 95*, 2304-2311.

55.   Pirillo, A., Uboldi, P., Kuhn, H., and Catapano, A. L. (2006) 15-Lipoxygenase-mediated modification of high-density lipoproteins impairs SR-BI- and ABCA1-dependent cholesterol efflux from macrophages, *Biochimica et biophysica acta 1761*, 292-300.

56.   Pallast, S., Arai, K., Wang, X., Lo, E. H., and van Leyen, K. (2009) 12/15-Lipoxygenase targets neuronal mitochondria under oxidative stress., *Journal of neurochemistry 111*, 882-889.

57.   van Leyen, K., Duvoisin, R. M., Engelhardt, H., and Wiedmann, M. (1998) A function for lipoxygenase in programmed organelle degradation, *Nature 395*, 392-395.

58.   Funk, C. D. (2005) Leukotriene modifiers as potential therapeutics for cardiovascular disease, *Nature reviews. Drug discovery 4*, 664-672.

59.   Wenzel, S. E., and Kamada, A. K. (1996) Zileuton: the first 5-lipoxygenase inhibitor for the treatment of asthma, *Ann Pharmacother 30*, 858-864.

60.   O'Byrne, P. M., Israel, E., and Drazen, J. M. (1997) Antileukotrienes in the Treatment of Asthma, *Annals of Internal Medicine 127*, 472-480.

61.   Drazen, J. M., Israel, E., and O'Byrne, P. M. (1999) Treatment of asthma with drugs modifying the leukotriene pathway, *The New England journal of medicine 340*, 197-206.

62.   Berger, W., De Chandt, M. T., and Cairns, C. B. (2007) Zileuton: clinical implications of 5-Lipoxygenase inhibition in severe airway disease, *International Journal of Clinical Practice 61*, 663-676.

63. Muller-Peddinghaus, R. (1997) Potential anti-inflammatory effects of 5-lipoxygenase inhibition--exemplified by the leukotriene synthesis inhibitor BAY X 1005, *J Physiol Pharmacol 48*, 529-536.

64. Spanbroek, R., Grabner, R., Lotzer, K., Hildner, M., Urbach, A., Ruhling, K., Moos, M. P., Kaiser, B., Cohnert, T. U., Wahlers, T., Zieske, A., Plenz, G., Robenek, H., Salbach, P., Kuhn, H., Radmark, O., Samuelsson, B., and Habenicht, A. J. (2003) Expanding expression of the 5-lipoxygenase pathway within the arterial wall during human atherogenesis, *Proceedings of the National Academy of Sciences of the United States of America 100*, 1238-1243.

65. Lotzer, K., Funk, C. D., and Habenicht, A. J. (2005) The 5-lipoxygenase pathway in arterial wall biology and atherosclerosis, *Biochimica et biophysica acta 1736*, 30-37.

66. Weinblatt, M. E., Kremer, J. M., Coblyn, J. S., Helfgott, S., Maier, A. L., Petrillo, G., Henson, B., Rubin, P., and Sperling, R. (1992) Zileuton, a 5-lipoxygenase inhibitor in rheumatoid arthritis, *The Journal of rheumatology 19*, 1537-1541.

67. Klickstein, L. B., Shapleigh, C., and Goetzl, E. J. (1980) Lipoxygenation of arachidonic acid as a source of polymorphonuclear leukocyte chemotactic factors in synovial fluid and tissue in rheumatoid arthritis and spondyloarthritis, *The Journal of clinical investigation 66*, 1166-1170.

68. Serhan, C. N., Sheppard, K. A., and Fiore, S. (1990) Lipoxin formation: evaluation of the role and actions of leukotriene A4, *Advances in Prostaglandin Thromboxane and Leukotriene Research 20*, 54-62.

69. Funk, C. D., Furci, L., and Fitzgerald, G. A. (1990) Molecular cloning of the human platelet 12-lipoxygenase, *Trans Assoc Am Physicians 103*, 180-186.

70. Funk, C. D., Furci, L., and FitzGerald, G. A. (1990) Molecular cloning, primary structure, and expression of the human platelet/erythroleukemia cell 12-lipoxygenase, *Proceedings of the National Academy of Sciences of the United States of America 87*, 5638-5642.

71.	Funk, C. D., Funk, L. B., FitzGerald, G. A., and Samuelsson, B. (1992) Characterization of human 12-lipoxygenase genes, *Proceedings of the National Academy of Sciences of the United States of America 89*, 3962-3966.

72.	Thomas, C. P., Morgan, L. T., Maskrey, B. H., Murphy, R. C., Kuhn, H., Hazen, S. L., Goodall, A. H., Hamali, H. A., Collins, P. W., and O'Donnell, V. B. (2010) Phospholipid-esterified eicosanoids are generated in agonist-activated human platelets and enhance tissue factor-dependent thrombin generation, *Journal of Biological Chemistry 285*, 6891-6903.

73.	Ikei, K. N., Yeung, J., Apopa, P. L., Ceja, J., Vesci, J., Holman, T. R., and Holinstat, M. (2012) Investigations of human platelet-type 12-lipoxygenase: role of lipoxygenase products in platelet activation, *Journal of lipid research*.

74.	Bleich, D., Chen, S., Gu, J. L., and Nadler, J. L. (1998) The role of 12-lipoxygenase in pancreatic -cells (Review), *International journal of molecular medicine 1*, 265-272.

75.	Hedrick, C. C., Kim, M. D., Natarajan, R. D., and Nadler, J. L. (1999) 12-Lipoxygenase products increase monocyte:endothelial interactions, *Advances in experimental medicine and biology 469*, 455-460.

76.	Nozawa, K., Tuck, M. L., Golub, M., Eggena, P., Nadler, J. L., and Stern, N. (1990) Inhibition of lipoxygenase pathway reduces blood pressure in renovascular hypertensive rats, *American Journal of Physiology 259*, H1774-1780.

77.	Kuhn, H., and O'Donnell, V. B. (2006) Inflammation and immune regulation by 12/15-lipoxygenases, *Progress in lipid research 45*, 334-356.

78.	Hussain, H., Shornick, L. P., Shannon, V. R., Wilson, J. D., Funk, C. D., Pentland, A. P., and Holtzman, M. J. (1994) Epidermis Contains Platlet-Type 12-Lipoxygenase that is Overexpressed in Germinal Layer Keratinocytes in Psoriasis, *Am. J. Physiol. 266*, C243-C253.

79.	Anton, R., Camacho, M., Puig, L., and Vila, L. (2002) Hepoxilin B3 and its enzymatically formed derivative trioxilin B3 are incorporated into

phospholipids in psoriatic lesions, *The Journal of investigative dermatology 118*, 139-146.

80. Ding, X. Z., Iversen, P., Cluck, M. W., Knezetic, J. A., and Adrian, T. E. (1999) Lipoxygenase inhibitors abolish proliferation of human pancreatic cancer cells., *Biochemical and biophysical research communications 261*, 218-223.

81. Connolly, J. M., and Rose, D. P. (1998) Enhanced angiogenesis and growth of 12-lipoxygenase gene-transfected MCF-7 human breast cancer cells in athymic nude mice, *Cancer Lett 132*, 107-112.

82. Steele, V. E., Holmes, C. A., Hawk, E. T., Kopelovich, L., Lubet, R. A., Crowell, J. A., Sigman, C. C., and Kelloff, G. J. (1999) Lipoxygenase inhibitors as potential cancer chemopreventives., *Cancer Epidemiol. Biomark. Prev. 8*, 467-483.

83. Krishnamoorthy, S., Jin, R., Cai, Y., Maddipati, K. R., Nie, D., Pages, G., Tucker, S. C., and Honn, K. V. (2010) 12-Lipoxygenase and the regulation of hypoxia-inducible factor in prostate cancer cells, *Experimental cell research 316*, 1706-1715.

84. Jiang, W. G., Douglas-Jones, A., and Mansel, R. E. (2003) Levels of expression of lipoxygenases and cyclooxygenase-2 in human breast cancer, *Prostaglandins, leukotrienes, and essential fatty acids 69*, 275-281.

85. Boeglin, W. E., Kim, R. B., and Brash, A. R. (1998) A 12R-lipoxygenase in human skin: mechanistic evidence, molecular cloning, and expression, *Proceedings of the National Academy of Sciences of the United States of America 95*, 6744-6749.

86. Sun, D., McDonnell, M., Chen, X. S., Lakkis, M. M., Li, H., Isaacs, S. N., Elsea, S. H., Patel, P. I., and Funk, C. D. (1998) Human 12(R)-lipoxygenase and the mouse ortholog. Molecular cloning, expression, and gene chromosomal assignment, *The Journal of biological chemistry 273*, 33540-33547.

87.   Furstenberger, G., Epp, N., Eckl, K. M., Hennies, H. C., Jorgensen, C., Hallenborg, P., Kristiansen, K., and Krieg, P. (2007) Role of epidermis-type lipoxygenases for skin barrier function and adipocyte differentiation, *Prostaglandins & other lipid mediators 82*, 128-134.

88.   Jobard, F., Lefevre, C., Karaduman, A., Blanchet-Bardon, C., Emre, S., Weissenbach, J., Ozguc, M., Lathrop, M., Prud'homme, J. F., and Fischer, J. (2002) Lipoxygenase-3 (ALOXE3) and 12(R)-lipoxygenase (ALOX12B) are mutated in non-bullous congenital ichthyosiform erythroderma (NCIE) linked to chromosome 17p13.1, *Human molecular genetics 11*, 107-113.

89.   Lesueur, F., Bouadjar, B., Lefevre, C., Jobard, F., Audebert, S., Lakhdar, H., Martin, L., Tadini, G., Karaduman, A., Emre, S., Saker, S., Lathrop, M., and Fischer, J. (2007) Novel mutations in ALOX12B in patients with autosomal recessive congenital ichthyosis and evidence for genetic heterogeneity on chromosome 17p13, *The Journal of investigative dermatology 127*, 829-834.

90.   Zheng, Y., Yin, H., Boeglin, W. E., Elias, P. M., Crumrine, D., Beier, D. R., and Brash, A. R. (2011) Lipoxygenases mediate the effect of essential fatty acid in skin barrier formation: a proposed role in releasing omega-hydroxyceramide for construction of the corneocyte lipid envelope, *The Journal of biological chemistry 286*, 24046-24056.

91.   Tang, D. G., Bhatia, B., Tang, S., and Schneider-Broussard, R. (2007) 15-lipoxygenase 2 (15-LOX2) is a functional tumor suppressor that regulates human prostate epithelial cell differentiation, senescence, and growth (size), *Prostaglandins & other lipid mediators 82*, 135-146.

92.   Tang, S., Bhatia, B., Maldonado, C. J., Yang, P., Newman, R. A., Liu, J., Chandra, D., Traag, J., Klein, R. D., Fischer, S. M., Chopra, D., Shen, J., Zhau, H. E., Chung, L. W., and Tang, D. G. (2002) Evidence that arachidonate 15-lipoxygenase 2 is a negative cell cycle regulator in normal prostate epithelial cells, *The Journal of biological chemistry 277*, 16189-16201.

93.   Shappell, S. B., Manning, S., Boeglin, W. E., Guan, Y. F., Roberts, R. L., Davis, L., Olson, S. J., Jack, G. S., Coffey, C. S., Wheeler, T. M., Breyer, M. D., and Brash, A. R. (2001) Alterations in lipoxygenase and cyclooxygenase-2

catalytic activity and mRNA expression in prostate carcinoma, *Neoplasia 3*, 287-303.

94.   Hsi, L. C., Wilson, L. C., and Eling, T. E. (2002) Opposing effects of 15-lipoxygenase-1 and -2 metabolites on MAPK signaling in prostate. Alteration in peroxisome proliferator-activated receptor gamma, *The Journal of biological chemistry 277*, 40549-40556.

95.   Wiesner, R., Suzuki, H., Walther, M., Yamamoto, S., and Kuhn, H. (2003) Suicidal inactivation of the rabbit 15-lipoxygenase by 15S-HpETE is paralleled by covalent modification of active site peptides, *Free radical biology & medicine 34*, 304-315.

96.   Kuhn, H., Belkner, J., Wiesner, R., and Brash, A. R. (1990) Oxygenation of biological membranes by the pure reticulocyte lipoxygenase, *The Journal of biological chemistry 265*, 18351-18361.

97.   Funk, C. D. (2006) Lipoxygenase pathways as mediators of early inflammatory events in atherosclerosis, *Arteriosclerosis, thrombosis, and vascular biology 26*, 1204-1206.

98.   Kelavkar, U. P., Glasgow, W., Olson, S. J., Foster, B. A., and Shappell, S. B. (2004) Overexpression of 12/15-lipoxygenase, an ortholog of human 15-lipoxygenase-1, in the prostate tumors of TRAMP mice, *Neoplasia 6*, 821-830.

99.   Kelavkar, U. P., Cohen, C., Kamitani, H., Eling, T. E., and Badr, K. F. (2000) Concordant induction of 15-lipoxygenase-1 and mutant p53 expression in human prostate adenocarcinoma: correlation with Gleason staging, *Carcinogenesis 21*, 1777-1787.

100.   Bhattacharya, S., Mathew, G., Jayne, D. G., Pelengaris, S., and Khan, M. (2009) 15-lipoxygenase-1 in colorectal cancer: a review, *Tumour Biol 30*, 185-199.

101.   Yigitkanli, K., Pekcec, A., Karatas, H., Pallast, S., Mandeville, E., Joshi, N., Smirnova, N., Gazaryan, I., Ratan, R. R., Witztum, J. L., Montaner, J., Holman, T. R., Lo, E. H., and van Leyen, K. (2013) Inhibition of 12/15-

lipoxygenase as therapeutic strategy to treat stroke, *Annals of neurology 73*, 129-135.

102.   van Leyen, K. (2013) Lipoxygenase: An Emerging Target for Stroke Therapy, *CNS Neurol Disord Drug Targets*.

103.   Kronke, G., Katzenbeisser, J., Uderhardt, S., Zaiss, M. M., Scholtysek, C., Schabbauer, G., Zarbock, A., Koenders, M. I., Axmann, R., Zwerina, J., Baenckler, H. W., van den Berg, W., Voll, R. E., Kuhn, H., Joosten, L. A., and Schett, G. (2009) 12/15-lipoxygenase counteracts inflammation and tissue damage in arthritis, *Journal of immunology 183*, 3383-3389.

104.   Sigal, E., and Nadel, J. A. (1991) The airway epithelium and arachidonic acid 15-lipoxygenase, *The American review of respiratory disease 143*, S71-74.

105.   Profita, M., Vignola, A. M., Sala, A., Mirabella, A., Siena, L., Pace, E., Folco, G., and Bonsignore, G. (1999) Interleukin-4 enhances 15-lipoxygenase activity and incorporation of 15(S)-HETE into cellular phospholipids in cultured pulmonary epithelial cells, *American journal of respiratory cell and molecular biology 20*, 61-68.

106.   Schewe, T., Rapoport, S. M., and Kuehn, H. (1986) Enzymology and physiology of reticulocyte lipoxygenase : comparison with other lipoxygenases, *Adv. Enzymol. Relat. Areas Mol. Biol 58*, 191-272.

107.   Rapoport, S. M., and Schewe, T. (1986) The maturational breakdown of mitochondria in reticulocytes, *Biochimica et biophysica acta 864*, 471-495.

108.   Moskowitz, M. A., Lo, E. H., and Iadecola, C. (2010) The science of stroke: mechanisms in search of treatments, *Neuron 67*, 181-198.

109.   Roger, V. L., Go, A. S., Lloyd-Jones, D. M., Adams, R. J., Berry, J. D., Brown, T. M., Carnethon, M. R., Dai, S., de Simone, G., Ford, E. S., Fox, C. S., Fullerton, H. J., Gillespie, C., Greenlund, K. J., Hailpern, S. M., Heit, J. A., Ho, P. M., Howard, V. J., Kissela, B. M., Kittner, S. J., Lackland, D. T., Lichtman, J. H., Lisabeth, L. D., Makuc, D. M., Marcus, G. M., Marelli, A., Matchar, D. B., McDermott, M. M., Meigs, J. B., Moy, C. S., Mozaffarian, D., Mussolino, M. E., Nichol, G., Paynter, N. P., Rosamond, W. D., Sorlie, P. D.,

Stafford, R. S., Turan, T. N., Turner, M. B., Wong, N. D., and Wylie-Rosett, J. (2011) Heart disease and stroke statistics--2011 update: a report from the American Heart Association, *Circulation 123*, e18-e209.

110.   Lo, E. H. (2008) A new penumbra: transitioning from injury into repair after stroke, *Nat Med 14*, 497-500.

111.   Lo, E. H., Moskowitz, M. A., and Jacobs, T. P. (2005) Exciting, radical, suicidal: how brain cells die after stroke, *Stroke; a journal of cerebral circulation 36*, 189-192.

112.   Lo, E. H., Dalkara, T., and Moskowitz, M. A. (2003) Mechanisms, challenges and opportunities in stroke, *Nat Rev Neurosci 4*, 399-415.

113.   Dirnagl, U., Iadecola, C., and Moskowitz, M. A. (1999) Pathobiology of ischaemic stroke: an integrated view, *Trends in neurosciences 22*, 391-397.

114.   Ratan, R. R., Ryu, H., Lee, J., Mwidau, A., and Neve, R. L. (2002) In vitro model of oxidative stress in cortical neurons., *Methods Enzymol 352*, 183-190.

115.   Dargusch, R., and Schubert, D. (2002) Specificity of resistance to oxidative stress, *Journal of neurochemistry 81*, 1394-1400.

116.   Mytilineou, C., Kramer, B. C., and Yabut, J. A. (2002) Glutathione depletion and oxidative stress, *Parkinsonism Relat Disord 8*, 385-387.

117.   Ankarcrona, M., Dypbukt, J. M., Bonfoco, E., Zhivotovsky, B., Orrenius, S., Lipton, S. A., and Nicotera, P. (1995) Glutamate-induced neuronal death: a succession of necrosis or apoptosis depending on mitochondrial function, *Neuron 15*, 961-973.

118.   Zhang, Y., Wang, H., Li, J., Jimenez, D. A., Levitan, E. S., Aizenman, E., and Rosenberg, P. A. (2004) Peroxynitrite-induced neuronal apoptosis is mediated by intracellular zinc release and 12-lipoxygenase activation, *The Journal of neuroscience : the official journal of the Society for Neuroscience 24*, 10616-10627.

119. Crack, P. J., and Taylor, J. M. (2005) Reactive oxygen species and the modulation of stroke, *Free radical biology & medicine 38*, 1433-1444.

120. Chan, P. H. (1996) Role of oxidants in ischemic brain damage, *Stroke; a journal of cerebral circulation 27*, 1124-1129.

121. Chan, P. H. (2001) Reactive oxygen radicals in signaling and damage in the ischemic brain, *Journal of cerebral blood flow and metabolism : official journal of the International Society of Cerebral Blood Flow and Metabolism 21*, 2-14.

122. van Leyen, K., Siddiq, A., Ratan, R. R., and Lo, E. H. (2005) Proteasome inhibition protects HT22 neuronal cells from oxidative glutamate toxicity., *Journal of neurochemistry 92*, 824-830.

123. Seiler, A., Schneider, M., Forster, H., Roth, S., Wirth, E. K., Culmsee, C., Plesnila, N., Kremmer, E., Radmark, O., Wurst, W., Bornkamm, G. W., Schweizer, U., and Conrad, M. (2008) Glutathione peroxidase 4 senses and translates oxidative stress into 12/15-lipoxygenase dependent- and AIF-mediated cell death, *Cell metabolism 8*, 237-248.

124. Pallast, S., Arai, K., Pekcec, A., Yigitkanli, K., Yu, Z., Wang, X., Lo, E. H., and van Leyen, K. (2010) Increased nuclear apoptosis-inducing factor after transient focal ischemia: a 12/15-lipoxygenase-dependent organelle damage pathway., *Journal of cerebral blood flow and metabolism : official journal of the International Society of Cerebral Blood Flow and Metabolism 30*, 1157-1167.

125. Loscalzo, J. (2008) Membrane redox state and apoptosis: death by peroxide, *Cell metabolism 8*, 182-183.

126. Reddy, M. A., Thimmalapura, P. R., Lanting, L., Nadler, J. L., Fatima, S., and Natarajan, R. (2002) The oxidized lipid and lipoxygenase product 12(S)-hydroxyeicosatetraenoic acid induces hypertrophy and fibronectin transcription in vascular smooth muscle cells via p38 MAPK and cAMP response element-binding protein activation. Mediation of angiotensin II effects, *Journal of Biological Chemistry 277*, 9920-9928.

127. Chipuk, J. E., Kuwana, T., Bouchier-Hayes, L., Droin, N. M., Newmeyer, D. D., Schuler, M., and Green, D. R. (2004) Direct activation of Bax by p53 mediates mitochondrial membrane permeabilization and apoptosis, *Science 303*, 1010-1014.

128. Endo, H., Kamada, H., Nito, C., Nishi, T., and Chan, P. H. (2006) Mitochondrial translocation of p53 mediates release of cytochrome c and hippocampal CA1 neuronal death after transient global cerebral ischemia in rats, *The Journal of neuroscience : the official journal of the Society for Neuroscience 26*, 7974-7983.

129. Cui, L., Zhang, X., Yang, R., Liu, L., Wang, L., Li, M., and Du, W. (2010) Baicalein is neuroprotective in rat MCAO model: role of 12/15-lipoxygenase, mitogen-activated protein kinase and cytosolic phospholipase A2, *Pharmacology, biochemistry, and behavior 96*, 469-475.

130. Jin, G., Arai, K., Murata, Y., Wang, S., Stins, M. F., Lo, E. H., and van Leyen, K. (2008) Protecting against Cerebrovascular Injury: Contributions of 12/15-lipoxygenase to edema formation following transient focal ischemia, *Stroke; a journal of cerebral circulation 39*, 2538-2543.

131. van Leyen, K., Arai, K., Jin, G., Kenyon, V., Gerstner, B., Rosenberg, P. A., Holman, T. R., and Lo, E. H. (2008) Novel lipoxygenase inhibitors as neuroprotective reagents, *Journal of neuroscience research 86*, 904-909.

132. al., E. J. e. (2007) Lipoxygenases- A challenging problem in enzyme inhibition and drug development, *Current Enzyme Inhibition 3*, 119-132.

133. Brash, A. R., Boeglin, W. E., and Chang, M. S. (1997) Discovery of a second 15S-lipoxygenase in humans, *Proceedings of the National Academy of Sciences of the United States of America 94*, 6148-6152.

134. Brash, A. R., Jisaka, M., Boeglin, W. E., Chang, M. S., Keeney, D. S., Nanney, L. B., Kasper, S., Matusik, R. J., Olson, S. J., and Shappell, S. B. (1999) Investigation of a second 15S-lipoxygenase in humans and its expression in epithelial tissues, *Advances in experimental medicine and biology 469*, 83-89.

135.   Subbarayan, V., Krieg, P., Hsi, L. C., Kim, J., Yang, P., Sabichi, A. L., Llansa, N., Mendoza, G., Logothetis, C. J., Newman, R. A., Lippman, S. M., and Menter, D. G. (2006) 15-Lipoxygenase-2 gene regulation by its product 15-(S)-hydroxyeicosatetraenoic acid through a negative feedback mechanism that involves peroxisome proliferator-activated receptor gamma, *Oncogene 25*, 6015-6025.

136.   Jiang, W. G., Watkins, G., Douglas-Jones, A., and Mansel, R. E. (2006) Reduction of isoforms of 15-lipoxygenase (15-LOX)-1 and 15-LOX-2 in human breast cancer, *Prostaglandins, leukotrienes, and essential fatty acids 74*, 235-245.

137.   Suraneni, M. V., Schneider-Broussard, R., Moore, J. R., Davis, T. C., Maldonado, C. J., Li, H., Newman, R. A., Kusewitt, D., Hu, J., Yang, P., and Tang, D. G. (2010) Transgenic expression of 15-lipoxygenase 2 (15-LOX2) in mouse prostate leads to hyperplasia and cell senescence, *Oncogene 29*, 4261-4275.

138.   Goodey, N. M., and Benkovic, S. J. (2008) Allosteric regulation and catalysis emerge via a common route, *Nat Chem Biol 4*, 474-482.

139.   Nordlund, P., and Reichard, P. (2006) Ribonucleotide reductases, *Annu Rev Biochem 75*, 681-706.

140.   Reichard, P. (2002) Ribonucleotide reductases: the evolution of allosteric regulation, *Arch Biochem Biophys 397*, 149-155.

141.   Kolberg, M., Strand, K. R., Graff, P., and Andersson, K. K. (2004) Structure, function, and mechanism of ribonucleotide reductases, *Biochimica et biophysica acta 1699*, 1-34.

142.   Ivanov, I., Rathmann, J., Myagkova, G., and Kuhn, H. (2001) Soybean lipoxygenase-1 oxygenates synthetic polyenoic fatty acids with an altered positional specificity: evidence for inverse substrate alignment, *Biochemistry 40*, 10223-10229.

143.   Gardner, H. W. (1989) Soybean Lipoxygenase-1 Enzymatically Forms Both (9S)-and (13S)-Hydroperoxides From Linoleic Acid by a pH-Dependent Mechanism., *Biochim. Biophys. Acta 1001*, 274-281.

144.   Walther, M., Roffeis, J., Jansen, C., Anton, M., Ivanov, I., and Kuhn, H. (2009) Structural basis for pH-dependent alterations of reaction specificity of vertebrate lipoxygenase isoforms, *Biochimica et biophysica acta 1791*, 827-835.

145.   Leblebicioglu, B., Lim, J. S., Cario, A. C., Beck, F. M., and Walters, J. D. (1996) pH changes observed in the inflamed gingival crevice modulate human polymorphonuclear leukocyte activation in vitro, *Journal of periodontology 67*, 472-477.

146.   Vijayvergiya, C., De Angelis, D., Walther, M., Kuhn, H., Duvoisin, R. M., Smith, D. H., and Wiedmann, M. (2004) High-level expression of rabbit 15-lipoxygenase induces collapse of the mitochondrial pH gradient in cell culture, *Biochemistry 43*, 15296-15302.

Chapter 2

Inhibition of 12/15-lipoxygenase as therapeutic strategy to treat stroke

2.1 Introduction

Acute stroke drug therapy in the United States currently remains limited to tissue plasminogen activator (tPA), a protease with significant side effects including increased bleeding. Because of the need to rule out a hemorrhagic stroke, CT or MRI imaging is required before tPA can be administered, narrowing the time window for tPA use. Currently only 1-5% of eligible patients are treated[1, 2].

Following experimental stroke, several oxidative stress-related pathways are activated, which contribute to enhanced ischemia/reperfusion injury[3-6]. 12/15-lipoxygenase (12/15-LOX) is increased in both neurons and endothelial cells in the peri-infarct area[7, 8], contributing to delayed cell death in the penumbra, weakening of the blood – brain barrier, and edema formation. Previous studies using lipoxygenase inhibitors have demonstrated infarct size reduction in mice and rats[9-14], and improved behavioral deficits in rabbits[15].

We have recently introduced novel lipoxygenase inhibitors, which were able to protect cultured neuronal and oligodendrocytic cells against oxidative stress[16]. In this study, we investigated 12/15-LOX activity in the ischemic brain, and we tested the inhibitor LOXBlock-1 in mouse models of cerebral ischemia and hemorrhage for its potential as acute phase therapy for ischemic stroke.

2.2 Materials and Methods

All animal experiments were performed following protocols approved by the Massachusetts General Hospital Institutional Animal Care and Use Committee in accordance with the National Institutes of Health Guide for the Care and Use of Laboratory Animals. Both the surgeon carrying out the operations, and the investigators evaluating data, were blinded as to treatment groups.

2.2 Materials and Methods

2.2.1 Oxidative Glutamate Toxicity in HT22 Cells

Glutathione depletion was induced in HT22 cells by glutamate treatment, and LDH release into the medium was measured to detect cell death as described[16-18]. Briefly, HT22 cells were cultured in DMEM containing 10% fetal bovine serum and penicillin / streptomycin (all media from Invitrogen). For viability experiments, cells were seeded at 5×10^5 cells/well in 24-well plates (Corning) and treated when approximately 70% confluent. Treatment consisted of exchanging the medium to 1 ml fresh culturing medium and adding 5 mM glutamate (stock solution 400 mM in PBS) in the presence or absence of DMSO (maximum 0.1% final concentration) as control or the indicated concentrations of LOXBlock-1. Lactate dehydrogenase (LDH) content was determined separately for the cell extracts and corresponding media using a Cytotoxicity Detection Kit (Roche), and the percentage of LDH released to the medium calculated after subtracting the corresponding background value. To determine levels of the 12/15-LOX metabolite 12-hydroxy-eicosatetraenoic acid (12-HETE), we cultured HT22 cells in 75 cm^2 flasks in DMEM medium without phenol red, supplemented with 5% FBS, and treated the cells the

48

next day when cells were 50-70% confluent. 24 hours later, the eicosanoid-containing fraction was isolated via Sep-Pak C-18 column, and 12-HETE was detected with a 12-HETE EIA kit (Assay Designs), used according to the manufacturer's instruction. Three independent experiments were evaluated.

2.2.2 Transcription Factor Activation Assays

Cell-based reporter assays were used to measure activation of NRF2 and HIF1α pathways. Varied concentrations (0.015-12 μM) of LOXBlock-1 and a positive control (TBHQ for Neh2-luc reporter cell line[19] and ciclopirox for HIF1 ODD-luc reporter cell line[20]) were tested in 96-format white, flat-bottom plates. Cells were plated at the density of 25,000 cells per well using a WellMate multichannel dispenser from Matrix (Thermo Fisher Scientific) and grown overnight on DMEM/F12+GlitaMAX (100 μl per well). Then the activator was added, and the plates were incubated for 3 hr; the medium was removed, cells lysed, and luciferase activity was measured on a luminometer Lmax11384 (Molecular Devices) with BrightGloTM reagent (Promega). The titration was performed in triplicate. The reporter activation was normalized to the background luminescence.

2.2.3 Mouse Transient Focal Cerebral Ischemia Models

The standard intraluminal middle cerebral artery occlusion method was used to induce transient focal cerebral ischemia in CD-1 mice as previously described[8]. General anesthesia was maintained with 1-1.5% isoflurane via facemask. Laser-Doppler flowmetry was used to confirm adequate induction of focal ischemia and successful cerebral reperfusion (3 mm lateral to bregma). Perfusion

reductions were monitored during ischemia as a percentage of pre-ischemia baselines. Body temperature was monitored and maintained at 36.5-37.5°C with a feedback heating pad. In this study, we used two types of transient focal cerebral ischemia models. First, in a 90-minute transient occlusion model, brain infarct was assessed at 24 hours after onset of ischemia. Second, in a 60-minutes of focal cerebral ischemia model, both histological and sensorimotor function measurements were assessed up to 14 days after ischemia. In all the in vivo experiments, investigators were blinded to the treatment groups.

2.2.4 Infarction Volumes

Male CD-1 mice were obtained from Charles River Laboratories. 5 minutes before induction of ischemia, mice received either DMSO vehicle, or 50 mg/kg LB-1 dissolved in DMSO, by intraperitoneal injection. At 24 hours after 90 minutes of focal cerebral ischemia, following transcardial perfusion with PBS to remove blood, mice were sacrificed. Ischemic brain damage was assessed by 2,3,5-triphenyltetrazolium hydrochloride (TTC) staining on 1-mm brain slices. In separate experiments, at 14 days after 60 minutes of transient focal cerebral ischemia, we used hematoxylin & eosin staining in 20-µm coronal sections (with a 1-mm interval). Infarct volumes were quantitated with a standard computer-assisted image analysis technique (Image-J). The indirect method was used (contralateral volume minus uninfarcted ipsilateral volume) to measure the brain infarction volume.

2.2.5 Preparation of Brain Homogenates and Isolation of Eicosanoid Fraction

The standard intraluminal 60 minutes middle cerebral artery occlusion filament method was used to induce transient focal cerebral ischemia in CD-1 mice as described above. After transcardial perfusion with PBS to eliminate blood, brain hemispheres from the ipsilateral (ischemic) and the non-ischemic contralateral side were separately frozen. Subsequently, they were homogenized in 5 µl Cell Lysis buffer (Cell Signaling) / mg weight with 20 strokes in a Dounce homogenizer, centrifuged for 15 minutes at 10000 x g. The supernatant was acidified to pH 3.5, centrifuged again, and the supernatant of this second spin was applied to a Sep-Pak C-18 column. The eluate of the C-18 column was concentrated in a SpeedVac vacuum centrifuge and analyzed using a commercially available 12-HETE EIA kit (Assay Designs), or subjected to analysis by HPLC/MS.

2.2.6 HPLC /MS analysis

The samples were dried under vacuum, re-suspended in methanol, centrifuged and supernatant was transferred to eppendorf tubes and stored at -20º C until analyzed by Finnigan LTQ liquid chromatography tandem mass spectrometry (LC−MS/MS) system. An internal control, deuterated (d_4) - PGE_2 (d_4-PGE_2) was added to each sample prior to injection on LC-MS to account for the variation in the detector response and it was assumed that the change in detector response for internal control and LOX products of interest would be similar. A Thermo Electron Corp. Aquasil (3 μm, 100 mm × 2.1 mm) C-18 column was used to separate the lipoxygenase products with an elution protocol consisting of 0.2 ml/min flow rate and a linear gradient from 40% ACN, 59.9% H_2O, and 0.1% THF to 48% ACN, 67.9 %

H_2O, and 0.1% THF, followed by an isocratic step of 55% ACN, 44.9% H_2O, and 0.1% THF. The corresponding LOX metabolites were detected using selective ion monitoring analysis [(m/z =318.7 to 319.7 for 12-HETE and 15-HETE),(m/z =334.7 to 335.7 for LTB$_4$), (m/z =354.7 to 355.7 for d$_4$-PGE$_2$) and (m/z =623.8 to 624.8 for LTC$_4$)] in negative ion mode and then identified by fragmentation pattern (12-HETE - parent ion at m/z 319 and fragments at m/z 179 and 163; 15-HETE - parent ion at m/z 319 and fragments at m/z 219 and 175; LTB$_4$ - parent ion at m/z 335 and fragments at m/z 203 and 195; d$_4$-PGE$_2$ - parent ion at m/z 355 and fragments at m/z 337,319 and 275; LTC$_4$ - parent ion at m/z 624 and fragments at m/z 606, 495 and 272) from MS-MS[21, 22]. The electro spray voltage was set to 5.0 kV and a global acquisition MS mode was used. The MS-MS scan was performed for the five most abundant precursor ions. The Collision Induced Dissociation (CID) was used for MS-MS with collision energy of 35 eV. The peak intensities of LOX products were normalized to the d$_4$- PGE$_2$ intensities. The amount of 12-HETE, 15 HETE, LTB$_4$ and LTC$_4$ in the samples was estimated using a standard curve generated from respective pure products with concentrations ranging from 0 μM to 10 μM along with a constant amount of d$_4$-PGE$_2$ added in each sample. The assays are linear in the concentration range used for the standard curve of 12-HETE, 15-HETE, LTB$_4$ and LTC$_4$ with R^2 values of 0.906, 0.933, 0.988 and 0.998 respectively.

2.2.7 Immunohistochemistry

Immunohistochemistry was performed on formalin-fixed sections, according to Pallast et al[23]. Brains were perfused transcardially first with PBS, then with 4%

formalin. They are then rapidly removed and stored in 4% formalin overnight. The next day, brains are transferred to buffer containing 15% sucrose for 24 hours, then 30% sucrose. Sections were cut to 20-µm coronal sections on a freezing microtome. After staining with primary antibodies and fluorescent-tagged secondary antibodies, sections are analyzed on a Zeiss LSM 5 Pascal scanning confocal microscope. Antibodies used for double staining were a rabbit polyclonal antiserum raised against the C-terminal peptide of 12/15-LOX and affinity purified against the peptide used for immunization, and a mouse monoclonal antibody MDA2, which recognizes malondialdehyde-modified lysine residues[24, 25].

2.2.8 Sensorimotor Function Assessments

Mice were tested and scored for neurological deficits using a Neurological Severity Score, 24 hours after onset of ischemia, and in a Corner Test 1, 4, 7, and 14 days after MCAO. One day before focal ischemic injury, mice were also tested to obtain pre-injury baselines.

2.2.9 Neurological Severity Score

A 10 point neurological score was employed with slight modifications[26]. The score consists of 10 individual clinical parameters, including tasks on motor function, alertness, and physiological behavior, whereby 1 point is given for failure. A maximal NSS of 10 point indicates severe neurological dysfunction with failure at all tasks (**Table 2.1**).

Table 2.1

Exit circle: Ability and initiative to exit circle of 30 cm diameter (time limit: 3 minutes)

Mono-Hemiparesis: Paresis of upper and/or lower limb of the contralateral side

Straight Walk: Alertness, initiative, and motor ability to walk straight, once the mouse is put on the floor

Startle Reflex: Initiative reflex; the mouse will react to a loud hand clap

Seeking Behavior: Physiological Behavior as a sign of "interest" in the environment

Beam Balancing: Ability to balance on a beam of 7 mm width for at least 10 seconds

Round Stick Balancing: Ability to balance on a round stick of 5 mm diameter for at least 10 seconds

Beam Walk 3 cm: Ability to cross a 30 cm long beam of 3 cm width

Beam Walk 2 cm: Same task, increased difficulty on a 2 cm wide beam

Beam Walk 1 cm: Same task, increased difficulty on a 1 cm wide beam

2.2.10 Corner Test

This test was carried out as previously described with slight modifications[27]. Briefly the mouse was placed between two rectangular pieces of wood (30x20x1 cm) joined with a hinge at an angle of 30° with a small opening along the joint. Mice were encouraged to enter the corner formed by the wooden boards. When the mouse entered into the deep part of the corner, both sides of the vibrissae were stimulated together by the two boards. Then the mouse reared forward and upward, then turned back to face the open end. Trials in which the mouse turned without rearing were excluded. Ten trials with a complete rearing were performed for

each mouse and the direction of rearing and turning was recorded. Following MCAO to the right side of the brain, mice initially have a strong tendency to turn to the right. This test detected integrated sensorimotor function as it involves both stimulation of the vibrissae (sensory/neglect) and rearing (motor response).

2.2.11 Induction of Intracerebral Hemorrhage

The standard intrastriatal collagenase model was used to make an Intracerebral Hemorrhage Model, in CD-1 mice[28]. Briefly, while the mice were under isofluorane anesthesia (1.5%) with spontaneous respiration in a nitrous oxide/oxygen mixture, a small borehole was drilled via the following coordinates from the bregma: 0.0 mm anterior, 2 mm lateral. A 32-gauge 0.5 µl microinjection needle (Hamilton, 7000) series was lowered 3.5 mm depth in the borehole with a stereotactic frame into the right striatum. During a period of 5 minutes, 0.5 µL of saline containing 0.075 U collagenase VII-S (Sigma) was injected. The needle was left in place for 10 minutes and then slowly removed over 5 minutes. Body temperature was monitored and maintained at 36.5-37.5°C with a feedback heating pad. Afterward, the borehole was sealed with bone wax, the scalp was sutured closed, and the mice were allowed to recover. The whole surgical procedure lasted approximately 35 minutes for each mouse.

2.2.12 Measuring Hemorrhagic Blood Volume by Quantitative Hemoglobin

Content Determination

55

24 hours after hemorrhage induction, transcardial perfusion with PBS was performed under deep (5%) isofluorane anesthesia. Brains were removed, separated into left and right hemispheres. Ipsilateral (hemorrhagic side) are homogenized in 900 µl, 1x Cell Lysis buffer (Cell Signaling) with 20 strokes in a Dounce homogenizer, centrifuged for 15 minutes at 13000 rpm. The 12.5 µl supernatant was added to 50 µL Drabkins reagant. With use of a photometer, absorption rates were determined at 540 nm, and hemorrhagic blood volumes were calculated for the ipsilateral brain on the basis of a standard curve.

2.2.13 Functional Outcome Assessment: Hanging Wire Test

At 24 hours after hemorrhage induction, neurological deficits were assessed on a standard hanging wire test, which was described before[28, 29]. Briefly, mice were suspended by its forelimbs on a wire stretched between two posts 60 cm above a foam pillow. The period of time in seconds until the mouse fell was recorded. We scored the mice; 1=0-29 seconds, 2=30-60 seconds, 3=no fall off in 60 seconds. The posture of the four limbs and tail and the movement of the mouse were recorded as different scores; 0=fall off in the first 30 seconds, 1=is not able to bring all four paws to the wire, 2=uses all four paws and tail to stay on the wire but does not move to the left or right, 3=like 2, but also gains some distance on the wire, 4= like 2 and the mice reaches the post holding the hanging wire, 5= like 2 but also climbs down the side of the post to the table. The test was repeated 3 times for each mouse.

2.2.14 Distal MCAO Experiments

To study LOXBlock-1 in a model of tPA-induced thrombolysis, C57Bl6J mice were treated with ferric chloride ($FeCl_3$) to cause occlusion of the distal middle cerebral artery[30]. Mice were kept under anesthesia with 1.5 % isoflurane in a nitrous oxide/oxygen mixture via facemask. The body temperature was monitored by a rectal probe and maintained at 37±0.3°C by a homoeothermic blanket control unit. Briefly, mice were placed in a stereotaxic frame, the scalp was opened and right temporal muscle was dissected. The area between zygomatic arch and squamous bone was thinned by a high-speed drill and cooled with saline. The trace of MCA was visualized and thin bony film was lifted up by forceps. After that a laser-Doppler flowmetry probe was placed 2 mm posterior, 6 mm lateral to the bregma to monitor the regional cerebral blood flow (rCBF). After obtaining a stable epoch of the pre-ischemic rCBF, a piece of 10 % $FeCl_3$ saturated filter paper was placed over the intact dura mater along the trace of MCA and the rCBF was continuously monitored during the next 3 hours. After 2 hours of ischemia, either 50 mg/kg LOXBlock-1, or DMSO vehicle was injected intraperitoneally. Then intravenous tPA (10 mg/kg, Activase®, Genentech Inc.) was administered in 20 minutes. Neurological deficit was rated by using modified neurological severity score 24 hours after ischemia.

Mice were sacrificed following cardiac perfusion with saline 24 hours after ischemia. Brains were removed and photographed, and then tissues were immersed in 4% paraformaldehyde overnight. Cryoprotection was obtained with 15% and 30% sucrose solutions at 4 °C. 20 μm thick frozen coronal sections were taken. After hydrating with PBS for 5 min, sections were incubated in diaminobenzidine

(DAB) staining solution (Vector, USA) for 15 min and washed with PBS for 5 min. in the presence of hemoglobin, hydrogen peroxide oxidizes DAB and it gives a dark-brown color. DAB specifically marks hemorrhage area and non-hemorrhagic areas are not stained[31, 32]. Nissl staining was used to see background. For this purpose 0.5 % cresyl violet in 0.1% acetic acid solution was applied for 2 minutes and sections were washed with water. Then dehydration was obtained by 70 %, 95 % and 100 % alcohol for 30 sec in each and xylene was used for immersion. The border of each DAB stained area was drawn by using NIH Image J and hemorrhage area (mm2) was calculated by a summation of them.

For distal MCAO experiments 8 mice were used (n=4/group). There was no significant difference in ischemia and reperfusion levels between groups. In vehicle treated group rCBF drop was 30 ± 2 % and reperfusion rate was 74 ± 15 % and in the LOXBlock-1 treated group, ischemia rate was 26 ± 6 % and reperfusion rate was 79 ± 19 %. Hemorrhage area was significantly higher in vehicle treated group (2.2 ± 0.4 mm^2) comparing to LOXBlock-1 treated group (0.4 ± 0.1 mm^2) ($p<0.05$). The vehicle treated group showed a more severe neurological deficit than the LOXBlock-1 group, but the difference was only borderline significant (not shown; $p=0.05$).

2.2.15 Human brain tissue samples

A 59 year old male with a history of hypertension and diabetes mellitus type II, who suffered an acute ischemic stroke, due to a severe right carotid stenosis (atherothrombotic stroke) was included in the study[33]. CT scan showed an infarct in the territory of the right Middle Cerebral Artery. The patient did not receive

tPA and died 87 hours after stroke onset. It took 4 h from death to the necropsic study (post-mortem). On autopsy and during macroscopic examination, morphological features and last available neuroimages were used to guide brain tissue sampling from ischemic ipsilateral, or from contralateral hemisphere. Infarcted area was delineated by an experienced neuropathologist (mainly through the consistence and colour of the parenchyma) and 1 cm^3 of the contiguous tissue was obtained as peri-infarct, which was confirmed by histopathological microscopic examination. Histological examination showed severe ischemic necrosis in the whole MCA territory, with extensive neuronal necrosis and no signs of neurodegenerative disease. The second patient was a 77 year old female with probable atrial fibrillation, presenting with ischemic stroke affecting the left MCA. This patient developed hemorrhagic transformation following thrombolytic treatment, and died 77 hours after stroke onset. Samples for immunohistochemistry were immediately fixed with 4% paraformaldehyde and kept at -80ºC until use. This study was approved by the Ethics Committee of the Hospital Vall d'Hebron [PR(HG)85/04]. Informed consent was acquired from relatives prior to the autopsy.

2.2.16 Statistical analysis

For parametric and continuously variable measurements, we used ANOVA followed by Tukey-Kramer posthoc tests. For nonparametric ordinal data (e.g. functional outcomes), we used non-parametric Kruskal-Wallis followed by post-hoc Mann-Whitney tests. P values less than 0.05 were considered significant.

2.3 Results

Dose-ranging studies showed that 200 nM LOXBlock-1, which itself lacks antioxidant activity[16], protected HT22 neuronal cells against oxidative glutamate toxicity (**Figure 2.1A**). Correspondingly, glutamate-induced elevation of the 12/15-LOX metabolite 12-hydroxyeicosatetraenoic acid (12-HETE) was also significantly suppressed by LOXBlock-1 (**Figure 2.1B**). Two major iron-dependent pathways counteracting oxidative stress are mediated by NRF2 and HIF1a, and many traditional LOX inhibitors act by iron chelation. To rule out that LOXBlock-1 protected HT22 cells by activating these pathways, we used cell-based reporter assays[19, 20]. Neither NRF2 nor HIF1α were significantly activated (**Figure 2.1C** and **D**, respectively), suggesting that neuroprotection in our HT22 experiments was specific to the 12/15-LOX pathway.

Biochemical effects of 12/15-LOX were next examined in vivo. The brains of mice were analyzed at 12 or 24 hours after 60 minutes transient focal cerebral ischemia. 12/15-LOX activity was measured by assaying 12-HETE by enzyme immunoassay, which showed a marked increase in the ipsilateral brain at 12 and 24 hours post-ischemia (**Figure 2.1E**). The identity of 12-HETE was confirmed by HPLC and mass spectrometry (**Figure 2.1F**). At 24 hours, immunostaining with antibody MDA2[24, 34] detected an increase in malondialdehyde-conjugated lysine in cells of the ischemic peri-infarct area, which were also 12/15-LOX positive (Figure 1G). Malondialdehyde is a breakdown product formed by oxidation of arachidonic acid, a substrate for 12/15-LOX.

To determine if these results are relevant to human stroke, we performed immunostaining with the 12/15-LOX and MDA2 antibodies. Cell-specific staining for both antigens was detected in the penumbra surrounding the core infarct, but not on the contralateral side of the brain (**Figure 2.2A**). Higher magnification of the ipsilateral staining pattern and overlay with a nuclear stain again showed colocalization of 12/15-LOX with the MDA2 epitope (**Figure 2.2B**). In a second patient, we combined 12/15-LOX staining with an antibody to apoptosis-inducing factor AIF, which showed both antigens increased in the peri-infarct region of the brain, compared to the contralateral side (**Figure 2.2C**). The staining pattern closely resembles that found in our previously published mouse experiments, where both 12/15-LOX and AIF were also increased coincidentally in the peri-infarct region[23].

Consistent with a damaging role for increased 12/15-LOX activity, intraperitoneal administration of the 12/15-LOX inhibitor LOXBlock-1 significantly reduced infarct size 24 hours after focal cerebral ischemia (**Figure 2.3A**). Showing specificity, LOXBlock-1 also reduced the amount of 12-HETE in the ischemic hemisphere (**Figure 2.3B**). Neuroprotection was sustained long-term. Even 14 days post-ischemia, LOXBlock-1-treated mice still had significantly smaller infarct sizes compared to vehicle controls (**Figure 2.3C**). Behavioral testing supported this result, with LOXBlock-1 treated mice showing a reduced Neurological Severity Score in the acute phase, and returning towards pre-injury baseline in the Corner Test by Day 14, while vehicle-treated mice retained a significant deficit (**Supplementary Figure 1**).

A major issue for any acute phase stroke therapy is until what time after stroke onset treatment will provide a benefit. LOXBlock-1 proved to still protect when given 4 hours after induction of ischemia, and even at 6 hours still showed a trend towards protection, although this was not statistically significant (**Figure 2.3D**).

In a safety study, we tested the effects of LOXBlock-1 in a mouse model of collagenase-induced hemorrhage. LOXBlock-1 did not alter hematoma volumes (**Figure 2.3E**) or worsen neurological outcomes (**Supplementary Figure 2**), suggesting it does not increase hemorrhagic injury to the brain.

Finally, we investigated the effects of LOXBlock-1 when combined with tPA in a model of tPA-associated hemorrhagic transformation. Intravenous administration of tPA two hours after onset of clotting allowed for efficient reperfusion (not shown), but led to hemorrhage in C57Bl6J mice. This was significantly reduced by intraperitoneal injection of LOXBlock-1 (**Figures 2.3F and G**), demonstrating that 12/15-LOX inhibition may provide benefits when co-administered with tPA.

2.4 Discussion

Our main findings are that 12/15-LOX inhibition by LOXBlock-1 efficiently protected against oxidative stress-related cell death, both in neuronal HT22 cells, and in mouse models of transient focal ischemia. In an established mouse model of stroke, 12/15-LOX activity was increased. 50 mg/kg LOXBlock-1 was sufficient to reduce elevated 12-HETE in the ischemic brain, and to provide long-lasting protection against ischemic stroke. Furthermore, LOXBlock-1 still protected when administered 4 hours, possibly even six hours after onset of ischemia. Importantly, LOXBlock-1

did not have adverse effects in a mouse hemorrhage model, and actually reduced hemorrhage associated with tPA administration. Because increased 12/15-LOX was also detected in the peri-infarct region of a human stroke victim, these results may translate well to human stroke.

Glutathione depletion in HT22 cells is an established cell culture model of oxidative stress-related toxicity. Cell death in these cells, as in immature primary cortical neurons and in primary oligodendrocytic cells, depends on 12/15-LOX[15, 16, 35-38]. The effective concentration for half-maximal rescue of HT22 cells by LOXBlock-1 (EC$_{50}$) was around 300 nM, suggesting reasonable efficacy for an enzyme inhibitor. Release of 12-HETE into the culture medium is presumably not part of the death mechanism; addition of exogenous 12-HETE does not affect viability of HT22 cells[17]. Instead, an intracellular mechanism of lipid peroxidation in endoplasmic reticulum and mitochondria, followed by translocation of apoptosis-inducing factor AIF to the nucleus likely kills the cell[23]. Nevertheless, the detection of 12-HETE provides a good readout for 12/15-LOX inhibition both in cell culture, and in the ischemic brain. Here, the decrease of 12-HETE in the ischemic hemisphere of LOXBlock-1 treated mice suggests that the inhibitor reaches its target in the brain. 12-HETE was still elevated 24 hours after MCAO, and a recent biomarker study found increased HETE levels up until 7 days in the plasma of stroke patients[39], suggesting that lipoxygenase inhibition may be beneficial even at relatively late times of administration. From the initial studies identifying LOXBlock-1[16, 40], we know that it also inhibits the human version of 12/15-LOX, termed 15-lipoxygenase-1. Our

case study shows increased 12/15-LOX after stroke in two human stroke cases as well (**Figure 2.2**). LOXBlock-1 may thus also protect against 12/15-LOX related brain damage in humans.

Because of its propensity to cause bleeding, tPA administration currently requires time-consuming imaging to rule out a hemorrhagic stroke. A drug that does not worsen hemorrhage could be given earlier, before advanced imaging by CT or MRI. While no current hemorrhage model can completely reflect the complexities of both intracerebral (ICH) and subarachnoid (SAH) hemorrhagic strokes, it is significant that LOXBlock-1 does not have adverse effects in the collagenase-induced hemorrhage model. Should this be confirmed, or LOXBlock-1 even provide a benefit to victims of ICH or SAH, this would raise the intriguing possibility of giving a neuroprotective drug already in the ambulance, or directly upon arrival in the hospital and initial stroke diagnosis.

A further possible use for 12/15-LOX inhibition may be as an adjuvant to tPA thrombolysis. As a first step to investigate this possibility, we used a mouse model of clot-induced distal MCAO. We found surprisingly high levels of hemorrhagic transformation when we reperfused after two hours using tPA, which in humans typically occurs when tPA is given at later time points. We used tPA at 10 mg/kg. This the standard dose for tPA in rodents, but tenfold higher than in humans, possibly explaining the difference in timing. Nevertheless, the striking finding here is that LOXBlock-1 administered at the same time as tPA can significantly reduce hemorrhage (**Figure 2.3 F-G**), suggesting that combining tPA with LOXBlock-1 may

be a useful therapeutic strategy. Further studies will be required to determine whether administration at the same time is required, and to find a suitable time window for this combination treatment.

In summary, we found increased 12/15-LOX activity following ischemia, and have tested a novel inhibitor of 12/15-LOX for its utility as a neuroprotectant in vitro, as well as in mouse models of transient focal ischemia. The robust protection shown by LOXBlock-1 suggests it is a strong candidate for a successful acute phase stroke treatment.

Acknowledgements

2.5 Figures

Figure 2.1 LOXBlock-1 targets increased 12/15-LOX activity in oxidatively stressed neuronal cells, and 12/15-LOX activity is increased in the ischemic brain. **A)** Neuronal HT22 cells are protected against oxidative glutamate toxicity by nanomolar levels of LOXBlock-1 (***$p<0.001$). **B)** 5 µM LOXBlock-1 brings increased levels of 12-HETE in the medium back down to baseline (**$p<0.01$ against control, or glutamate plus LOXBlock-1 treated cells). **C)** LOXBlock-1 (n) does not activate NRF2 in the Neh2-luc reporter assay (with tertiary butylhydroquinone (l) as positive control). **D)** Likewise, LOXBlock-1 (n) does not activate HIF1α in a HIF1 ODD-luc reporter assay (ciclopirox (m) as positive control). **E)** 12-HETE was significantly increased in the ipsilateral hemisphere both 12 and 24 hours after transient focal ischemia (*$p<0.05$, ***$p<0.001$; sham n=6 brains, 12hours n=3 brains, 24hours n=5 brains). **F)** The identity of 12-HETE was confirmed by HPLC/Mass Spectrometry analysis. The smaller peak for 15-HETE in the HPLC profile (top panel) is also a 12/15-LOX product. **G)** 24h after transient focal ischemia, LOX co-localizes with a marker for malondialdehyde-modified proteins, MDA2 in the peri-infarct cortex. Nuclei appear as blue stain (To-Pro-3) in the merged picture; scale bar = 20 µm
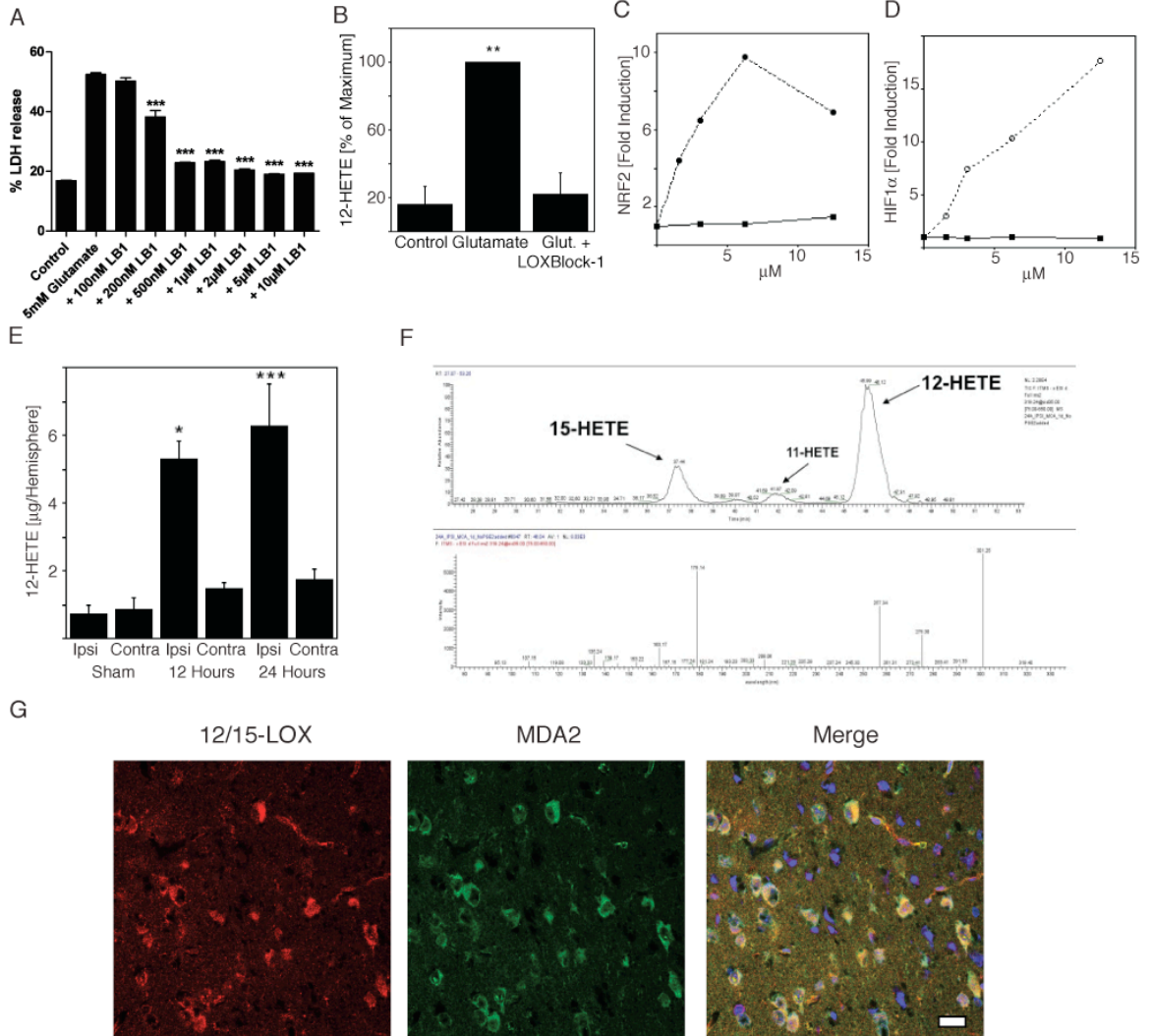
Figure 2.1

Figure 2.2 12/15-LOX co-localizes with the oxidative stress marker MDA2 in the infarcted human brain. **A)** 12/15-LOX is increased in the peri-infarct region of a human brain 87 hours after an ischemic stroke, compared to the contralateral side (scale bar 50 nm). **B)** Co-localization of 12/15-LOX in the peri-infarct area with MDA2, merged with nuclear stain To-Pro-3 (scale bar 20 nm). **C)** In a second human brain, 12/15-LOX co-localizes with AIF, and both are clearly increased on the infarcted vs the contralateral side (scale bar 20 nm).

Figure 2.2

A

Ipsilateral   Contralateral

12/15-LOX

MDA2

B

12/15-LOX   MDA2   Merge

C

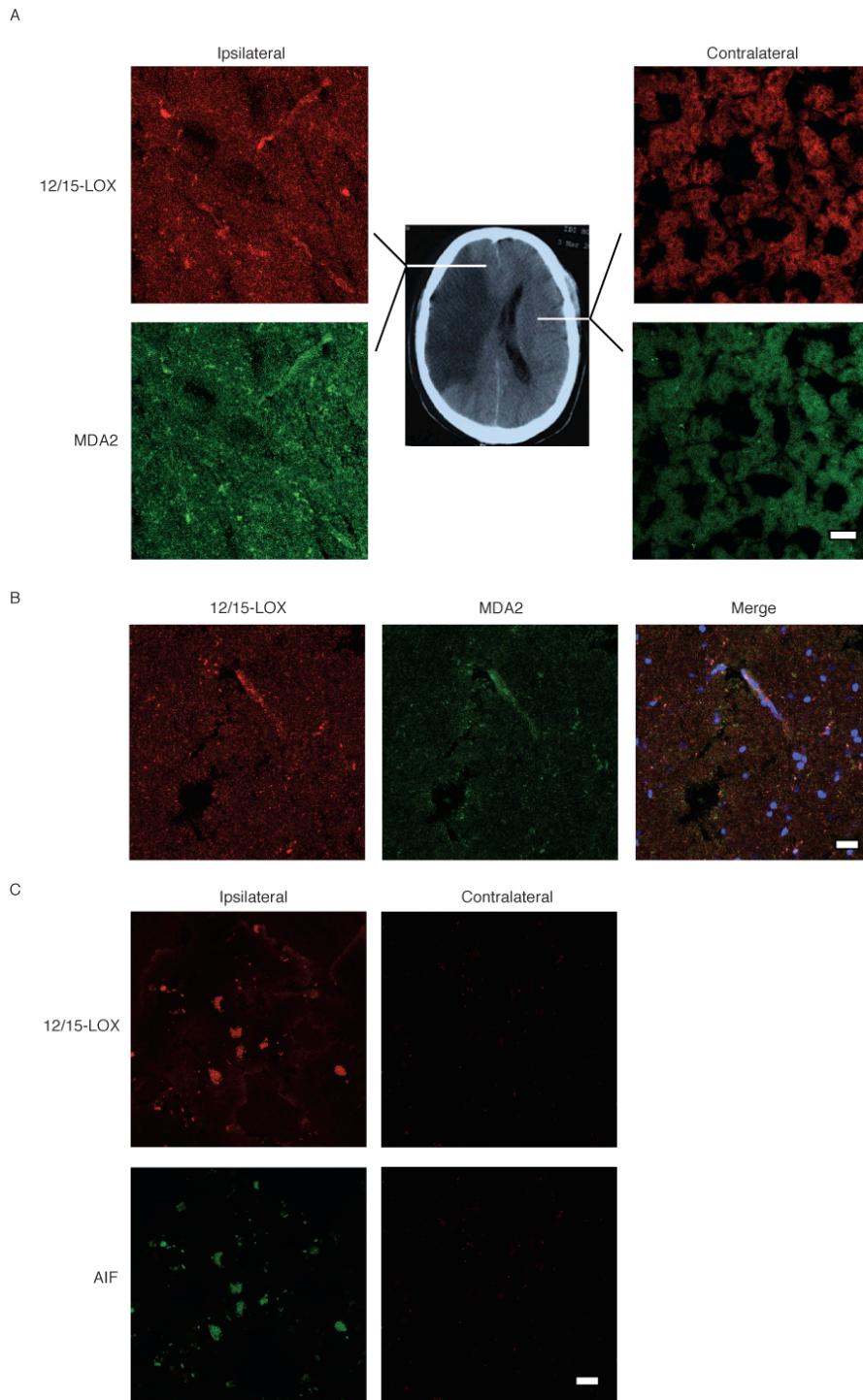Ipsilateral   Contralateral

12/15-LOX

AIF

Figure 2.3 LOXBlock-1 efficiently protects against transient focal ischemia in mice, and does not worsen outcome after hemorrhage. **A)** Treatment with 50 mg/kg LOXBlock-1 significantly reduced infarct size 24 hours after 90 minutes of MCAO (**$p<0.01$; n=12 per group). **B)** Levels of 12-HETE were lower in the ischemic brain hemisphere of LOXBlock-1 treated mice (n=11 for vehicle, n=10 for LOXBlock-1). **C)** Infarct sizes remained smaller 14 days after MCAO (**$p<0.01$; n=12 per group). **D)** Delayed administration of LOXBlock-1 retains efficacy against MCAO-induced brain injury (**$p<0.01$ at 2 hours with n=8 per group; *$p<0.05$ at 4 hours). **E)** Hemorrhage volume after collagenase administration was not increased by LOXBlock-1 (n=7 per group). **F)** Following tPA thrombolysis in an embolic clot model, vehicle-treated mice exhibit brain hemorrhage, which is reduced by LOXBlock-1 treatment. **G)** Quantitative evaluation of DAB-stained brain sections confirms a significant reduction in hemorrhage by treatment with LOXBlock-1 (**$p<0.01$).

Figure 2.3
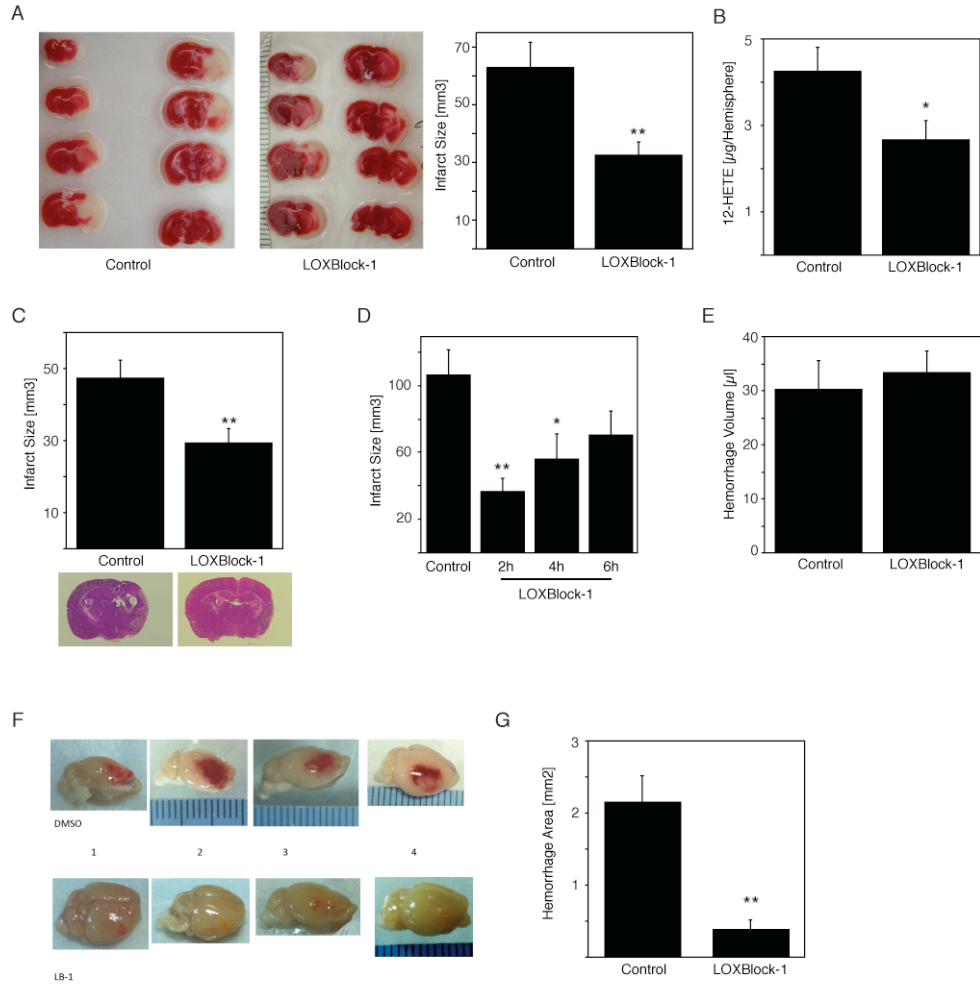
2.6 Supplementary Figures

Supplementary Figure 1

Behavioral tests in the long-term outcome study show protection by LOXBlock-1 in the MCAO model. **A)** To determine the acute severity of brain injury in this model, we used a standard ten point Neurological Severity Score. 24 hours after MCAO, LOXBlock-1 treated mice show significantly reduced injury (**$p<0.01$ compared to vehicle-treated). **B)** To gauge long-term recovery, we used an established Corner Test. Mice initially have a strong preference for right-hand turns following MCAO, which becomes less pronounced over time. In our experiment, vehicle treated mice retained a significant deficit after 14 days (*$p<0.05$ compared to pre-injury baseline), while LOXBlock-1 treated mice were not significantly different from the pre-injury baseline (n.s. = non-significant).
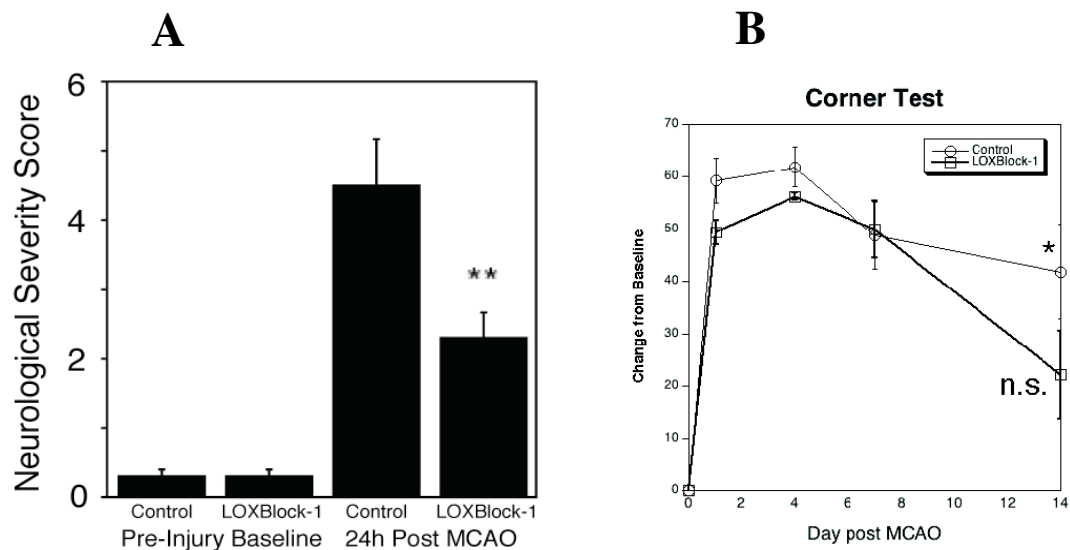
Supplementary Figure 2:

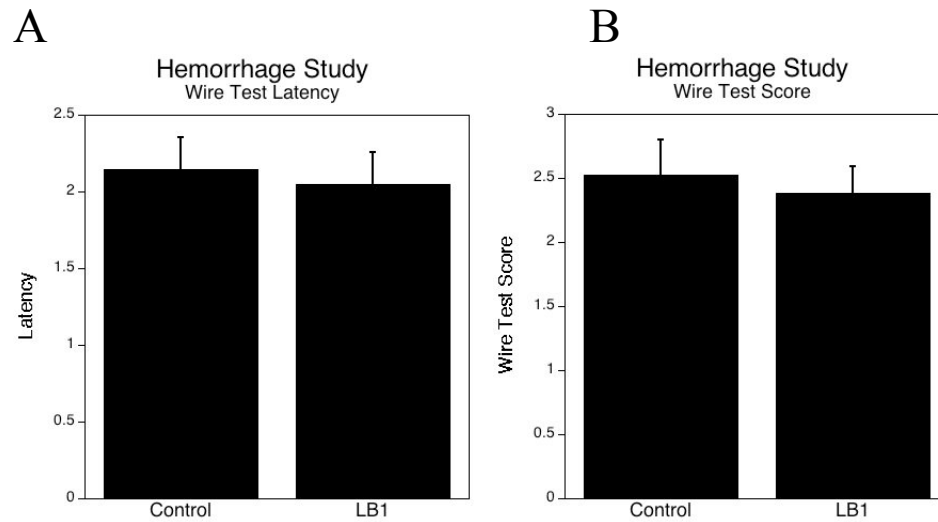LOXBlock-1 does not worsen behavioral outcome following hemorrhagic injury. Neither latency **(A)**, nor score **(B)** in a hanging wire test were adversely affected by LOXBlock-1 treatment. No significant differences were found between groups.

2.7 References:

1. Investigators., C. A. S. P. R. C. (2005) Prioritizing interventions to improve rates of thrombolysis for ischemic stroke, *Neurology 64*, 654-659.

2. Roger, V. L., Go, A. S., Lloyd-Jones, D. M., Adams, R. J., Berry, J. D., Brown, T. M., Carnethon, M. R., Dai, S., de Simone, G., Ford, E. S., Fox, C. S., Fullerton, H. J., Gillespie, C., Greenlund, K. J., Hailpern, S. M., Heit, J. A., Ho, P. M., Howard, V. J., Kissela, B. M., Kittner, S. J., Lackland, D. T., Lichtman, J. H., Lisabeth, L. D., Makuc, D. M., Marcus, G. M., Marelli, A., Matchar, D. B., McDermott, M. M., Meigs, J. B., Moy, C. S., Mozaffarian, D., Mussolino, M. E., Nichol, G., Paynter, N. P., Rosamond, W. D., Sorlie, P. D., Stafford, R. S., Turan, T. N., Turner, M. B., Wong, N. D., and Wylie-Rosett, J. (2011) Heart disease and stroke statistics--2011 update: a report from the American Heart Association, *Circulation 123*, e18-e209.

3. Moskowitz, M. A., Lo, E. H., and Iadecola, C. (2010) The science of stroke: mechanisms in search of treatments, *Neuron 67*, 181-198.

4. Niizuma, K., Endo, H., and Chan, P. H. (2009) Oxidative stress and mitochondrial dysfunction as determinants of ischemic neuronal death and survival, *J Neurochem 109 Suppl 1*, 133-138.

5. Saito, A., Maier, C. M., Narasimhan, P., Nishi, T., Song, Y. S., Yu, F., Liu, J., Lee, Y. S., Nito, C., Kamada, H., Dodd, R. L., Hsieh, L. B., Hassid, B., Kim, E. E., Gonzalez, M., and Chan, P. H. (2005) Oxidative stress and neuronal death/survival signaling in cerebral ischemia, *Mol Neurobiol 31*, 105-116.

6. Hardingham, G. E., and Lipton, S. A. (2011) Regulation of neuronal oxidative and nitrosative stress by endogenous protective pathways and disease processes, *Antioxid Redox Signal 14*, 1421-1424.

7. Jin, G., Arai, K., Murata, Y., Wang, S., Stins, M. F., Lo, E. H., and van Leyen, K. (2008) Protecting against cerebrovascular injury: contributions of 12/15-lipoxygenase to edema formation after transient focal ischemia, *Stroke 39*, 2538-2543.

8.   van Leyen, K., Kim, H. Y., Lee, S. R., Jin, G., Arai, K., and Lo, E. H. (2006) Baicalein and 12/15-lipoxygenase in the ischemic brain, *Stroke; a journal of cerebral circulation 37*, 3014-3018.

9.   Khanna, S., Roy, S., Slivka, A., Craft, T. K., Chaki, S., Rink, C., Notestine, M. A., DeVries, A. C., Parinandi, N. L., and Sen, C. K. (2005) Neuroprotective properties of the natural vitamin E alpha-tocotrienol, *Stroke; a journal of cerebral circulation 36*, 2258-2264.

10.   Cui, L., Zhang, X., Yang, R., Liu, L., Wang, L., Li, M., and Du, W. (2010) Baicalein is neuroprotective in rat MCAO model: role of 12/15-lipoxygenase, mitogen-activated protein kinase and cytosolic phospholipase A2, *Pharmacology, biochemistry, and behavior 96*, 469-475.

11.   Zhou, Y., Fang, S. H., Ye, Y. L., Chu, L. S., Zhang, W. P., Wang, M. L., and Wei, E. Q. (2006) Caffeic acid ameliorates early and delayed brain injuries after focal cerebral ischemia in rats, *Acta Pharmacol Sin 27*, 1103-1110.

12.   Munsiff, A. V., Chander, P. N., Levine, S., and Stier, C. T., Jr. (1992) The lipoxygenase inhibitor phenidone protects against proteinuria and stroke in stroke-prone spontaneously hypertensive rats, *Am J Hypertens 5*, 56-63.

13.   Nishi, H., Watanabe, T., Sakurai, H., Yuki, S., and Ishibashi, A. (1989) Effect of MCI-186 on brain edema in rats, *Stroke; a journal of cerebral circulation 20*, 1236-1240.

14.   Abe, K., Yuki, S., and Kogure, K. (1988) Strong attenuation of ischemic and postischemic brain edema in rats by a novel free radical scavenger, *Stroke; a journal of cerebral circulation 19*, 480-485.

15.   Lapchak, P. A., Maher, P., Schubert, D., and Zivin, J. A. (2007) Baicalein, an antioxidant 12/15-lipoxygenase inhibitor improves clinical rating scores following multiple infarct embolic strokes, *Neuroscience 150*, 585-591.

16.   van Leyen, K., Arai, K., Jin, G., Kenyon, V., Gerstner, B., Rosenberg, P. A., Holman, T. R., and Lo, E. H. (2008) Novel lipoxygenase inhibitors as neuroprotective reagents, *J Neurosci Res 86*, 904-909.

17.   Pallast, S., Arai, K., Wang, X., Lo, E. H., and van Leyen, K. (2009) 12/15-Lipoxygenase targets neuronal mitochondria under oxidative stress, *J Neurochem 111*, 882-889.

18.   van Leyen, K., Siddiq, A., Ratan, R. R., and Lo, E. H. (2005) Proteasome inhibition protects HT22 neuronal cells from oxidative glutamate toxicity, *Journal of neurochemistry 92*, 824-830.

19.   Smirnova, N. A., Haskew-Layton, R. E., Basso, M., Hushpulian, D. M., Payappilly, J. B., Speer, R. E., Ahn, Y. H., Rakhman, I., Cole, P. A., Pinto, J. T., Ratan, R. R., and Gazaryan, I. G. (2011) Development of neh2-luciferase reporter and its application for high throughput screening and real-time monitoring of nrf2 activators, *Chem Biol 18*, 752-765.

20.   Smirnova, N. A., Rakhman, I., Moroz, N., Basso, M., Payappilly, J., Kazakov, S., Hernandez-Guzman, F., Gaisina, I. N., Kozikowski, A. P., Ratan, R. R., and Gazaryan, I. G. (2010) Utilization of an in vivo reporter for high throughput identification of branched small molecule regulators of hypoxic adaptation, *Chem Biol 17*, 380-391.

21.   Kim, H. Y., and Sawazaki, S. (1993) Structural analysis of hydroxy fatty acids by thermospray liquid chromatography/tandem mass spectrometry, *Biol Mass Spectrom 22*, 302-310.

22.   The LIPID MAPS–Nature Lipidomics Gateway, http://www.lipidmaps.org.

23.   Pallast, S., Arai, K., Pekcec, A., Yigitkanli, K., Yu, Z., Wang, X., Lo, E. H., and van Leyen, K. (2010) Increased nuclear apoptosis-inducing factor after transient focal ischemia: a 12/15-lipoxygenase-dependent organelle damage pathway, *J Cereb Blood Flow Metab 30*, 1157-1167.

24.   Palinski, W., Yla-Herttuala, S., Rosenfeld, M. E., Butler, S. W., Socher, S. A., Parthasarathy, S., Curtiss, L. K., and Witztum, J. L. (1990) Antisera and monoclonal antibodies specific for epitopes generated during oxidative modification of low density lipoprotein, *Arteriosclerosis 10*, 325-335.

25.   Yla-Herttuala, S., Rosenfeld, M. E., Parthasarathy, S., Glass, C. K., Sigal, E., Witztum, J. L., and Steinberg, D. (1990) Colocalization of 15-lipoxygenase

mRNA and protein with epitopes of oxidized low density lipoprotein in macrophage-rich areas of atherosclerotic lesions, *Proc Natl Acad Sci U S A 87*, 6959-6963.

26.   Chen, Y., Constantini, S., Trembovler, V., Weinstock, M., and Shohami, E. (1996) An experimental model of closed head injury in mice: pathophysiology, histopathology, and cognitive deficits, *J Neurotrauma 13*, 557-568.

27.   Zhang, L., Schallert, T., Zhang, Z. G., Jiang, Q., Arniego, P., Li, Q., Lu, M., and Chopp, M. (2002) A test for detecting long-term sensorimotor dysfunction in the mouse after focal cerebral ischemia, *J Neurosci Methods 117*, 207-214.

28.   Foerch, C., Arai, K., Jin, G., Park, K. P., Pallast, S., van Leyen, K., and Lo, E. H. (2008) Experimental model of warfarin-associated intracerebral hemorrhage, *Stroke 39*, 3397-3404.

29.   Wang, X., Liu, J., Zhu, H., Tejima, E., Tsuji, K., Murata, Y., Atochin, D. N., Huang, P. L., Zhang, C., and Lo, E. H. (2008) Effects of neuroglobin overexpression on acute brain injury and long-term outcomes after focal cerebral ischemia, *Stroke 39*, 1869-1874.

30.   Karatas, H., Erdener, S. E., Gursoy-Ozdemir, Y., Gurer, G., Soylemezoglu, F., Dunn, A. K., and Dalkara, T. (2011) Thrombotic distal middle cerebral artery occlusion produced by topical FeCl(3) application: a novel model suitable for intravital microscopy and thrombolysis studies, *Journal of cerebral blood flow and metabolism : official journal of the International Society of Cerebral Blood Flow and Metabolism 31*, 1452-1460.

31.   Garcia-Yebenes, I., Sobrado, M., Zarruk, J. G., Castellanos, M., Perez de la Ossa, N., Davalos, A., Serena, J., Lizasoain, I., and Moro, M. A. (2011) A mouse model of hemorrhagic transformation by delayed tissue plasminogen activator administration after in situ thromboembolic stroke, *Stroke 42*, 196-203.

32.   Wakisaka, Y., Chu, Y., Miller, J. D., Rosenberg, G. A., and Heistad, D. D. (2010) Spontaneous intracerebral hemorrhage during acute and chronic hypertension in mice, *J Cereb Blood Flow Metab 30*, 56-69.

33. Cuadrado, E., Rosell, A., Colome, N., Hernandez-Guillamon, M., Garcia-Berrocoso, T., Ribo, M., Alcazar, A., Ortega-Aznar, A., Salinas, M., Canals, F., and Montaner, J. (2010) The proteome of human brain after ischemic stroke, *J Neuropathol Exp Neurol 69*, 1105-1115.

34. Weismann, D., Hartvigsen, K., Lauer, N., Bennett, K. L., Scholl, H. P., Charbel Issa, P., Cano, M., Brandstatter, H., Tsimikas, S., Skerka, C., Superti-Furga, G., Handa, J. T., Zipfel, P. F., Witztum, J. L., and Binder, C. J. (2011) Complement factor H binds malondialdehyde epitopes and protects from oxidative stress, *Nature 478*, 76-81.

35. Li, Y., Maher, P., and Schubert, D. (1997) A role for 12-lipoxygenase in nerve cell death caused by glutathione depletion, *Neuron 19*, 453-463.

36. Khanna, S., Roy, S., Ryu, H., Bahadduri, P., Swaan, P. W., Ratan, R. R., and Sen, C. K. (2003) Molecular basis of vitamin E action: tocotrienol modulates 12-lipoxygenase, a key mediator of glutamate-induced neurodegeneration, *The Journal of biological chemistry 278*, 43508-43515.

37. Wang, H., Li, J., Follett, P. L., Zhang, Y., Cotanche, D. A., Jensen, F. E., Volpe, J. J., and Rosenberg, P. A. (2004) 12-Lipoxygenase plays a key role in cell death caused by glutathione depletion and arachidonic acid in rat oligodendrocytes, *Eur J Neurosci 20*, 2049-2058.

38. Zhang, Y., Wang, H., Li, J., Jimenez, D. A., Levitan, E. S., Aizenman, E., and Rosenberg, P. A. (2004) Peroxynitrite-induced neuronal apoptosis is mediated by intracellular zinc release and 12-lipoxygenase activation, *The Journal of neuroscience : the official journal of the Society for Neuroscience 24*, 10616-10627.

39. Seet, R. C., Lee, C. Y., Chan, B. P., Sharma, V. K., Teoh, H. L., Venketasubramanian, N., Lim, E. C., Chong, W. L., Looi, W. F., Huang, S. H., Ong, B. K., and Halliwell, B. (2011) Oxidative damage in ischemic stroke revealed using multiple biomarkers, *Stroke 42*, 2326-2329.

40. Kenyon, V., Chorny, I., Carvajal, W. J., Holman, T. R., and Jacobson, M. P. (2006) Novel human lipoxygenase inhibitors discovered using virtual screening with homology models, *J Med Chem 49*, 1356-1363.

Chapter 3

Potent and Selective Inhibitors of Human Reticulocyte 15- Lipoxygenase-1 as Anti-Stroke Therapies.

3.1 Introduction

Human Lipoxygenases (LOX) are non-heme, iron-containing enzymes, which catalyze the dioxygenation of 1,4-cis, cis-pentadiene-containing polyunsaturated fatty acids (e.g., linoleic acid (LA) and arachidonic acid (AA)) to form hydroperoxy-fatty acids.[1, 2] The nomenclature of the LOX isozymes is based on the carbon position (e.g. 5, 12 or 15) at which they oxidize arachidonic acid to form the corresponding hydroperoxyeicosatetraenic acid (HPETE),[3] which are reduced to the hydroxyeicosatetraenoic acid (HETE) by intracellular glutathione peroxidases.[4] Human lipoxygenases and their metabolites have been implicated in numerous diseases including inflammation, asthma, cancer, diabetes, thrombosis and neurodegenerative diseases.[5-10] 5-LOX has been implicated in cancer,[11] asthma,[12, 13] COPD,[14] allergic rhinitis,[15] osteoarthritis,[16, 17] and atherosclerosis.[18-20] Platelet-type 12-LOX, another important biomolecule, has been implicated in diabetes,[21, 22] blood coagulation,[23] psoriasis,[24] and cancer. [25, 26] Reticulocyte 15-lipoxygenase-1 (15-LOX-1, aka 12/15-LOX) has also emerged as an attractive therapeutic target by pharmaceutical industry, particularly for its role in atherogenesis.[5, 6] However, despite its promise as a therapeutic target, 15-LOX-1 is complicated by the fact that it has been implicated in both promoting [7, 9, 27] and inhibiting disease progression.[28-30] A more straightforward therapeutic benefit of a

15-LOX-1 inhibitor is minimizing the brain damage that occurs after an ischemic stroke event.[31, 32] One of the major traits of neuronal cell death after a stroke event is the accumulation of reactive oxygen species (ROS).[33-35] ROSs in turn activate 15-LOX-1 leading to the production of lipid hydroperoxides (such as HPETE) and exacerbate the oxidative stress conditions.[36-39] Interestingly, 15-LOX-1 is the only human LOX able to efficiently oxygenate the membrane bound, esterified polyenolic unsaturated fatty acids directly.[40-42] This suggests that overexpression of 15-LOX-1 not only contributes to neuronal damage indirectly through the production of HPETE, but also through direct oxidation of organelle membranes. As proof of principle, we demonstrated that a 15-LOX-1 knock-out (KO) mouse model resulted in a reduced infarct size of ~40%, compared to the wild-type.[43, 44] Moreover, several reports have shown via immunohistochemistry that 15-LOX-1 levels (aka 12/15-LOX) are increased in both neurons and endothelial cells following middle cerebral artery occlusion (MCAO, ischemic stroke).[43, 45] Consequently, these broad implications of 15-LOX-1 in stroke regulation emphasize the need for small molecule inhibitors, which effectively cross the blood brain barrier and target affected tissue. Our laboratory for the last 12 years,[46-52] and others,[53-56] have attempted to identify potent and selective 15-LOX-1 inhibitors, but with limited success. Unfortunately, many of these inhibitors are reductive and/or promiscuous polyphenolic/terpene based terrestrial natural products, such as boswellic acid (IC$_{50}$ = 1 μM),[57] nor-dihydroguaiaretic acid (NDGA) (IC$_{50}$ = 0.5 μM),[47] and baicalein (IC$_{50}$ = 2 μM)[51] as shown in **Figure 3.2**. Computational docking methods were used to identify novel,

80

non-reductive inhibitors, but the potency and selectivity of these compounds remained undesirable (**LOXBlock-1, Figure 3.2**).[31] The most drug-like 15-LOX-1 inhibitors that had been published prior to our investigations were those reported by researchers at Bristol-Myers Squibb (BMS) between 2005 and 2011. Their original publication in 2005 described the identification of tryptamine-based compounds (**37l**, **Figure 3.2**) which exhibited low nanomolar potency versus rabbit 15-LOX-1 and modest selectivity against both 5-hLO and 12-hLO, but they had generally unfavorable physical properties (solubility and Logp).[54] The same group later described the identification of imidazole-based compounds (**21n**, **Figure 3.2**)[55] and pyrazole-based compounds (**15i**, **Figure 3.2**),[53] with improved properties (e.g solubility), but these compounds still were reported to have unacceptable PK properties for use *in vivo*.

This lack of potent, selective and biologically active 15-LOX-1 inhibitors, inspired our initial effort to the discovery of **ML094** (**Figure 3.2**).[52] This probe compound was identified via quantitative high-throughput screen (qHTS) of 74,290 small molecules followed by medicinal chemistry optimization. While **ML094** was optimized for highly potent activity (14 nM) and selectivity, the loss of the terminal ester, a potential esterase substrate, resulted in a complete loss of activity. Moreover, we were unable to observe activity of **ML094** in a cellular context, which limited its biological utility.

As mentioned above, 15-LOX-1 has been implicated in stroke, which is the fourth-leading cause of death in the United States and the leading cause of

disability.[58, 59] However only tPA is an approved FDA treatment and is only used in less than 5% of stroke victims. Therefore, a potent, selective and biologically active inhibitor of 15-LOX-1 would be highly desirable to probe its role in stroke. Our previously discovered inhibitor, LOXBlock-1 (**Figure 3.2**), demonstrated good activity in mouse models for stroke however it is non-selective.[31] Moreover, these 2-amino-3-carbonyl thiophene derivatives are annotated as PAINS (pan assay interference compounds) for being "promiscuous, non-specific and reactive", which speaks to the need for the identification of other specific inhibitors to interrogate 15-LOX-1 biology *in vivo*. From our original HTS, we developed the 1,3,4-oxadiazole-2-thiol chemotype (**ML094, Figure 3.2**) as a selective and potent inhibitor against 15-LOX-1 (19 nM), however it was not active *in-vivo*.[52] We therefore re-screened the top hits from this HTS and discovered another novel scaffold that is chemically tractable and amenable to chemical modification at various positions of the molecule allowing for rapid exploration of the SAR profile. As such, in this investigation, we discuss the discovery, SAR and biological activity of a novel oxazole-4-carbonitrile core scaffold with nanomolar potency, selectivity over related eicosanoid producing enzymes.

3.2 Results and Discussion

3.2.1 Initial screening and optimization of novel chemotype

We previously screened a diverse collection of 74,290 compounds, utilizing a colorimetric method for detecting the LOX hydroperoxide product and uncovered numerous compounds with potency against 15-LOX-1.[52] **ML094**, from our previous

publication, was discovered from this batch of potent compounds but it had low therapeutic value due to its low *in-vivo* activity. Therefore, the remaining potent 15-LOX-1 inhibitors were screened in order to discover an inhibitor with better *in-vivo* activity and a novel oxazole-4-carbonitrile core scaffold discovered. Our initial round of analogues was focused around modification of our lead compound **1 (ML351)**, with the general synthesis is represented in **Figure 3.1**.

To investigate requirements for optimal 15-LOX-1 inhibition, we conducted detailed SAR analysis of the lead molecule as shown in **Tables 3.1-3.3** (analogs **1-40**). Initially, the 1-naphthyl group in the left side of the molecule was replaced with various aryl and heterocyclic groups as shown in **Table 3.1**. The bioisosteric replacement of 1-naphthyl with 2,3-dichlorophenyl (**7**) or 3,4-dichlorophenyl (**8**) groups showed comparable albeit slightly lower potencies (IC_{50} = 0.46 µM and 0.81 µM respectively vs. 0.20 µM for **1 aka ML351**). Replacement with 2-naphthyl group showed reduced potency (analog **2**, IC_{50} = 1.3 µM) compared to the 1-naphthyl substitution, which based on space-filling analysis, agreed with the findings we observed for dichloro analogs **7** and **8**. Several other modifications, including saturated rings or heterocyclic rings at this region (compounds **3-6** and **9-18**), also resulted in reduced potency. Thus, in general the 1-naphthyl group appeared to be optimal for maximal 15-LOX-1 inhibition as variations in size and electrostatics in this region were not well tolerated. Accordingly, the 1-naphthyl group was held constant while other regions of the molecule were explored for further SAR (**Tables 3.2 & 3.3**).

Having explored modifications to the 1-naphthyl moiety, our next focus was to explore modifications of the *N*-methyl side chain at the 5-position as shown in **Table 3.2** (analogs **19-31**). Removal of the methyl group, affording the primary amine, drastically reduced potency (analog **19**, IC_{50} = 25 µM) and di-methylation reduced potency as well, albeit less so (analog **20**, IC_{50} = 3.7 µM). Modifications of the methyl group with other alkyl substitutions, such as ethyl, *n*-propyl, *n*-butyl and *n*-pentyl groups, were tolerated (analogs **21-25**), with comparable or even improved potency being observed. However, replacing the methyl group with a branched alkyl group (analog **26**) or cycloalkyl groups (analogs **30-31**) significantly reduced the potency. Larger groups such as benzyl (compound **28**, IC_{50} = 5.6 µM) or phenyl substituted analogs (analog **29**, IC_{50} = 5.6 µM) also showed diminished 15-LOX-1 activity. Overall, these data suggested that the mono-alkylation with straight chain alkyl groups is critical for optimal 15-LOX-1 inhibition.

Finally, we turned our attention to optimization of the 1,3-oxazole core and its substitution pattern (**Table 3.3**). Replacing the 1,3-oxazole core with a 1,3-thiazole ring (analog **32**, IC_{50} = 0.55 µM) resulted in a two-fold decrease in potency. This could be partly attributed to the difference in size and hardness/softness of the sulfur and oxygen atoms in the thiazole and oxazole rings respectively. The diminished potency trend continued further with completely diminished activity for the pyridine (**39**, IC_{50} > 40 µM) and pyrimidine analogs (**40**, IC_{50} > 40 µM). Attempts to mimic the interaction of the oxazole core were unsuccessful with the *N*-methyl/oxadiazole derivative (analog **35**, IC_{50} > 40 µM) or the thiadiazole analog **36** (IC_{50} > 40 µM).

Interchanging the positions of the 1-naphthyl group and the -NHMe group (analogs **33-34**) led to complete loss of activity. In summary, this chemotype showed very tight SAR and our efforts to make several changes around the molecule resulted in similar or lower potency, with exception to analogs **21-23,** which showed marginally improved potency. Despite this improved potency of some of the synthesized analogs, analog **1** (**ML351**) was declared the probe because we had conducted more extensive biological studies on this compound and the added lipophilicity of compounds **21-23** would only decrease the already marginal aqueous solubility. The summary of the SAR results from the medicinal chemistry optimization is depicted in **Figure 3.3**.

3.2.2 Biological Evaluation of ML351

Given the results of our SAR investigations, which provided compounds with low nM potency against 15-LOX-1, we then determined the selectivity of a few of our top analogues against related human LOX isozymes (5-LOX, 12-LOX and 15-LOX-2). From the four 15-LOX-1 inhibitors tested, **ML351**, **7**, **8**, and **32**, all displayed excellent selectivity against all 3 isozymes (**Table 3.4**). We were encouraged by these findings because few compounds reported in the literature have achieved nM potency towards 15-LOX-1 while maintaining excellent selectivity towards other isozymes. Moreover, we investigated whether these analogs inhibited cyclooxygenase-1 (COX-1) and/or COX-2 and it was determined that none of them displayed inhibition (<10% at 15 μM). In summary, **ML351** demonstrates excellent selectivity toward a several related enzymes.

3.2.3 Mechanistic Investigations

As the LOX inhibitors are known to exhibit a variety of inhibitory mechanisms, different biochemical methods were used to assess the specific mechanism for this novel class of inhibitors. To investigate if the mechanism was reductive in nature, the UV-vis pseudoperoxidase activity assay was performed on four selected analogs and no degradation of the hydroperoxide product was observed at 234 nm, indicating a non-reductive inhibitory mechanism. Additionally, there was no elongation of enzymatic lag phase when these inhibitors were used, supporting a non-reductive inhibitory mechanism. To investigate nature of inhibition further, steady-state kinetics were performed using compound **ML351** by monitoring the formation of 15-HPETE as a function of substrate and inhibitor concentration in the presence of 0.01% Triton X-100. Replots of K_M/V_{max} and $1/V_{max}$ versus inhibitor concentration yielded linear plots (**Figure 3.4 and 3.5**), with K_i equaling 0.1 +/- 0.002 μM and $K_i^{'}$ equaling 1.2 +/- 0.02 μM. These parameters are defined as the equilibrium constants of dissociation from the catalytic (K_i) and secondary sites ($K_i^{'}$), respectively. The K_i is in good agreement with the IC_{50} value and due to the greater than 10-fold difference between K_i and K_i', we assume the secondary site to be the allosteric site,[60] which is consistent with our previous studies of 15-LOX-1 inhibition.[61]

3.2.4 *In vitro* ADME and *in vivo* PK profile

Our previously declared probe for 15-LOX-1 inhibition, **ML094**, demonstrated excellent potency and selectivity but lacked solubility, cell permeability

and microsomal stability ($T_{1/2}$ <2 mins). Moreover, this compound possessed an essential ester moiety that was susceptible to intracellular and plasma esterases rendering it inactive and thus limiting its utility in advanced biological models. Thus, we are encouraged by *in vitro* ADME (**Table 3.5**) and *in vivo* PK properties (**Table 3.6**) of **ML351**. This represents a vast improvement over the majority of compounds reported previously (*vide infra*). Despite the low molecular weight (249 Da), and favorable log D (pH 7.4) of 2.6 which was obtained by Analiza Inc. using their "scaled-down shake flask lipophilicity method", most analogs exhibited poor solubility. The aqueous kinetic solubility in PBS buffer was determined to be 1.2 µM, which is about 7 times the *in vitro* IC_{50}. Empirically, we did observe a vast improvement in the solubility in the 15-LOX assay buffer (data not shown), which was encouraging and suggests that solubility was not a detrimental factor in the biochemical studies. Importantly, the compound demonstrated favorable PAMPA permeability (passive) and acceptable Caco-2 permeability of >1 (1.5 cm/s^{-6}) with no evidence of efflux (efflux ratio: 0.7) suggesting the compound is not susceptible to the action of P-glycoprotein 1 (Pgp), a well-characterized ABC-transporter. Moreover, **ML351** was stable in various aqueous solutions (pH 2, pH 7.4, pH 9) and mouse plasma. In addition, **ML351** exhibited minimal CYP inhibition of the 2D6 and 3A4 isoforms at 10.3% and 3.5% inhibition respectively. Microsomal stability appears to be species dependent with **ML351** possessing moderate stability to rat liver microsomes (18 minutes) while being less stable to mouse liver microsomes (5.5 mins). The compounds were completely stable in the absence of NADPH, suggesting

a CYP-mediated degradation. Given our interest in testing compound **ML351** in proof of concept mouse models of stroke, we obtained *in vivo* PK data on **ML351** (**Table 3.6**) and found a suitable formulation for **ML351** (10% Solutol, 10% Cremophor EL, 20% PEG400 in saline). As anticipated from the microsomal stability studies, **ML351** has a relatively fast half-life in both plasma and brain ($T_{1/2}$ = ~ 1 h) with a C_{max} of 13.8 µM in plasma (69 times *in vitro* IC_{50}) and 28.8 µM in brain (144 times *in vitro* IC_{50}). Encouragingly, **ML351** has a brain/plasma ratio of 2.8 which demonstrates favorable BBB permeability and suggested that this compound was suitable for *in vivo* POC models of ischemic stroke (*vide infra*).

3.2.5 Cell Activity and *In vivo* efficacy

After having established the SAR profile and *in vitro* ADME/*in vivo* PK properties of **ML351,** we then sought to determine the efficacy in mouse models of ischemic stroke. However, before doing so we tested the ability of **ML351** to protect mouse HT-22 neuronal cells from glutamate-induced oxidative cell death. This cell-based assay has been previously shown to depend on glutathione depletion and subsequent activation of 12/15-LOX which leads to the production of peroxides, influx of Ca^{2+} and ultimately cell death.[62, 63] A point of clarification is that human reticulocyte 15-LOX-1 has also historically been called 12/15-LOX, due to its high sequence identity (78%) and similar reaction specificity with that of mouse leukocyte 12-LOX. Both proteins are products of the ALOX15 gene. Animal studies are further complicated by the differences in sequence homology between the human enzymes and the species of interest. Thus, given that our initial POC animal studies involve

mice we needed to determine the *in vitro* activity of **ML351** against mouse 12/15-LOX (m12/15-LOX) to ensure that we retained activity against the related enzyme. However, given that isolated recombinant m12/15-LOX is very difficult to work with, we used activity in mouse HT-22 neuronal cells as a surrogate. Thus, **ML351** was tested in the mouse HT-22 neuronal cell assay (**Figure 3.6B**), which monitors oxidative cell death after 12-LOX is induced with glutamate (5 mM) addition. It was found that **ML351** had an EC_{50} value of ~5 µM and that 10 µM of **ML351** was able to significantly reduce the 12/15-LOX product (12-HETE) in HT-22 cells, suggesting on target activity within the cell (**Figure 3.6A**). With the encouraging *in vitro* activity (HT-22 cells) and *in vivo* PK data in hand, we decided to progress **ML351** into *in vivo* efficacy models. For these initial studies we chose the permanent focal ischemia model in mice (**Figure 3.7 A, B**), which has been shown to mimic the pathophysiological mechanisms following ischemic injury.[64] The advantage of this model is that it does not inflict surgical trauma, and has a low mortality compared to other methods. The thrombosis event in the middle cerebral artery (MCA) is induced by topical application of $FeCl_3$ to the intact dura mater, leading to a cortical infarct. Laser Doppler flowmetry is used to monitor blood flow reduction and infarct size is measured following sacrifice at 24 hours by staining of 1 mm brain slice with 2,3,5-triphenylterazolium hydrochloride (TTC). For the initial POC studies, DMSO was used as the vehicle for direct comparison, since the van Leyen laboratory had previously used this formulation in the "LOXBlock-1" studies mentioned above. [31] However, we plan to utilize the more acceptable formulation (10% Solutol, 10%

Cremophor EL, 20% PEG400 in saline) for future *in vivo* efficacy studies of **ML351**. Gratifyingly, IP administration of **ML351** administered 2 hours after the induced ischemia resulted in a ~30% reduction in infarct size (p < 0.01) as shown in **Figure 3.7 B**. By comparison, the 12/15-LOX KO mouse resulted in a ~40% reduction in infarct size, suggesting the results for **ML351** are quite promising.

3.3 Conclusion

Our initial efforts to identify a stroke relevant 15-LOX-1 inhibitor (**ML094**) thru a HTS proved unsuccessful due to its inactivity in our mouse *ex vivo* model.[52] Fortunately, re-interrogation of the HTS data revealed a 15-LOX-1 inhibitor (**ML351**), with better "drug-like" properties and more importantly mouse *ex vivo* activity. Our initial medicinal chemistry efforts, described herein, provided important SAR to guide future investigations, but we were unable to significantly improve potency and the tolerability for the structural changes are limited. The most significant loss of inhibition was observed at the 1-naphthyl position, where almost all substitutions resulted in significant loss in activity with the exception of its bio-isosteric dichloro analogs (analog **7** and **8**), that only showed a slight decrease in activity. Modifications of the methyl group on the N-methyl side chain were not well tolerated either, indicating the straight chain, mono alkylated amine was critical for potency. Moreover, the only substitution tolerated for 1,3 oxazole core ring was the replacement with a 1,3 diazole (analog **32**), which resulted in a two fold decrease in the potency. The cyanide group on the oxazole core was found to be essential, with modifications completely abolishing activity. With these modifications, the SAR

90

profile of the **ML351** chemotype was developed and 3 more analogs (**7**,**8** and **32**) were selected for further biochemical studies and mechanistic investigation. 5-LOX, 12-LOX, 15-LOX-2, COX-1 and COX-2 were not inhibited by this chemotype. Most importantly, **ML351** is active in both mouse neuronal cells (HT22) and in reducing the infarct size of stroke-induced mice. This later result is significant since **ML351** is the first human 15-LOX-1 inhibitor that is not active against human 12-LOX but against mouse 12/15-LOX, as seen by its effectiveness in our mouse stroke model. This is an unusual quality of **ML351** since it was previously determined that human 12-LOX inhibitors were more likely to inhibit mouse 12/15-LOX than human 15-LOX-1 inhibitors. This is most likely due a greater similarity between the active sites of human 12-LOX and mouse 12/15-LOX, as seen by the preference of both LOX isozymes to produce 12-HpETE. This critical quality of **ML351** is significant because it maintains the human LOX selectivity, which is beneficial to a human therapeutic, but is also functional in a mouse stroke model, which is critical to developing its biological efficacy.

3.4 Experimental Section

3.4.1 General Methods for Chemistry

All air or moisture sensitive reactions were performed under positive pressure of nitrogen with oven-dried glassware. Anhydrous solvents such as dichloromethane, *N,N*-dimethylforamide (DMF), acetonitrile, methanol and triethylamine were purchased from Sigma-Aldrich. Preparative purification was performed on a Waters semi-preparative HPLC system. The column used was a Phenomenex Luna C18 (5

micron, 30 x 75 mm) at a flow rate of 45 mL/min. The mobile phase consisted of acetonitrile and water (each containing 0.1% trifluoroacetic acid). A gradient of 10% to 50% acetonitrile over 8 minutes was used during the purification. Fraction collection was triggered by UV detection (220 nm). Analytical analysis was performed on an Agilent LC/MS (Agilent Technologies, Santa Clara, CA). Method 1: A 7 minute gradient of 4% to 100% Acetonitrile (containing 0.025% trifluoroacetic acid) in water (containing 0.05% trifluoroacetic acid) was used with an 8 minute run time at a flow rate of 1 mL/min. A Phenomenex Luna C18 column (3 micron, 3 x 75 mm) was used at a temperature of 50 °C. Method 2: A 3 minute gradient of 4% to 100% Acetonitrile (containing 0.025% trifluoroacetic acid) in water (containing 0.05% trifluoroacetic acid) was used with a 4.5 minute run time at a flow rate of 1 mL/min. A Phenomenex Gemini Phenyl column (3 micron, 3 x 100 mm) was used at a temperature of 50 °C. Purity determination was performed using an Agilent Diode Array Detector for both Method 1 and Method 2. Mass determination was performed using an Agilent 6130 mass spectrometer with electrospray ionization in the positive mode. ^{1}H NMR spectra were recorded on Varian 400 MHz spectrometers. Chemical shifts are reported in ppm with undeuterated solvent (DMSO-d_6 at 2.49 ppm) as internal standard for DMSO-d_6 solutions. All of the analogs tested in the biological assays have purity greater than 95%, based on both analytical methods. High resolution mass spectrometry was recorded on Agilent 6210 Time-of-Flight LC/MS system. Confirmation of molecular formula was accomplished using electrospray ionization in the positive mode with the Agilent Masshunter software (version B.02).

3.4.2 General procedure for the formation of ML351 (Figure 3.1)

Step A: A mixture of 1-naphthoic acid (1.36 g, 7.90 mmol, 1 eq.) and 2-aminomalononitrile.TsOH (2.0 g, 7.90 mmol, 1 eq.) in ethyl acetate (15 mL) was added TEA (3.30 mL, 23.7 mmol, 3 eq.) followed by 50 % solution of propylphosphonic anhydride ($T_3P^®$) in ethyl acetate (12.56 g, 19.74 mmol, 2.5 eq.). The reaction was allowed to stir at room temperature for 12 h then diluted with ethyl acetate. The organic layer was successively washed with water, saturated bicarbonate solution, brine and dried with $MgSO_4$, and concentrated *in vacuo*. The crude product was purified on a biotage flash$^®$ system eluting with 50% ethyl acetate in hexanes containing 0.1 % triethylamine to provide a yellow solid: 2.2 g (Yield: 81%)

Step B: A mixture of 5-amino-2-(naphthalen-1-yl)oxazole-4-carbonitrile (0.42 g, 1.79 mmol, 1 eq.), paraformaldehyde (0.11 g, 3.57 mmol, 2 eq.) and sodium methoxide (0.096 g, 1.79 mmol, 1 eq.) in methanol (10 mL) was stirred at 65° C in for 3 h until a clear mixture was obtained. The reaction mixture was cooled and sodium borohydride (0.135 g, 3.57 mmol, 2 eq.) was added slowly and stirred further at room temperature for 1 h. The crude product was extracted with ethyl acetate and successively washed with water and brine. The ethyl acetate layer was dried with $MgSO_4$, and concentrated *in vacuo*. The crude product was purified on a biotage flash$^®$ system eluting with 30% ethyl acetate in hexanes containing 0.1 % triethylamine to provide of 5-(methylamino)-2-(naphthalen-1-yl)oxazole-4-carbonitrile (**ML351/NCGC00070329**) as a colorless solid: 0.12 g (Yield: 27 %).

ML351: *5-(methylamino)-2-(naphthalen-1-yl)oxazole-4-carbonitrile*

(**NCGC00070329**): LC-MS Retention Time: t_1 (Method 1) = 6.011 min and t_2 (Method 2) = 2.42 min; ^{1}H NMR (400 MHz, DMSO-d_6) δ 9.15 (dq, *J* = 8.7 and 0.9 Hz, 1H), 8.44 (brs, 1H), 8.10 − 7.99 (m, 3H), 7.74 − 7.57 (m, 3H), 3.07 − 3.01 (m, 3H).; ^{13}C NMR (400 MHz, DMSO-d_6) δ 161.9, 161.9, 149.5, 134.1, 134.0, 131.2, 129.2, 128.3, 127.2, 127.2, 127.0, 126.9, 125.8, 125.8, 125.8, 125.7, 122.1, 116.5, 116.5, 84.1, 84.1, 84.1, 29.7, 29.7, 29.6; HRMS (ESI) *m/z* (M+H)$^+$ calcd. for $C_{15}H_{12}N_3O$, 250.0975; found 250.0975.

(4-(8-Hydroxyquinolin-6-yl)phenyl)(piperazin-1-yl)methan-one

(NCGC00262513)**:** LC-MS Retention Time: t_1 (Method 1) = 1.905 min and t_2 (Method 2) = 3.048 min; ^{1}H NMR (400 MHz, DMSO-d_6) δ 9.11 (ddq, *J* = 8.7, 1.5, 0.7 Hz, 1H), 8.14 − 7.93 (m, 3H), 7.78 − 7.50 (m, 4H), 2.92 (dd, *J* = 4.9, 0.6 Hz, 3H), 2.50 (p, *J* = 1.9 Hz, 1H).; HRMS (ESI) *m/z* (M+H)$^+$ calcd. for $C_{13}H_{12}N_3O$, 226.0975; found 226.0976.

3-(4-Aminopiperidin-1-yl)-8-hydroxyquinoline-5-carboxylic acid

(NCGC00319032)**:** LC-MS Retention Time: t_1 (Method 1) = 2.814 min and t_2 (Method 2) = 3.756 min; ^{1}H NMR (400 MHz, DMSO-d_6) δ 8.88 (ddt, *J* = 8.5, 1.4, 0.8 Hz, 1H), 8.17 (q, *J* = 4.7 Hz, 1H), 8.07 − 7.98 (m, 2H), 7.77 (dd, *J* = 7.2, 1.2 Hz, 1H), 7.71 − 7.53 (m, 3H), 3.01 (d, *J* = 4.7 Hz, 3H); HRMS (ESI) *m/z* (M+H)$^+$ calcd. for $C_{15}H_{12}N_3S$, 266.0754; found 266.0746.

(3-(8-Hydroxyquinolin-6-yl)phenyl)(4-methylpiperazin-1-yl)methanone

(NCGC00263290)**:** LC-MS Retention Time: t_1 (Method 1) = 1.803 min and t_2

(Method 2) = 2.759 min; ^{1}H NMR (400 MHz, DMSO-d_6) δ 8.45 (d, J = 5.2 Hz, 1H), 8.25 (m, 1H), 8.04 (ddd, J = 15.4, 7.7, 2.2 Hz, 2H), 7.71 – 7.51 (m, 4H), 6.92 (d, J = 5.2 Hz, 1H), 2.88 (s, 3H); HRMS (ESI) m/z (M+H)$^+$ calcd. for $C_{15}H_{14}N_3$, 236.1189; found 236.1182.

3-(8-Hydroxyquinolin-6-yl)-N-(3-(piperazin-1-yl)-   propyl)benzamide (NCGC00263300): LC-MS Retention Time: t_1 (Method 1) = 6.895 min and t_2 (Method 2) = 3.909 min; ^{1}H NMR (400 MHz, DMSO-d_6) ^{1}H NMR (400 MHz, DMSO-d_6) δ 9.18 – 9.11 (m, 1H), 8.57 (t, J = 5.9 Hz, 1H), 8.10 – 7.99 (m, 3H), 7.74 – 7.58 (m, 3H), 3.45 – 3.38 (m, 2H), 1.68 – 1.56 (m, 2H), 1.48 – 1.33 (m, 2H), 0.94 (t, J = 7.4 Hz, 3H); HRMS (ESI) m/z (M+H)$^+$ calcd. for $C_{18}H_{18}N_3O$, 292.1444; found 292.1453.

***N*-(3-(dimethylamino)propyl)-4-(8-hydroxyquinolin-3-yl)benzamide (NCGC00263283):** LC-MS Retention Time: t_1 (Method 1) = 2.975 min and t_2 (Method 2) = 3.857 min; ^{1}H NMR (400 MHz, DMSO-d_6) ^{1}H NMR (400 MHz, DMSO-d_6) δ 9.14 (t, J = 6.2 Hz, 1H), 9.10 – 9.04 (m, 1H), 8.10 – 7.96 (m, 3H), 7.71 – 7.54 (m, 3H), 7.49 – 7.35 (m, 4H), 7.34 – 7.25 (m, 1H), 4.61 (d, J = 6.2 Hz, 2H); HRMS (ESI) m/z (M+H)$^+$ calcd. for $C_{21}H_{16}N_3O$, 326.1288; found 326.1295.

3.5 Materials and Methods

3.5.1 Materials

Different commercial fatty acids as lipoxygenase substrates, were purchased from Nu Chek Prep, Inc. (MN, USA). The fatty acids were further re-purified using a Higgins HAISIL column (5 μm, 250 X 10 mm) C-18 column. An isocratic elution of

85% solvent A (99.9% methanol and 0.1% acetic acid): 15% solvent B (99.9% water and 0.1% acetic acid) was used to purify all the fatty acids. Post purification, the fatty acids were stored at -80 °C for a maximum of 6 months. Lipoxygenase product 13-(S)-HPODE was generated by reacting the linoleic acid (LA) with soybean LOX-1. The product generation protocol involved reacting 50 μM substrate in 500 mL of 100 mM Borate buffer pH 9.2 with soybean LOX-1. A small sample from the big reaction was monitored on the UV Spectrometer till complete turnover. The products were then extracted using dichloromethane, reduced with trimethylphosphite, evaporated to dryness and reconstituted in methanol. The products were HPLC purified using an isocratic elution of 75% A (99.9% methanol and 0.1% acetic acid): 25% B (99.9% water and 0.1% acetic acid). The products were tested for their purity using LC-MS/MS and were found to have > 98% purity. Ovine COX-1 (Cat. No. 60100) and human COX-2 (Cat. No. 60122) were purchased from Cayman chemicals. All other chemicals were of high quality and used without further purification.

3.5.2 Methods

3.5.2.1 Overexpression and Purification of Lipoxygenases

Different lipoxygenases such as, human reticulocyte 15-lipoxygenase-1 (15-LOX-1), human epithelial 15-lipoxygenase-2 (15-LOX-2), human platelet 12-lipoxygenase (12-LOX) were expressed as N-terminal His_6-tagged proteins and were purified via immobilized metal affinity chromatography (IMAC) using Ni-NTA resins for 15-LOX-1 and 15-LOX-2, whereas Ni-IDA resin for 12-LOX.[65],[66]The protein purity was evaluated by SDS-PAGE analysis and was found to be greater than 90%.

Human 5-lipoxygenase (5-LOX) was expressed as a non-tagged protein and used as a crude ammonium sulfate protein fraction, as published previously.[67]

3.5.2.2 High-throughput Screen (HTS)

Materials

Dimethyl sulfoxide (DMSO) ACS grade was from Fisher, while ferrous ammonium sulfate, Xylenol Orange (XO), sulfuric acid, and Triton X-100 were obtained from Sigma-Aldrich.

Compound library

A 74,290 compound library was screened in 7 to 15 concentrations ranging from 0.7 nM to 57 μM. The library included 61,548 diverse small drug-like molecules that are part of the NIH Small Molecule Repository. A collection of 1,372 compounds from the Centers of Methodology and Library Development at Boston University (BUCMLD) and University of Pittsburgh (UPCMLD) were added to the library. Several combinatorial libraries from Pharmacopeia, Inc. totaled 2,419 compounds. An additional 1,963 compounds from the NCI Diversity Set were included. Lastly, 6,925 compounds with known pharmacological activity were added to provide a large and diverse screening collection.

HTS protocol and analysis

All screening operations were performed on a fully integrated robotic system (Kalypsys Inc, San Diego, CA) as described elsewhere. Three μL of enzyme (40 nM 15-hLO-1, final concentration) was dispensed into 1536-well Greiner black clear-bottom assay plate. Compounds and controls (23 nL) were transferred via

Kalypsys PinTool equipped with 1536-pin array. The plate was incubated for 15 min at room temperature, and then a 1 µL aliquot of substrate solution (50 µM arachidonic acid final concentration) was added to start the reaction. The reaction was stopped after 6.5 min by the addition of 4 µL FeXO solution (final concentrations of 200 µM Xylenol Orange (XO) and 300 µM ferrous ammonium sulfate in 50 mM sulfuric acid). After a short spin (1000 rpm, 15 sec), the assay plate was incubated at room temperature for 30 minutes. The absorbances at 405 and 573 nm were recorded using ViewLux high throughput CCD imager (Perkin-Elmer, Waltham, MA) using standard absorbance protocol settings. During dispense, enzyme and substrate bottles were kept submerged into +4 °C recirculating chiller bath to minimize degradation. Plates containing DMSO only (instead of compound solutions) were included approximately every 50 plates throughout the screen to monitor any systematic trend in the assay signal associated with reagent dispenser variation or decrease in enzyme specific activity.

Data was analyzed in a similar method as described elsewhere. Briefly, assay plate-based raw data was normalized to controls and plate-based data corrections were applied to filter out background noise. All concentration response curves (CRCs) were fitted using in-house developed software (http://ncgc.nih.gov/pub/openhts/). Curves were categorized into four classes: complete response curves (Class 1), partial curves (Class 2), single point actives (Class 3) and inactives (Class 4). Compounds with the highest quality, Class 1 and Class 2 curves, were prioritized for follow-up.

3.5.2.3 Lipoxygenase UV-Vis Assay

The inhibitor compounds were screened initially using one concentration point on a Perkin-Elmer Lambda 40 UV/Vis spectrophotometer. The percent inhibition was determined by comparing the enzyme rates of the control (DMSO solvent) and the inhibitor sample by following the formation of the conjugated diene product at 234 nm ($\varepsilon = 25,000 \ M^{-1}cm^{-1}$). The reactions were initiated by adding either of ~ 40 nM 12-LOX, 40 nM 15-LOX-1, 0.5 μM 15-LOX-2 or 5-10 μL of 5-LOX crude extract to a cuvette with a 2mL reaction buffer constantly stirred using a magnetic stir bar at room temperature (22° C). Reaction buffers used for various lipoxygenase were as follows- 25 mM HEPES (pH 7.3), 0.3 mM $CaCl_2$, 0.1 mM EDTA, 0.2 mM ATP, 0.01% Triton X-100, 10 μM AA for the crude, ammonium sulfate precipitated 5-LOX; 25 mM Hepes (pH 8), 0.01% Triton X-100, 10 μM AA for 12-LOX and 25 mM Hepes buffer (pH 7.5), 0.01% Triton X-100, 10 μM AA for 15-LOX-1 and 15-LOX-2. The substrate concentration was quantitatively determined by allowing the enzymatic reaction to go to completion in the presence of 15-LOX-2. For the inhibitors that showed more than 50% inhibition at the one point screens, IC_{50} values were obtained by determining the enzymatic rate at various inhibitor concentrations and plotted against inhibitor concentration, followed by a hyperbolic saturation curve fit (assuming total enzyme concentration $[E] \ll K_i^{app}$, so $IC_{50} \sim K_i^{app}$). It should be noted that all of the potent inhibitors displayed greater than 80% maximal inhibition, unless stated in the tables. Inhibitors were stored at -20° C in DMSO.

3.5.2.4 Pseudo-peroxidase Assay

The pseudo-peroxidase activity rates were determined with BWb70c as the positive control, 13-(S)-HPODE as the oxidizing product and 15-LOX-1 on a Perkin-Elmer Lambda 40 UV/Vis spectrometer. Activity was determined by monitoring the decrease at 234 nm (product degradation) in buffer (50 mM Sodium Phosphate (pH 7.4), 0.3 mM $CaCl_2$, 0.1 mM EDTA, 0.01% Triton X100, and 20 μM 13-(S)-HPODE). About 0.6 nmoles of 15-LOX-1 were added to 2 mL buffer containing 20 μM 13-(S)-HPODE, constantly stirred with a rotating stir bar (22 °C). Reaction was initiated by addition of 20 μM inhibitor (1:1 ratio to product). The percent consumption of 13-(S)-HPODE was recorded and loss of product less than 20% was not considered as viable redox activity. Individual controls were conducted with inhibitor alone with product and enzyme alone with product. These negative controls formed the baseline for the assay, reflecting non-pseudoperoxidase dependent hydroperoxide product decomposition. To rule out the auto-inactivation of the enzyme from pseudo-peroxidase cycling, 15-LOX-1 residual activities were measured after the assay was complete. 20 μM AA was added to the reaction mixture and the residual activity was determined by comparing the initial rates with inhibitor and 13-(S)-HPODE versus inhibitor alone, since the inhibitor by itself inherently lowers the rate of the oxygenation. Activity is characterized by direct measurement of the product formation with the increase of absorbance at 234 nm.

3.5.2.5 Steady-State Inhibition Kinetics.

The steady-state kinetics experiments were performed with the parent analogue, compound **1** (**ML351**) to determine the mode of inhibition. The inhibitor concentrations ranging from 0, 0.05, 2 and 5 µM were used. Reactions were initiated by adding approximately 40-60 nM 15-LOX-1 to a constantly stirring 2 mL cuvette containing 1 – 20 µM AA in 25 mM HEPES buffer (pH 7.5), in the presence of 0.01% Triton X-100. Lipoxygenase rates were determined by monitoring the formation of the conjugated product, 15-HPETE, at 234 nm ($\varepsilon = 25\ 000\ M^{-1}\ cm^{-1}$) with a Perkin-Elmer Lambda 40 UV/Vis spectrophotometer. The substrate concentration was quantitatively determined by allowing the enzymatic reaction to proceed to completion using 15-LOX-2. Kinetic data were obtained by recording initial enzymatic rates, at varied substrate and inhibitor concentrations, and subsequently fitted to the Henri-Michaelis-Menten equation, using KaleidaGraph (Synergy) to determine the microscopic rate constants, V_{max} (µmol/min/mg) and V_{max}/K_M (µmol/min/mg/µM). These rate constants were subsequently replotted with $1/V_{max}$ and K_M/V_{max} versus inhibitor concentration, yielding K_i' and K_i, respectively.

3.5.2.6 Cyclooxygenase Assay

About 2-5 µg of either COX-1 or COX-2 were added to buffer containing 0.1 M Tris-HCl buffer (pH 8.0), 5 mM EDTA, 2 mM phenol and 1 µM hematin at 37 ° C. The inhibitors were added to the reaction cell, followed by an incubation of 5 minutes with either of the COX enzymes. The reaction was then initiated by adding 100 µM AA in the reaction cell. Data was collected using a Hansatech DW1 oxygen electrode and the consumption of oxygen was recorded. Indomethacin and the solvent DMSO,

were used as positive and negative controls, respectively and the percent inhibition of the enzyme was calculated by comparing the rates from samples and the controls.

3.5.2.7 HT22 Cell Culture Assay

Glutathione depletion was induced in HT22 cells by glutamate treatment, and LDH release into the medium was measured to detect cell death as described.[62] Briefly, HT22 cells were cultured in DMEM containing 10% fetal bovine serum and penicillin / streptomycin (all media from Invitrogen). For viability experiments, cells were seeded at 1 x 10^4 cells/well in 96-well plates (Corning) and treated 18h later, when the cells were approximately 50-70% confluent. Treatment consisted of exchanging the medium to 100 µl fresh culturing medium and adding 5 mM glutamate (stock solution 0.5 M in PBS) in the presence or absence of DMSO (maximum 0.1% final concentration) as control or the indicated concentrations of **ML351**. Lactate dehydrogenase (LDH) content was determined separately for the cell extracts and corresponding media using a Cytotoxicity Detection Kit (Roche), and the percentage of LDH released to the medium calculated after subtracting the corresponding background value. To determine levels of the 12/15-LOX metabolite 12-hydroxy-eicosatetraenoic acid (12-HETE), we cultured HT22 cells in 75 cm^2 flasks in DMEM medium without phenol red, supplemented with 5% FBS, and treated the cells the next day when cells were 50-70% confluent. 24 hours later, the eicosanoid-containing fraction was isolated via Sep-Pak C-18 column, and 12-HETE was detected with a 12-(S)-HETE ELISA kit, purchased from Enzo Life Sciences

(Catalog # ADI-900-050), and used according to the manufacturer's instruction. Three independent experiments were evaluated.

3.5.2.8 Distal MCAO Model of Permanent Focal Ischemia in Mice

To study **ML351** in a model of distal middle cerebral artery occlusion (distal MCAO), [64] C57Bl6J mice were treated with ferric chloride ($FeCl_3$) to cause occlusion of the distal middle cerebral artery. Mice were kept under anesthesia with 1.5 % isoflurane in a nitrous oxide/oxygen mixture via facemask. The

body temperature was monitored by a rectal probe and maintained at $37\pm0.3°$ C by a homoeothermic blanket control unit. Briefly, mice were placed in a stereotaxic frame, the scalp was opened and right temporal muscle was dissected. The area between zygomatic arch and squamous bone was thinned by a high-speed drill and cooled with saline. The trace of MCA was visualized and thin bony film was lifted up by forceps. After that a laser-Doppler flowmetry probe was placed 2 mm posterior, 6 mm lateral to the bregma to monitor the regional cerebral blood flow (rCBF). After obtaining a stable epoch of the pre-ischemic rCBF, a piece of 10% $FeCl_3$ saturated filter paper was placed over the intact dura mater along the trace of MCA and the rCBF was continuously monitored during the next 3 hours. After 2 hours of ischemia, either 50 mg/kg **ML351**, or DMSO vehicle was injected intraperitoneally. Following sacrifice at 24 hours, brains were sectioned into 1mm slices, and infarct sizes were determined by staining with 2,3,5-triphenyltetrazolium chloride (TTC), using the indirect method (infarct volume = contralateral volume minus uninfarcted ipsilateral volume).

3.6 Acknowledgment

3.7 Figures

Figure 3.1 Synthetic route to ML351.
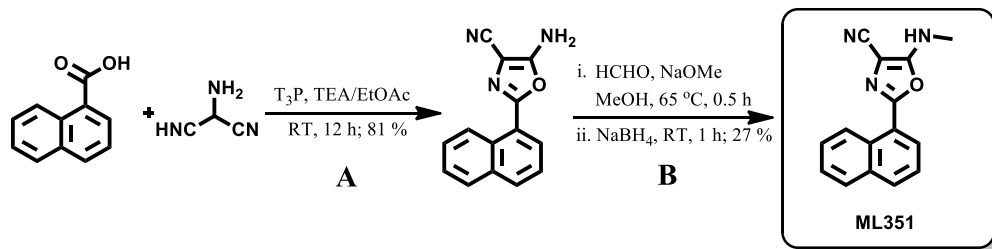
Figure 3.2 Representative examples of previously reported 15-hLO-1 inhibitors
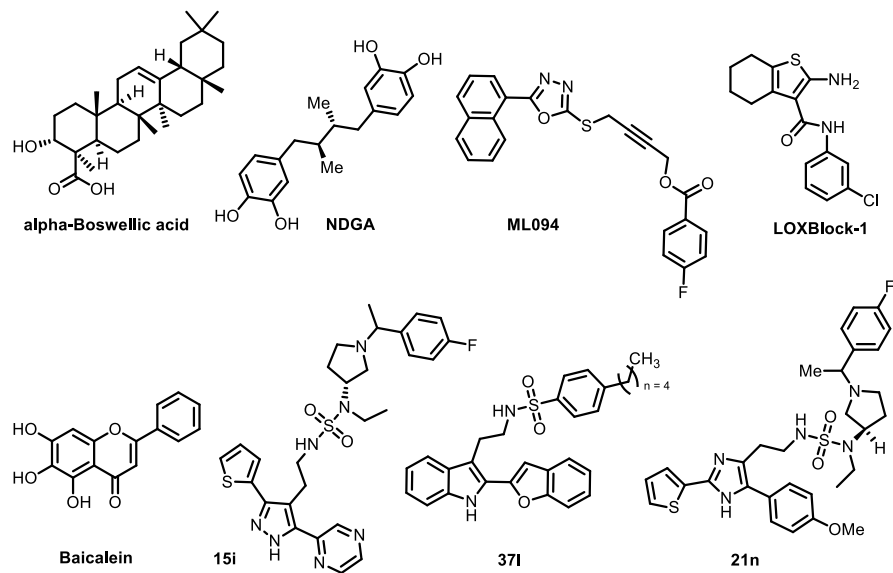
Figure 3.3 SAR summary of JMD2E probe, ML351

-1,3-oxazole ring is optimal
-1,3-thiazole is tolerated
-Other heterocyles are not tolerated

-Heterocycles decrease potency
-Other aryl groups decrease potency
-2,3-dichlorophenyl showed comparable
 potency

-CN group is essential
-Moving CN group reduced potency
-Other groups such as ester group
 also decreased the potency

ML351

-N-alkyl groups improve potency in the order of
Pentyl<Methyl<Ethyl~Butyl~Propyl
-Larger groups such as aryl, acetyl, cycloalkyl
reduced potency, as did branched alkyl (*i*Pr).

Figure 3.4 Steady-state kinetics data for the determination of *K*i for 15-LOX-1 with ML351. Plot of K_M/Vmax versus Inhibitor concentration is the secondary re-plot of the inhibition data, which yielded a K_i of 0.1 ± 0.002 µM.
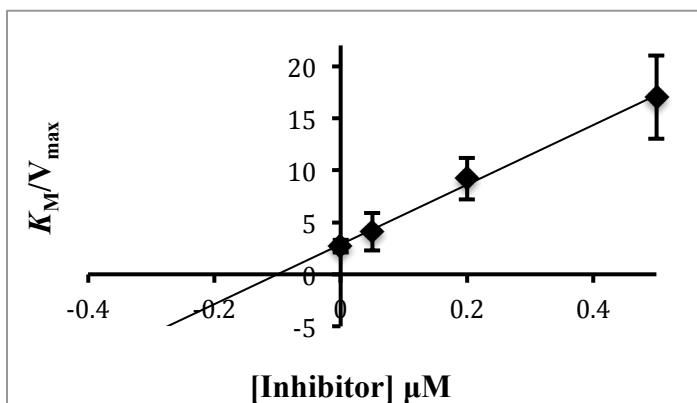
Figure 3.5 Steady-state kinetics data for the determination of K$_i$' for 15-LOX-1 with ML351. Plot of 1/Vmax (y-intercept, V$_{max}$ units are μmol/min/mg) versus [Inhibitor] (μM) is the secondary re-plot of the inhibition data, which yielded a K$_i$' of 1.2 ± 0.02 μM.
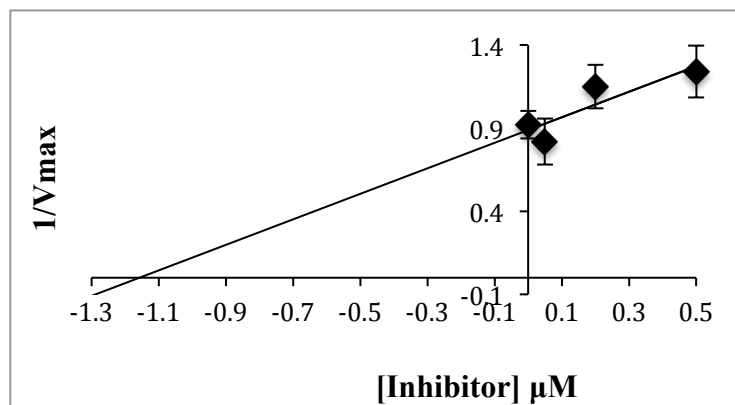
Figure 3.6 (A) Inhibition of 12-HETE in HT-22 cells by ML351 following treatment with glutamate (5 mM). **(B)** Protection of Glutamate (5 mM) induced HT-22 death by increasing amounts of ML351;(12% death rate with no glutamate added, normalized to 100%); ** $p < 0.1$, *** $P < 0.001$.
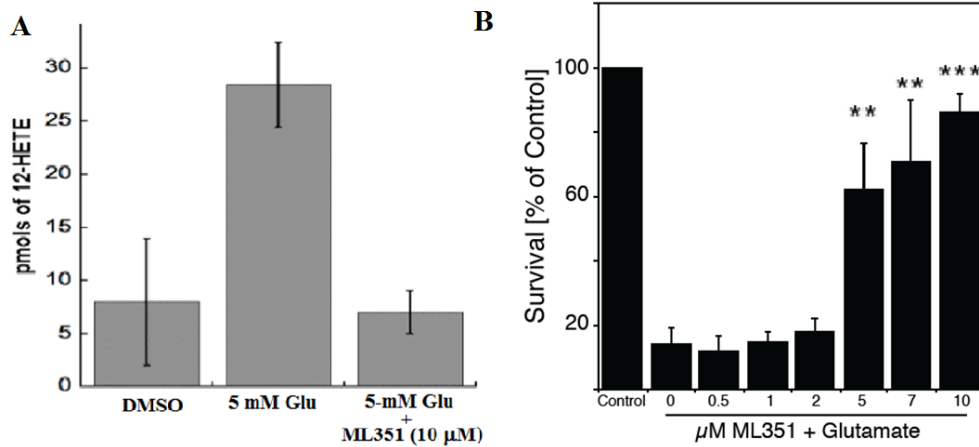
Figure 3.7 (A) Reduced infarct size in 12/15-LOX KO mice (ALOX15[(-/-)]) compared to wild-type C57BL6 mice; *p<0.05. ML351. (B) Activity of ML351 (50 mpk) administered via IP in mouse distal MCAO model of permanent focal ischemia. ** p < 0.01

3.8 Tables

Table 3.1. Variations to compound ML351 (analogs 2-18)

All Compounds synthesized at NCGC. IC$_{50}$ values were measured using the UV-Vis assay in triplicate.

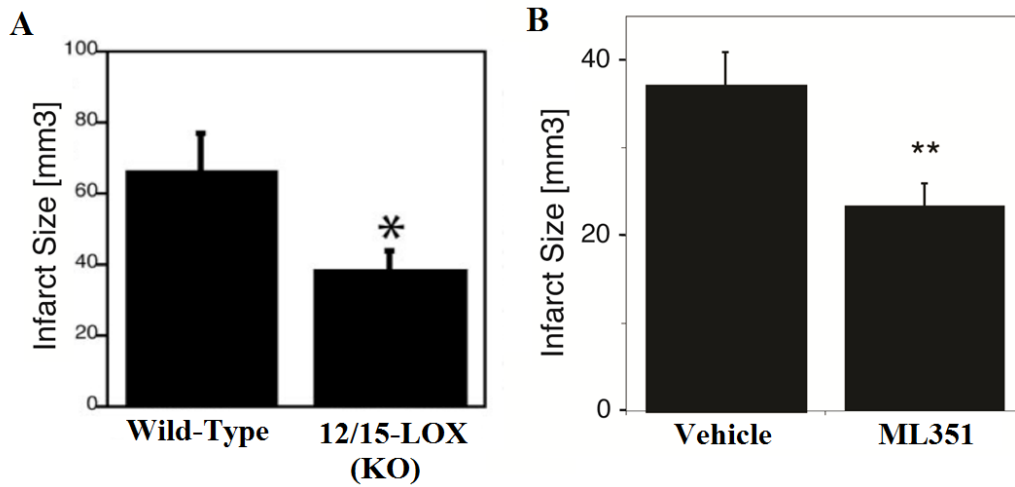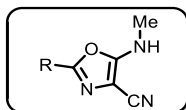| Entry	Internal ID[a]	SID	CID	Structure	IC$_{50}$[b] (μM) [$\pm$ SD (μM)]
1	ML351 NCGC00070329	104223766	664510		0.20 [0.04]
2	NCGC00262509	XXXXX	XXXXX		1.3 [0.5][c]
3	NCGC00262516	160844118	70701456		3.4 [1][c]
4	NCGC00262515	160844117	70701463		3.6 [0.5]
5	NCGC00262517	160844119	70701448		0.73
6	NCGC00262732	160844122	70701454		>40
7	NCGC00262519	160844121	70701462		0.46 [0.06]
8	NCGC00262512	160844114	70701465		0.81 [0.2]
9	NCGC00262518	160844120	70701472		>40
10	NCGC00262510	160844135	70701452		7.6 [2]
11	NCGC00263292	160844135	70701452		>40
12	NCGC00249670	124398610	53257100		23 [13]
13	NCGC00262508	XXXXX	XXXXX		>40
14	NCGC00262511	160844113	70701458		3.9 [0.2]
15	NCGC00019649	124885079	661037		25 [4]
16	NCGC00183424	104224030	18822680		6.3 [0.5]
17	NCGC00183428	104224032	693672		15 [1]
18	NCGC00183425	104224031	49853164		>50

[a]All compounds synthesized at NCGC
[b]IC$_{50}$ values represent the half maximal (50%) inhibitory concentration as determined in the UV-Vis cuvette-based assay in triplicate
[c]Compound possesed low efficacy (<50%)

Table 3.2. Variations to compound ML351 (analogs 19-31)

All Compounds synthesized at NCGC. IC$_{50}$ values were measured using the UV-Vis assay in triplicate.

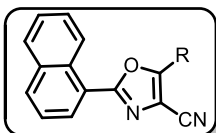| Entry	Internal ID[a]	SID	CID	Structure	IC$_{50}$[b] (μM) [$\pm$ SD (μM)]
1	ML351 NCGC00070329	104223766	664510	NHMe	0.20 [0.04]
19	NCGC00183395	104224014	44142076	NH$_2$	25 [10]
20	NCGC00183407	104224015	49853061	N(Me)$_2$	3.7 [1][c]
21	NCGC00072540	XXXXX	XXXXX	HN	0.12 [0.3]
22	NCGC00068736	XXXXX	XXXXX	HN	0.10 [0.3]
23	NCGC00263300	XXXXX	XXXXX	HN	0.12 [0.05]
24	NCGC00183420	104224027	49852806	HN	0.3 [0.04]
25	NCGC00068824	104223764	663890	HN	3.0 [1]
26	NCGC00068780	XXXXX	XXXXX	HN	>40
27	NCGC00183409	104224016	44142073	NHAc	10 [3]
28	NCGC00263283	160844126	70701475	HN—Ph	5.6 [5][c]
29	NCGC00263299	160844142	70701455	HN—Ph	0.53 [0.2][c]
30	NCGC00262733	160844146	70701470	HN—O	>25
31	NCGC00263294	160844137	70701464	HN—NH	>40

[a]All compounds synthesized at NCGC
[b]IC$_{50}$ values represent the half maximal (50%) inhibitory concentration as determined in the UV-Vis cuvette-based assay in triplicate
[c]Compound possesed low efficacy (<50%)

Table 3.3. Variations to compound ML351 (analogs 32-40)

All Compounds synthesized at NCGC. IC$_{50}$ values were measured using the UV-Vis assay in triplicate.

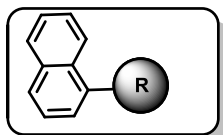| Entry	Internal ID[a]	SID	CID	Structure	IC$_{50}$[b] (μM) [± SD (μM)]
1	MLXXX NCGC00070329	104223766	664510		0.20 [0.04]
32	NCGC00319032	XXXXX	XXXXX		0.55 [0.06]
33	NCGC00263284	160844127	70701451		>40
34	NCGC00263295	160844138	70701459		>40
35	NCGC00262513	160844115	70701467		5.4 [1.8]
36	NCGC00262514	160844116	65644005		>40
37	NCGC00263296	160844139	70701466		>40
38	NCGC00263298	160844141	70701469		6.9 [10][c]
39	NCGC00263286	160844129	62197753		>40
40	NCGC00263290	160844133	63549790		>40

[a]All compounds synthesized at NCGC
[b]IC$_{50}$ values represent the half maximal (50%) inhibitory concentration as determined in the UV-Vis cuvette-based assay in triplicate
[c]Compound possesed low efficacy (<50%)

Table 3.4 Selectivity profiling of ML351 and other top compounds.

^{a}IC$_{50}$ values are reported in µM. ^{b} UV-vis pseudoperoxidase activity assay was performed (section 2.1.6) on all the four selected analogs and no degradation of the hydroperoxide product was observed at 234 nm, indicating a non-reductive inhibitory mechanism.

Analog	15-LOX-1^a	15-LOX-2^a	12-LOX^a	5-LOX^a	Redox Activity^b
ML351	0.02	>100	>100	> 50	No
7	0.46	>100	>100	>100	No
8	0.81	>100	>100	> 50	No
32	0.55	>100	> 40	>50	No

Table 3.5 ADME profile for ML351.

All experiments were conducted at Pharmaron Inc.[a] represents the stability in the presence of NADPH. The probe compound showed no degradation without NADPH present over a 1 hr period. [b] dextromethorphan was used as the substrate. [c] midazolam was used as the substrate.

Compd.	PBS buffer (pH 7.4) Solubility (μM)	Microsomal Stability $T_{1/2}$ (min)[a]		CYP 2D6 Inhibition @ 3μM[b]	CYP 3A4 Inhibition @ 3μM[c]	Permeability (10^{-6} cm/s)		Mouse Plasma Stability remaining at 2 hours
ML351	1.2	18 (rat)	5.5 (mouse)	10.3%	3.5%	723 (PAMPA)	1.5 (Caco-2)	100%

Table 3.6. *In vivo* PK (mouse) at 30 mpk IP for ML351.

All experiments were conducted at Pharmaron Inc. using male CD1 mice (6-8 weeks of age). Data was collected in triplicate at 8 time points over a 24 h period. [a] Formulated as a solution (10% Solutol, 10% Cremophor EL, 20% PEG400 in saline). [b]Brain to plasma ratio [AUC_{last}(brain)/ AUC_{last}(plasma)].

Compound	Tissue[a]	$T_{1/2}$ (h)	T_{max} (h)	C_{max} (µM)	AUC_{inf} (µM)	B/P Ratio[b]
ML351	Plasma	1.1	0.25	13.8	13	2.8
	Brain	1	0.5	28.8	35.5	

3.9   REFERENCES

1.   Solomon, E. I., Zhou, J., Neese, F., and Pavel, E. G. (1997) New Insights from Spectroscopy into the structure/function relationships of lipoxygenases, *Chem. Biol. 4*, 795-808.

2.   Brash, A. R. (1999) Lipoxygenases: Occurrence, Functions, Catalysis and Acquisition of Substrate, *J. Biol. Chem. 274*, 23679-23682.

3.   Ivanov, I., Heydeck, D., Hofheinz, K., Roffeis, J., O'Donnell, V. B., Kuhn, H., and Walther, M. (2010) Molecular enzymology of lipoxygenases, *Arch Biochem Biophys 503*, 161-174.

4.   Schnurr, K., Belkner, J., Ursini, F., Schewe, T., and Kuhn, H. (1996) The selenoenzyme phospholipid hydroperoxide glutathione peroxidase controls the activity of the 15-lipoxygenase with complex substrates and preserves the specificity of the oxygenation products, *J Biol Chem 271*, 4653-4658.

5.   Kuhn, H., Walther, M., and Kuban, R. J. (2002) Mammalian arachidonate 15-lipoxygenases: Structure, function, and biological implications, *Prostag. oth. Lipid M. 68-69*, 263-290.

6.   Haeggstrom, J., and Funk, C. D. (2011) Lipoxygenase and Leukotriene Pathways: Biochemistry, Biology, and Roles in Disease, *Chemical Reviews ASAP*.

7.   Dobrian, A. D., Lieb, D. C., Cole, B. K., Taylor-Fishwick, D. A., Chakrabarti, S. K., and Nadler, J. L. (2011) Functional and pathological roles of the 12- and 15-lipoxygenases, *Progress in lipid research 50*, 115-131.

8.   Natarajan, R., and Nadler, J. (1998) Role of lipoxygenases in breast cancer., *Front. Biosci. 3*, E81-88.

9.   Kuhn, H., Romisch, I., and Belkner, J. (2005) The role of lipoxygenase-isoforms in atherogenesis, *Mol Nutr Food Res 49*, 1014-1029.

10.   Khanapure, S. P., Garvey, D. S., Janero, D. R., and Letts, L. G. (2007) Eicosanoids in inflammation: biosynthesis, pharmacology, and therapeutic frontiers, *Curr Top Med Chem 7*, 311-340.

11. Tong, W. G., Ding, X. Z., Hennig, R., Witt, R. C., Standop, J., Pour, P. M., and Adrian, T. E. (2002) Leukotriene B4 receptor antagonist LY293111 inhibits proliferation and induces apoptosis in human pancreatic cancer cells, *Clinical cancer research : an official journal of the American Association for Cancer Research 8*, 3232-3242.

12. Wenzel, S. E., and Kamada, A. K. (1996) Zileuton: the first 5-lipoxygenase inhibitor for the treatment of asthma, *Ann Pharmacother 30*, 858-864.

13. O'Byrne, P. M., Israel, E., and Drazen, J. M. (1997) Antileukotrienes in the Treatment of Asthma, *Annals of Internal Medicine 127*, 472-480.

14. Berger, W., De Chandt, M. T., and Cairns, C. B. (2007) Zileuton: clinical implications of 5-Lipoxygenase inhibition in severe airway disease, *International Journal of Clinical Practice 61*, 663-676.

15. Muller-Peddinghaus, R. (1997) Potential anti-inflammatory effects of 5-lipoxygenase inhibition--exemplified by the leukotriene synthesis inhibitor BAY X 1005, *J Physiol Pharmacol 48*, 529-536.

16. Klickstein, L. B., Shapleigh, C., and Goetzl, E. J. (1980) Lipoxygenation of arachidonic acid as a source of polymorphonuclear leukocyte chemotactic factors in synovial fluid and tissue in rheumatoid arthritis and spondyloarthritis, *The Journal of clinical investigation 66*, 1166-1170.

17. Weinblatt, M. E., Kremer, J. M., Coblyn, J. S., Helfgott, S., Maier, A. L., Petrillo, G., Henson, B., Rubin, P., and Sperling, R. (1992) Zileuton, a 5-lipoxygenase inhibitor in rheumatoid arthritis, *The Journal of rheumatology 19*, 1537-1541.

18. Spanbroek, R., Grabner, R., Lotzer, K., Hildner, M., Urbach, A., Ruhling, K., Moos, M. P., Kaiser, B., Cohnert, T. U., Wahlers, T., Zieske, A., Plenz, G., Robenek, H., Salbach, P., Kuhn, H., Radmark, O., Samuelsson, B., and Habenicht, A. J. (2003) Expanding expression of the 5-lipoxygenase pathway within the arterial wall during human atherogenesis, *Proceedings of the National Academy of Sciences of the United States of America 100*, 1238-1243.

19. Funk, C. D. (2005) Leukotriene modifiers as potential therapeutics for cardiovascular disease, *Nature reviews. Drug discovery 4*, 664-672.

20. Lotzer, K., Funk, C. D., and Habenicht, A. J. (2005) The 5-lipoxygenase pathway in arterial wall biology and atherosclerosis, *Biochimica et biophysica acta 1736*, 30-37.

21. Bleich, D., Chen, S., Gu, J. L., and Nadler, J. L. (1998) The role of 12-lipoxygenase in pancreatic -cells (Review), *International journal of molecular medicine 1*, 265-272.

22. Hedrick, C. C., Kim, M. D., Natarajan, R. D., and Nadler, J. L. (1999) 12-Lipoxygenase products increase monocyte:endothelial interactions, *Advances in Experimental Medicine and Biology 469*, 455-460.

23. Thomas, C. P., Morgan, L. T., Maskrey, B. H., Murphy, R. C., Kuhn, H., Hazen, S. L., Goodall, A. H., Hamali, H. A., Collins, P. W., and O'Donnell, V. B. (2010) Phospholipid-esterified eicosanoids are generated in agonist-activated human platelets and enhance tissue factor-dependent thrombin generation, *Journal of Biological Chemistry 285*, 6891-6903.

24. Hussain, H., Shornick, L. P., Shannon, V. R., Wilson, J. D., Funk, C. D., Pentland, A. P., and Holtzman, M. J. (1994) Epidermis Contains Platlet-Type 12-Lipoxygenase that is Overexpressed in Germinal Layer Keratinocytes in Psoriasis, *Am. J. Physiol. 266*, C243-C253.

25. Connolly, J. M., and Rose, D. P. (1998) Enhanced angiogenesis and growth of 12-lipoxygenase gene-transfected MCF-7 human breast cancer cells in athymic nude mice, *Cancer Lett 132*, 107-112.

26. Ding, X. Z., Iversen, P., Cluck, M. W., Knezetic, J. A., and Adrian, T. E. (1999) Lipoxygenase inhibitors abolish proliferation of human pancreatic cancer cells., *Biochemical and biophysical research communications 261*, 218-223.

27. Schewe, T. (2002) 15-lipoxygenase-1: a prooxidant enzyme, *Biol Chem 383*, 365-374.

28.   Hennig, R., Kehl, T., Noor, S., Ding, X. Z., Rao, S. M., Bergmann, F., Furstenberger, G., Buchler, M. W., Friess, H., Krieg, P., and Adrian, T. E. (2007) 15-lipoxygenase-1 production is lost in pancreatic cancer and overexpression of the gene inhibits tumor cell growth, *Neoplasia 9*, 917-926.

29.   Bhattacharya, S., Mathew, G., Jayne, D. G., Pelengaris, S., and Khan, M. (2009) 15-lipoxygenase-1 in colorectal cancer: a review, *Tumour Biol 30*, 185-199.

30.   Kronke, G., Katzenbeisser, J., Uderhardt, S., Zaiss, M. M., Scholtysek, C., Schabbauer, G., Zarbock, A., Koenders, M. I., Axmann, R., Zwerina, J., Baenckler, H. W., van den Berg, W., Voll, R. E., Kuhn, H., Joosten, L. A., and Schett, G. (2009) 12/15-lipoxygenase counteracts inflammation and tissue damage in arthritis, *Journal of immunology 183*, 3383-3389.

31.   Yigitkanli, K., Pekcec, A., Karatas, H., Pallast, S., Mandeville, E., Joshi, N., Smirnova, N., Gazaryan, I., Ratan, R. R., Witztum, J. L., Montaner, J., Holman, T. R., Lo, E. H., and van Leyen, K. (2013) Inhibition of 12/15-lipoxygenase as therapeutic strategy to treat stroke, *Ann Neurol 73*, 129-135.

32.   van Leyen, K. (2013) Lipoxygenase: An Emerging Target for Stroke Therapy, *CNS Neurol Disord Drug Targets*.

33.   Ratan, R. R., Ryu, H., Lee, J., Mwidau, A., and Neve, R. L. (2002) In vitro model of oxidative stress in cortical neurons., *Methods Enzymol 352*, 183-190.

34.   Anthone, G. J., Bastidas, J. A., Orandle, M. S., and Yeo, C. J. (1990) Direct proabsorptive effect of octreotide on ionic transport in the small intestine, *Surgery 108*, 1136-1141; discussion 1141-1132.

35.   Moskowitz, M. A., Lo, E. H., and Iadecola, C. (2010) The science of stroke: mechanisms in search of treatments, *Neuron 67*, 181-198.

36.   Chan, P. H. (1996) Role of oxidants in ischemic brain damage, *Stroke 27*, 1124-1129.

37.   Haas, T. A., Bastida, E., Nakamura, K., Hullin, F., Admirall, L., and Buchanan, M. R. (1988) Binding of 13-HODE and 5-, 12- and 15-HETE to endothelial cells and subsequent platelet, neutrophil and tumor cell adhesion, *Biochimica et biophysica acta 961*, 153-159.

38.   Seiler, A., Schneider, M., Forster, H., Roth, S., Wirth, E. K., Culmsee, C., Plesnila, N., Kremmer, E., Radmark, O., Wurst, W., Bornkamm, G. W., Schweizer, U., and Conrad, M. (2008) Glutathione peroxidase 4 senses and translates oxidative stress into 12/15-lipoxygenase dependent- and AIF-mediated cell death, *Cell Metab 8*, 237-248.

39.   Mytilineou, C., Kramer, B. C., and Yabut, J. A. (2002) Glutathione depletion and oxidative stress, *Parkinsonism Relat Disord 8*, 385-387.

40.   Pallast, S., Arai, K., Pekcec, A., Yigitkanli, K., Yu, Z., Wang, X., Lo, E. H., and van Leyen, K. (2010) Increased nuclear apoptosis-inducing factor after transient focal ischemia: a 12/15-lipoxygenase-dependent organelle damage pathway., *J Cereb Blood Flow Metab 30*, 1157-1167.

41.   Pallast, S., Arai, K., Wang, X., Lo, E. H., and van Leyen, K. (2009) 12/15-Lipoxygenase targets neuronal mitochondria under oxidative stress., *J Neurochem 111*, 882-889.

42.   van Leyen, K., Duvoisin, R. M., Engelhardt, H., and Wiedmann, M. (1998) A function for lipoxygenase in programmed organelle degradation, *Nature 395*, 392-395.

43.   van Leyen, K., Kim, H. Y., Lee, S. R., Jin, G., Arai, K., and Lo, E. H. (2006) Baicalein and 12/15-lipoxygenase in the ischemic brain, *Stroke 37*, 3014-3018.

44.   Khanna, S., Roy, S., Slivka, A., Craft, T. K., Chaki, S., Rink, C., Notestine, M. A., DeVries, A. C., Parinandi, N. L., and Sen, C. K. (2005) Neuroprotective properties of the natural vitamin E alpha-tocotrienol, *Stroke 36*, 2258-2264.

45.   Jin, G., Arai, K., Murata, Y., Wang, S., Stins, M. F., Lo, E. H., and van Leyen, K. (2008) Protecting against Cerebrovascular Injury: Contributions of 12/15-

lipoxygenase to edema formation following transient focal ischemia, *Stroke 39*, 2538-2543.

46. Carroll, J., Jonsson, E. N., Ebel, R., Hartman, M. S., Holman, T. R., and Crews, P. (2001) Probing sponge-derived terpenoids for human 15-lipoxygenase inhibitors, *J Org Chem 66*, 6847-6851.

47. Whitman, S., Gezginci, M., Timmermann, B. N., and Holman, T. R. (2002) Structure-activity relationship studies of nordihydroguaiaretic acid inhibitors toward soybean, 12-human, and 15-human lipoxygenase, *J. Med. Chem. 45*, 2659-2661.

48. Amagata, T., Whitman, S., Johnson, T. A., Stessman, C. C., Loo, C. P., Lobkovsky, E., Clardy, J., Crews, P., and Holman, T. R. (2003) Exploring sponge-derived terpenoids for their potency and selectivity against 12-human, 15-human, and 15-soybean lipoxygenases, *J Nat Prod 66*, 230-235.

49. Cichewicz, R. H., Kenyon, V. A., Whitman, S., Morales, N. M., Arguello, J. F., Holman, T. R., and Crews, P. (2004) Redox inactivation of human 15-lipoxygenase by marine-derived meroditerpenes and synthetic chromanes: archetypes for a unique class of selective and recyclable inhibitors, *Journal of the American Chemical Society 126*, 14910-14920.

50. Vasquez-Martinez, Y., Ohri, R. V., Kenyon, V., Holman, T. R., and Sepulveda-Boza, S. (2007) Structure-activity relationship studies of flavonoids as potent inhibitors of human platelet 12-hLO, reticulocyte 15-hLO-1, and prostate epithelial 15-hLO-2, *Bioorganic & Medicinal Chemistry 15*, 7408-7425.

51. Deschamps, J. D., Kenyon, V. A., and Holman, T. R. (2006) Baicalein is a potent in vitro inhibitor against both reticulocyte 15-human and platelet 12-human lipoxygenases, *Bioorg Med Chem 14*, 4295-4301.

52. Rai, G., Kenyon, V., Jadhav, A., Schultz, L., Armstrong, M., Jameson, J. B., Hoobler, E., Leister, W., Simeonov, A., Holman, T. R., and Maloney, D. J. (2010) Discovery of potent and selective inhibitors of human reticulocyte 15-lipoxygenase-1, *Journal of medicinal chemistry 53*, 7392-7404.

53. Ngu, K., Weinstein, D. S., Liu, W., Langevine, C., Combs, D. W., Zhuang, S., Chen, X., Madsen, C. S., Harper, T. W., Ahmad, S., and Robl, J. A. (2011) Pyrazole-based sulfonamide and sulfamides as potent inhibitors of mammalian 15-lipoxygenase, *Bioorg Med Chem Lett 21*, 4141-4145.

54. Weinstein, D. S., Liu, W., Gu, Z., Langevine, C., Ngu, K., Fadnis, L., Combs, D. W., Sitkoff, D., Ahmad, S., Zhuang, S., Chen, X., Wang, F. L., Loughney, D. A., Atwal, K. S., Zahler, R., Macor, J. E., Madsen, C. S., and Murugesan, N. (2005) Tryptamine and homotryptamine-based sulfonamides as potent and selective inhibitors of 15-lipoxygenase, *Bioorg Med Chem Lett 15*, 1435-1440.

55. Weinstein, D. S., Liu, W., Ngu, K., Langevine, C., Combs, D. W., Zhuang, S., Chen, C., Madsen, C. S., Harper, T. W., and Robl, J. A. (2007) Discovery of selective imidazole-based inhibitors of mammalian 15-lipoxygenase: highly potent against human enzyme within a cellular environment, *Bioorg Med Chem Lett 17*, 5115-5120.

56. Malterud, K. E., and Rydland, K. M. (2000) Inhibitors of 15-lipoxygenase from orange peel, *J. Ag. Food Chem. 48*, 5576-5580.

57. Sailer, E. R., Schweizer, S., Boden, S. E., Ammon, H. P. T., and Safayhi, H. (1998) Characterization of an acetyl-11-keto-B-boswellic acid and arachidonate-binding regulatory site of 5-lipoxygenase using phoroaffinity labeling, *Eur. J. Biochem. 256*, 364-368.

58. Lo, E. H., Dalkara, T., and Moskowitz, M. A. (2003) Mechanisms, challenges and opportunities in stroke, *Nat Rev Neurosci 4*, 399-415.

59. Donnan, G. A., Fisher, M., Macleod, M., and Davis, S. M. (2008) Stroke, *Lancet 371*, 1612-1623.

60. Mogul, R., Johansen, E., and Holman, T. R. (2000) Oleyl sulfate reveals allosteric inhibition of Soybean Lipoxygenase-1 and Human 15-Lipoxygenase, *Biochemistry 39*, 4801-4807.

61. Wecksler, A. T., Kenyon, V., Deschamps, J. D., and Holman, T. R. (2008) Substrate specificity changes for human reticulocyte and epithelial 15-

lipoxygenases reveal allosteric product regulation, *Biochemistry 47*, 7364-7375.

62. Li, Y., Maher, P., and Schubert, D. (1997) A role for 12-lipoxygenase in nerve cell death caused by glutathione depletion, *Neuron 19*, 453-463.

63. Maher, P., Salgado, K. F., Zivin, J. A., and Lapchak, P. A. (2007) A novel approach to screening for new neuroprotective compounds for the treatment of stroke, *Brain Res 1173*, 117-125.

64. Karatas, H., Erdener, S. E., Gursoy-Ozdemir, Y., Gurer, G., Soylemezoglu, F., Dunn, A. K., and Dalkara, T. (2011) Thrombotic distal middle cerebral artery occlusion produced by topical FeCl(3) application: a novel model suitable for intravital microscopy and thrombolysis studies, *J Cereb Blood Flow Metab 31*, 1452-1460.

65. Ohri, R. V., Radosevich, A. T., Hrovat, K. J., Musich, C., Huang, D., Holman, T. R., and Toste, F. D. (2005) A Re(V)-catalyzed C-N bond-forming route to human lipoxygenase inhibitors, *Org Lett 7*, 2501-2504.

66. Chen, X. S., Brash, A. R., and Funk, C. D. (1993) Purification and characterization of recombinant histidine-tagged human platelet 12-lipoxygenase expressed in a baculovirus/insect cell system, *Eur J Biochem 214*, 845-852.

67. Robinson, S. J., Hoobler, E. K., Riener, M., Loveridge, S. T., Tenney, K., Valeriote, F. A., Holman, T. R., and Crews, P. (2009) Using enzyme assays to evaluate the structure and bioactivity of sponge-derived meroterpenes, *Journal of Natural Products 72*, 1857-1863.

Chapter 4

Investigations into the Allosteric and pH Effect on Substrate Specificity of Human

Epithelial 15-Lipoxygenase-2

4.1 Introduction

Lipoxygenases (LOX) represent a class of non-heme iron containing enzymes which catalyze the stereo-specific peroxidation of polyunsaturated fatty acids (PUFAs) containing at least one 1,4-cis-pentadiene moiety.[1-3] The mechanism of their action involves four primary steps –hydrogen abstraction, radical rearrangement, oxygen insertion and peroxy radical reduction.[4-7] There are three main types of human LOXs, 5-LOX, 12-LOX and 15-LOX, that are named according to their positional specificity with arachidonic acid (AA).[8] The crystal structures available from various LOXs indicate a single polypeptide chain folding into a two-domain structure.[9-15] The C-terminal catalytic domain primarily consists of α–helices and possesses the catalytically active non-heme iron, which is coordinated by endogenous ligands and a hydroxide ligand.[16] The smaller N-terminal domain consists of primarily β–sheets and resembles the C2-domain of human lipases, known as PLAT domains (Polycystin-1, Lipoxygenase, α-Toxin),[17] and has been implicated in membrane binding.[18, 19]

LOX react with various endogenous substrates, which differ in carbon chain length and number/position of unsaturation points.[20-23] Many of these LOX products are biologically active compounds that not only mediate cellular pathways but also

126

act as precursors for potent chemical mediators, such as leukotrienes,[24, 25] prostaglandins,[26] resolvins,[27-29] lipoxins[30] and protectins.[31] Specifically, the 15-LOX product of linoleic acid (LA), 13-(S)-hydroperoxy-9Z,11E-octadecadienoic acid (13-(S)-HPODE) (**Figure 4.1**), which is immediately reduced to 13-(S)- hydroxy-9Z,11E-octadecadienoic acid (13-(S)-HODE) in the cell,[32] is known to alleviate the epidermal hyper-proliferation in patients with psoriasis.[20, 33, 34] However, 13-(S)-HODE also up-regulates the MAP kinase signaling pathway, causing cell proliferation in prostate cancer.[35, 36] 15-(S)-5Z,8Z,11Z,13E-hydroxyeicosatetraenoic acid (15-(S)-HETE), the 15-LOX product of AA, leads to anti-inflammation by being an intermediate in the biosynthesis of lipoxins. [30, 37]

These 15-LOX products are produced by the two 15-LOX isoforms found in human tissue. Epithelial 15-Lipoxygenase-2 (15-LOX-2) is primarily expressed in normal human adult prostate tissue, as well as in lung, skin and cornea tissue,[38] while reticulocyte 15-lipoxygenase-1 (15-LOX-1) is primarily expressed in reticulocytes, as well as in eosinophils, macrophages, lung, brain, prostate and colon tissues.[39] 15-LOX-2 is highly homologous to murine 8-LOX (78% sequence identity),[40] but shares only 40% sequence identity with 15-LOX-1. 15-LOX-2 differs from 15-LOX-1 catalytically in that it exclusively oxygenates (>99%) at C_{15} of AA, compared to 90% for 15-LOX-1. 15-LOX-2 also reacts poorly with LA, while 15-LOX-1 reacts similarly with AA and LA.[39] In addition, the two human 15-LOXs respond differently to allosteric effector molecules. The LA product, 13-(S)-HODE, decreases

the k_{cat}/K_M AA/LA substrate specificity ratio for 15-LOX-2, whereas it increases the AA/LA ratio for 15-LOX-1.[41] The magnitudes of these substrate specificity changes are over four-fold,[41] which is comparable in magnitude to that observed for the allosteric regulation of ribonucleotide reductase (RNR) substrate specificity.[42, 43]

The minor AA product of 15-LOX-1, 12-(S)-HETE, changes the substrate specificity of 15-LOX-1 but not that of 15-LOX-2. 15-(S)-HETE, however, does not affect the substrate specificity of either 15-LOX isozyme, indicating that allosteric alteration of substrate specificity is a highly selective event. These earlier findings from steady-state kinetics of 15-LOX-1 were confirmed by a novel competitive substrate capture method developed by our lab, demonstrating saturating effects on the substrate specificity ratio of AA/LA with a $K_D = 1.2 \pm 0.1$ μM for perdeuterated 13-(S)-HPODE.[41] Interestingly, the addition of 13-(S)-HPODE showed no effect on 15-LOX-2 kinetics at pH 7.5, which contradicted the change between steady state kinetics and competitive substrate capture, 8.0 ±1.0 and 2.2 ±0.2 respectively This discrepancy was postulated to be due to a tight association of 13-(S)-HPODE with 15-LOX-2, thus saturating the allosteric binding site. It was also observed that the AA/LA substrate specificity ratio was pH dependent, changing from 1.4 ± 0.3 at pH 6.0 to 4.5 ± 0.5, at pH 10. The pH titration curve showed a pK_a of 7.7 ± 0.1, suggesting a charged interaction between 13-(S)-HPODE and a possible Histidine residue, whose neutral state lowered the affinity of 13-(S)-HPODE for 15-LOX-2.

128

However, these conclusions were tempered by the fact that LA is a very poor substrate of 15-LOX-2, which complicated the measurements.

Given the complexity of the allosteric properties of 15-LOX-2, the pH dependent substrate specificity ratio of AA/LA and the poor nature of the LA as substrate, the current paper expands the study of substrate specificity for 15-LOX-2 beyond the AA-LA pair and investigates the substrate preference of various PUFAs versus AA at different pH values. The current results demonstrate that the substrate specificity of 15-LOX-2 with C_{18} and C_{20} fatty acids is differentially altered by pH, indicating a distinct mechanism of catalysis for these two classes of LOXs substrates. In addition, LOX products affect substrate specificity in a similar manner to that of pH, suggestive of mechanism of actions with possibly shared components.

4.2 Materials and Methods

4.2.1 Materials

All the commercial fatty acids were purchased from Nu Chek Prep, Inc. (MN, USA). The fatty acids were further re-purified using a Higgins HAISIL column (5 μm, 250 X 10 mm) C-18 column. An isocratic elution of 85% A (99.9% methanol and 0.1% acetic acid): 15% B (99.9% water and 0.1% acetic acid) was used to purify all the fatty acids. Post purification, the fatty acids were stored at -80 °C for a maximum of 6 months. Different lipoxygenase products such as 13-(S)-HODE and 13-(S)-HOTrE(γ) were generated by reacting the appropriate substrate with 15-LOX-2. Briefly the protocol involved reacting 50 μM substrate in 500 mL of 25 mM Hepes

buffer pH 7.5 with 15-LOX-2. A small sample from the big reaction was monitored on the UV Spectrometer till complete turnover. The products were then extracted using dichloromethane, reduced with trimethylphosphite, evaporated to dryness and reconstituted in methanol. The products were HPLC purified using an isocratic elution of 75% A (99.9% methanol and 0.1% acetic acid): 25% B (99.9% water and 0.1% acetic acid). The products were tested for their purity using LC-MS/MS and were found to have > 98% purity. All other chemicals were of high quality and used without further purification.

4.2.2 Methods

4.2.2.1 Overexpression and purification 15-LOX-2

Purification of 15-LOX-2 was carried out using a construct encoding a fusion protein consisting of an N-terminal His8-tag fused to maltose. The parent plasmid used in these studies, pVP68K, is available from the Protein Structure Initiative Materials Repository, http://www.psimr.asu.edu. The 15-LOX-2 fusion was expressed using the pVP68K-102188 plasmid in *Escherichia coli* BL21 (DE3). For expression of 15-LOX-2, the host cells were grown to 0.6 OD at 37°C, the cells were then induced by dropping the temperature to 20° C and grown overnight (16 h). The cells were harvested in 2 L fractions at a velocity of 5,000 g, then snap frozen in liquid nitrogen. The cell pellets were re-suspended in buffer A (25 mM HEPES, pH 8, containing 150 mM NaCl), and lysed using a Power Laboratory Press. The cellular lysate was centrifuged at 40,000 g for 25 min, and the supernatant was loaded onto an

NTA-Ni affinity column. The column was washed with 15 mM imidazole in buffer A, followed by elution with 250 mM imidazole in buffer A (no NaCl). 15-LOX-2 fractions were collected, pooled together and then dialyzed in 25 mM HEPES, pH 7.5, containing 150 mM NaCl followed by overnight treatment with His_6-TEV protease at 4° C. The use of TEV protease was as previously described.[44] The proteolyzed sample was applied to an NTA-Co^{2+} column, and eluted in buffer A containing 15 mM imidazole, yielding greater then 90% purity. In this purification, the His_6-tagged TEV and un-cleaved His_8-MBP-15-LOX-2 fusion protein were bound to the columns. The resulting 15-LOX-2 was concentrated by ultrafiltration (30 kDa molecular mass cut-off), combined with glycerol to 20% (v/v) and then snap frozen under liquid nitrogen. The enzyme purity was evaluated by SDS-PAGE. Iron content of 15-LOX-2 was determined with a Thermo Element XR inductively coupled plasma mass spectrometer (ICP-MS), using scandium (EDTA) as an internal standard. Iron concentrations were compared to standard iron solutions. All the kinetics data was normalized to the iron content. The concentration of 15-LOX-2 was determined using the Bradford Assay, with Bovine Serum Albumin (BSA) as a protein standard. Briefly, Bradford protein dye reagent was diluted 1:5 using deionized water. Different solutions of BSA in deionized water were prepared, ranging from 0 mg/mL to 1 mg/mL (linear range of the assay for BSA). Diluted Bradford reagent and BSA stocks were mixed in 50:1 ratio, vortex and incubated for 5 minutes. Similarly, 15-LOX-2 samples with diluted Bradford reagent were made in duplicate. All the samples were

then spun down and absorbance was recorded at 595 nm on Perkin Elmer Lambda 40 instrument. The concentration of 15-LOX-2 was extrapolated from the standard curve of BSA.

4.2.2.2 Effect of pH on competitive substrate capture substrate specificity kinetics of 15-LOX-2

The competitive substrate capture method experiments were performed on several substrate pairs such as AA-LA (arachidonic acid - linoleic acid); AA-ALA (arachidonic acid - alpha linolenic acid); AA-GLA (arachidonic acid - gamma linolenic acid); AA-DGLA (arachidonic acid - dihomo gamma linoleic acid); AA-EPA (arachidonic acid- eicosapentaenoic acid) and AA-EDA (arachidonic acid - eicosadienoic acid) at pH 7.5 as well as at pH 8.5. The substrate mixtures were prepared with a molar ratio of ~1:1. The reaction was initiated by adding 20 nM 15-LOX-2 (normalized to the Fe content) to a 3 mL reaction cuvette using the following buffer conditions: 25 mM Hepes, pH 7.5 (or pH 8.5), room temperature and a total substrate concentration of 5 μM. The reaction was monitored at 234 nm with a Perkin-Elmer Lambda 40 spectrophotometer and quenched at 5% substrate turnover using 1% glacial acetic acid. The reaction mixture was then extracted with DCM, evaporated to dryness under vacuum. The dried sample was reconstituted in 100 μL methanol, centrifuged and stored at -20° C until analyzed by Finnigan LTQ liquid chromatography–tandem mass spectrometry (LC–MS/MS) system. A Thermo Electron Corp. Aquasil (3 μm, 100 mm × 2.1 mm) C-18 column was used to separate

the LO products with an elution protocol consisting of 0.2 mL /min flow rate and a linear gradient from 40% ACN, 59.9% H_2O, and 0.1% THF to 48% ACN, 67.9% H_2O, and 0.1% THF, followed by an isocratic step of 55% ACN, 44.9% H_2O, and 0.1% THF. The corresponding LO products were detected using selective ion monitoring analysis [(m/z = 318.7 to 319.7 for 11-(S)-HETE and 15-(S)-HETE); (m/z = 294.7 to 295.7 for 9-(S)-HODE and 13-(S)-HODE); (m/z = 292.7 to 293.7 for 9-(S)-HOTrE, 13-(S)-HOTrE and 9-(S)-HOTrE(γ), 13-(S)-HOTrE(γ)) ; (m/z = 320.7 to 321.7 for 15-(S)-HETrE and 11-(S)-HETrE); (m/z = 316.7 to 317.7 for 15-(S)-HEPE and 11-(S)-HEPE) and (m/z = 322.7 to 323.7 for 15-(S)-HEDE and 11-(S)-HEDE)] in negative ion mode and then identified by fragmentation pattern (15-(S)-HETE - parent ion at m/z 319 and fragments at m/z 219 and 175; 11-(S)-HETE - parent ion at m/z 319 and fragments at m/z 167 and 149; 9-(S)-HODE parent ion at m/z 295 and fragments at m/z 277 and 171; 13-(S)-HODE - parent ion at m/z 295 and fragments at m/z 277 and 195; 13-(S)-HOTrE parent ion at m/z 293 and fragments at m/z 223 and 195; 9-(S)-HOTrE parent ion at m/z 293 and fragments at m/z 231 and 171; 13-(S)-HOTrE(γ) parent ion at m/z 293 and fragments at m/z 231 and 193; 9-(S)-HOTrE(γ) parent ion at m/z 293 and fragments at m/z 169 and 141; 15-(S)-HETrE- parent ion at m/z 321 and fragments at m/z 303 and 221; 11-(S)-HETrE- parent ion at m/z 321 and fragments at m/z 303 and 217; 15-(S)-HEPE- parent ion at m/z 317 and fragments at m/z 219 and 175; 11-(S)-HEPE- parent ion at m/z 317 and fragments at m/z 167 and 149; 15-(S)-HEDE- parent ion at m/z 323 and fragments at m/z 305 and 223; 11-(S)-

HEDE- parent ion at *m/z* 323 and fragments at *m/z* 305 and 199) from MS-MS. The electrospray voltage was set to 5.0 kV and a global acquisition MS mode was used. The MS-MS scan was performed for the five most abundant precursor ions. The Collision Induced Dissociation (CID) was used for MS-MS with a collision energy of 35 eV. The peak areas of AA products (15-(S)-HETE and 11-(S)-HETE), LA products (13-(S)-HODE and 9-(S)-HODE), ALA products (13-(S)-HOTrE and 9-(S)-HOTrE), GLA products (13-(S)-HOTrE(γ), and 9-(S)-HOTrE(γ)), DGLA products (15-(S)-HETrE and 11-(S)-HETrE), EPA products (15-(S)-HEPE and 11-(S)-HEPE) and EDA products (15-(S)-HEDE and 11-(S)-HEDE) were integrated. The substrate specificity ratio of different substrates with respect to AA was then determined. This ratio was finally normalized based on the ratio of the substrates present in the substrate mixture.

4.2.2.3 Effect of pH on steady-state substrate specificity kinetics of 15-LOX-2

Lipoxygenase activity was assayed spectro-photometrically (Perkin Elmer lambda 40) by monitoring an increase in absorbance at 234 nm due to formation of a conjugated diene product (ε = 25 000 M^{-1} cm^{-1}). The reaction was carried out in 25 mM HEPES buffer (pH 7.5 or pH 8.5), constant ionic strength of 200 mM, room temperature, a final reaction volume of 2 mL and substrate concentrations ranging from 1 to 20 μM. Assays were initiated by adding 55-85 nM 15-LOX-2, (concentration normalized to iron content) and were constantly stirred using a magnetic stir bar. Assays for the different substrates were performed on the same day

to allow a direct comparison and minimize error between AA and GLA data. The substrate concentrations were quantitatively determined by allowing the enzymatic reaction to go to completion. Initial rates were recorded at each substrate concentration and fitted to the Michaelis-Menten equation using KaleidaGraph (Synergy) to determine k_{cat} and K_M values.

4.2.2.4 Effect of LOX products on steady-state substrate specificity kinetics of 15-LOX-2

The GLA steady-state kinetics experiments were performed in presence of two different lipoxygenase products, 13-(S)-HODE and 13-(S)-HOTrE(γ) at both pH with product concentrations ranging from 0, 5, 15 and 30 μM. For the AA kinetics, initially the effect of both the products was tested with and without 15 μM 13-(S)-HODE and 13-(S)-HOTrE (γ) at both pH values. Further, the effect of 13-(S)-HODE on AA kinetics was investigated in detail at lower concentrations of the product ranging from 0, 1, 3 and 5 μM at pH 7.5. Enzymatic assays were conducted using the same conditions as mentioned in the steady-state kinetics at different pH (25 mM Hepes, pH 7.5 or pH 8.5 at a constant ionic strength of 200 mM and at room temperature). However, the enzyme was incubated with product to facilitate their interaction, followed by an initiation of the reaction by adding the substrate.

4.3 Results and Discussion

4.3.1 Overexpression and purification 15-LOX-2

Methods developed for structural genomics studies of eukaryotic proteins were applied to the expression and purification of 15-LOX-2.[45] After 16 hours of low-temperature growth (20° C) and no IPTG induction, approximately 40 mgs of the His_6-MBP-fusion protein per 2 liter of medium was isolated, at approximately 80% purity after the first IMAC column. After cleavage of the His6-MBP tag with TEV protease[44] and subtractive IMAC, approximately 75% of the 15-LOX-2 was recovered, giving a final yield of approximately 30 mgs of pure protein per 2 liter of culture medium. The final 15-LOX-2 protein isolated from *E. coli* was 90% pure as judged by SDS-PAGE, which was comparable to the purity previously achieved using the SF9 expression system.[46] However, ICP-MS data indicated that the pure 15-LOX-2 had 50 ± 5% iron content, which is twice that of our previous 15-LOX-2 preparations.[41, 47, 48] The unique benefits of this expression and purification method were its high yield in *E. coli* and increased metal content, yielding a highly active protein.

4.3.2 Effect of pH on competitive substrate capture substrate specificity kinetics of 15-LOX-2

Previously, the substrate specificity of the AA/LA substrate pair was investigated utilizing a competitive substrate capture method,[41] which determined that 13-(S)-HODE affected the substrate specificity of 15-LOX-2 by binding to its allosteric site and that the effect was pH dependent.[48] In order to understand the pH effect further, our competitive substrate capture method was utilized to compare six

endogenous fatty acid substrates to AA, which differ in their chain length and degree of unsaturation (**Table 4.1**). 15-LOX-2 was reacted with different substrate pairs at pH 7.5 and at pH 8.5 and the product ratios indicated a pH dependence of the substrate specificity for some of the substrate pairs. All the substrate pairs that included AA and a C_{18} fatty acid (e.g. LA, ALA, GLA), showed a significant increase in their substrate specificity ratio at pH 8.5, relative to AA (**Table 4.1**). However, the longer C_{20} substrates, DGLA, EPA and EDA, did not show a significant change in their substrate specificity relative to AA, with increased pH. This suggested that relative to AA, pH preferentially affected the C_{18} substrate specificity but not the C_{20} substrate specificity, implicating a kinetic differentiation between the substrate classes with respect to pH.

4.3.3 Effect of pH on the steady-state substrate specificity kinetics of 15-LOX-2

To investigate the pH effect on substrate specificity for the C_{18} and C_{20} substrates further, steady-state kinetics were performed at different pH values on a select number of substrates. LA and ALA are difficult to use for these investigations since they are poor C_{18} substrates for 15-LOX-2, so all kinetics studies were performed on GLA instead, to minimize error. The kinetic data indicate that as pH increases, GLA becomes a poorer substrate, with both k_{cat} and k_{cat}/K_M decreasing with increasing pH (**Table 4.2**). However, both k_{cat} and k_{cat}/K_M values for AA increase with increasing pH. This pH effect results in a 3.4-fold increase in the k_{cat}/K_M AA/GLA ratio (0.63 at pH 7.5 to 2.1 at pH 8.5) and a 2.2-fold increase in the k_{cat} AA/GLA ratio

(0.83 at pH 7.5 to 1.8 at pH 8.5). The other C_{20} substrates, DGLA and EPA, also become better substrates with increasing pH and thus there is no pH dependence observed in their substrate specificity ratio relative to AA (**Table 4.2**). This observation that the substrate specificity ratio of AA relative to C_{18} substrates is pH dependent while the C_{20} substrates are not, is consistent with our competitive substrate capture data (**Table 4.1**) and indicates distinct catalytic mechanisms for both substrate capture (k_{cat}/K_M) and product release (k_{cat}) for C_{18} and C_{20} fatty acid substrates. The most likely explanation for this difference is length, since varying the unsaturation levels of the C_{20} and C_{18} substrates does not effect their pH dependence, as seen with both the steady-state and competitive capture data (**Tables 4.1 and 4.2**).

4.3.4 Effect of LOX products on steady-state substrate specificity kinetics of 15-LOX-2

The allosteric effect of 13-(S)-HODE was previously demonstrated to affect the AA/LA ratio, but it was difficult to investigate fully due to the poor kinetics of LA and the less active 15-LOX-2 preparation from SF9 cells.[41, 47, 48] With the discovery that GLA is a facile substrate and with the more active *E. coli* 15-LOX-2 preparation, the allosteric effects of the C_{18} LOX products, 13-(S)-HODE and 13-(S)-HOTrE(γ), were investigated with steady-state kinetics in order to more fully understand their enzymatic effects on both AA and GLA kinetics. The kinetic parameters of 15-LOX-2 with AA and GLA, with and without LOX products added, are listed in **Table 4.3**. It is observed that 13-(S)-HODE increases the k_{cat}/K_M of AA

138

(0.40 ± 0.02 $\mu M^{-1}s^{-1}$ to 0.66 ± 0.07 $\mu M^{-1}s^{-1}$), but decreases the k_{cat}/K_M of GLA (0.64 ± 0.02 $\mu M^{-1}s^{-1}$ to 0.29 ± 0.03 $\mu M^{-1}s^{-1}$). 13-(S)-HOTrE(γ) exerts a similar effect by increasing the k_{cat}/K_M for AA and decreasing the k_{cat}/K_M for GLA, albeit to a lesser extent (**Table 4.3**). As a result, the addition of 13-(S)-HODE and 13-(S)-HOTrE(γ) elicits a 3.7-fold and 2.3-fold increase in the k_{cat}/K_M ratio of AA/GLA, respectively. These increases in ratio are of comparable magnitude to the pH effect on k_{cat}/K_M (3.4-fold), suggesting a possible relationship in their molecular mechanism of substrate capture (k_{cat}/K_M) (*vide infra*). Interestingly, the k_{cat} AA/GLA ratio decreases with the addition of 13-(S)-HODE (1.3-fold) and 13-(S)-HOTrE(γ) (1.1-fold), which is the opposite as that seen for the pH effect, where the k_{cat} AA/GLA ratio increases 2.2-fold. These data represent a clear distinction between the allosteric and pH effects with respect to k_{cat}/K_M (substrate capture) and k_{cat} (product release).

4.3.5 Combined pH and product effects on the steady-state substrate specificity kinetics of 15-LOX-2

The above steady-state kinetic data demonstrate that both pH (**Table 4.2**) and the two LOX products at pH 7.5 (**Table 4.3**) affect the kinetic parameters of GLA and AA. The ability of 13-(S)-HODE and 13-(S)-HOTrE(γ) to affect the kinetics were then investigated at pH 8.5, in order to determine if pH affected the product effect. As seen in **Tables 4.4** and **4.5**, the pH does affect the product effect, but not in a similar manner against AA or GLA. Addition of 13-(S)-HODE decreases the k_{cat}/K_M for GLA by 55% at pH 7.5, but only decreases the k_{cat}/K_M for GLA by 43% at pH 8.5 (**Table

4.4). For k_{cat}, 13-(S)-HODE has little or no effect at either pH condition, emphasizing that allostery affects substrate capture primarily. The data for 13-(S)-HOTrE(γ) is similar to that of 13-(S)-HODE, when GLA is used as a substrate.

The pH and product effects are distinct when AA is used as a substrate. The addition of 13-(S)-HODE increases k_{cat}/K_M by 65% at pH 7.5, but increases it more (88%), at pH 8.5. For k_{cat}, 13-(S)-HODE has a slight decrease at both pH 7.5 or 8.5, mirroring the GLA data where allostery affects substrate capture primarily for AA. The kinetic data for 13-(S)-HOTrE(γ) displays comparable trends to that of 13-(S)-HODE for k_{cat}/K_M and k_{cat} with AA as the substrate, albeit with smaller changes with respect to k_{cat}/K_M.

The above data demonstrate that the pH and product effects are not completely independent of each other and are partially additive, increasing the AA/GLA substrate specificity significantly. For example, the k_{cat}/K_M AA/GLA substrate specificity ratio changes from 0.63 at pH 7.5 with no product present (**Tables 4.3** and **4.4**), to a ratio of 6.8 at pH 8.5 with 15 μM 13-(S)-HODE present. This is an 11-fold increase in substrate specificity when both effects are taken into account, well above the 4-fold change seen for ribonucleotide reductase.[42, 43] These combined effects could have significant consequences for the inflammation response under certain circumstances and we are currently investigating the structural determinants of both the pH and product effects in order to understand how both convey similar, yet semi-independent changes in substrate specificity.

140

4.3.6 Hyperbolic inhibition of 15-LOX-2 by LOX products

The overall trends for the 13-(S)-HODE and 13-(S)-HOTrE(γ) effects are comparable, however, their magnitudes are distinct. Addition of 15 μM of 13-(S)-HODE at pH 8.5 leads to a AA/GLA k_{cat}/K_M ratio of 6.8, but an addition of 15 μM of 13-(S)-HOTrE(γ) at pH 8.5 only leads to a AA/GLA k_{cat}/K_M ratio of 4.0. This data suggests that the additional double bond at C_6 for 13-(S)-HOTrE(γ) does register functional allosteric differences (**Figure 4.1**).This exquisite selectivity of the allosteric site is also demonstrated by the fact that 12-(S)-HETE and 15-(S)-HETE do not register an effect with 15-LOX-2,[41] while 13-(S)-HODE and 13-(S)-HOTrE(γ) do. Given this functional allosteric difference between 13-(S)-HODE and 13-(S)-HOTrE(γ), both products were titrated against 15-LOX-2, at both pH 7.5 and 8.5 with GLA as the substrate. From the data, it is observed that 15-LOX-2 exhibits a hyperbolic response to increasing amounts of 13-(S)-HOTrE(γ) with an increase in K_M(app) for GLA from 2.8 μM to ~9.8 μM (**Figure 4.2**) and a decrease in k_{cat}/K_M from 0.65 μM $^{-1}$s^{-1} to ~0.28 μM $^{-1}$s^{-1} (**Figure 4.3**). The saturation behavior of K_M(app) and k_{cat}/K_M is indicative of hyperbolic inhibition (i.e., partial inhibition), as seen previously for soybean 15-LOX-1 and the inhibitor, oleyl sulfate.[49, 50] This data indicates the presence of an allosteric binding site that affects the catalysis by changing the microscopic rate constants of 15-LOX-2, as described in **Scheme 4.1**. From **Scheme 4.1**, equations 1-4 allow for the determination of K_i, the strength of binding, α, the change in K_M and β, the change in k_{cat}.

141

$$1/v = (\alpha K_M/k_{cat})*[([I] + K_i)/(\beta[I] + \alpha K_i)]*1/[S] + 1/ k_{cat}*[([I] + \alpha K_i)/(\beta[I] + \alpha K_i)] \quad (1)$$

$$K_M (app) = (\alpha K_M)*[([I] + K_i)/([I] + \alpha K_i)] \quad (2)$$

$$k_{cat}/K_M = (k_{cat}/\alpha K_M)*[(\beta[I] + \alpha K_i)/([I] + K_i)] \quad (3)$$

$$k_{cat} = k_{cat}*[(\beta[I] + \alpha K_i)/([I] + \alpha K_i)] \quad (4)$$

A plot of K_M(app) with the addition of 13-(S)-HOTrE(γ) at pH 7.5, when fitted with equation 2, yielded an α of 3.5 ± 0.2 and a K_i of 4.9 ± 0.7 μM (**Figure 4.2**). The values of α and K_i were then utilized in equation 3 and fit to the k_{cat}/K_M data (**Figure 4.3**), which yielded a β of 1.2 ± 0.02. The value of β was also determined from the k_{cat} data with equation 4, with the above values of α and K_i applied (data not shown), which yielded a β of 1.2 ± 0.05 and matches well with the β value from the k_{cat}/K_M plot. These values indicate that the kinetics show mixed hyperbolic activation with $\alpha > 1$ and $\beta > 1$, with the majority of kinetic change being seen in the value of K_M ($\alpha = 3.5 \pm 0.2$) and only a slight effect on the k_{cat} value ($\beta = 1.2 \pm 0.02$). The hyperbolic data thus indicate the formation of a catalytically active ternary complex (I•E•S) with 15-LOX-2 and 13-(S)-HOTrE(γ) and strongly supports our previous finding of an allosteric site in 15-LOX-2.[48] Similarly, graphing of steady-state kinetic data of 15-LOX-2 with 13-(S)-HOTrE(γ) at pH 8.5 gave an α of 2.0 ± 0.1 and a K_i of 6.1 ± 1.5 from the K_M plot (**Figure 4.4**) and a β of 0.9 ± 0.04 n from the k_{cat}/K_M (**Figure 4.5**). From this data it is observed that the K_i value for 13-(S)-HOTrE(γ) shows little pH dependence, therefore, the change of the AA/GLA substrate specificity ratio, with changing pH , is not due to a change in the affinity of 13-(S)-

HOTrE(γ) at higher pH, as our lab had hypothesized previously for 13-(S)-HODE, with LA as the substrate.[48] A more plausible explanation for the decrease in both the α and the β values with increasing pH is that there is a pH dependent structural 15-LOX-2 change, which affects the allosteric pathway between the catalytic and allosteric sites, eliciting a change in substrate specificity.

Fitting the 13-(S)-HODE data in a similar manner, showed a similar effect on 15-LOX-2 and GLA at pH 7.5 as that of 13-(S)-HOTrE(γ), with an α value of 7.3 ± 0.06 and a K_i value of 9.8 ± 0.2 μM from the K_M plot (**Figure 4.6**), which is comparable to the previously determined K_D of 13-(S)-HODE to 15-LOX-1.[41] A β value of 1.6 ± 0.1 was determined from the k_{cat}/K_M plot (**Figure 4.7**). The α value is double that of the α value for 13-(S)-HOTrE(γ), indicative of a stronger allosteric effect on K_M, for 13-(S)-HODE. The K_i and β values are comparable to that of the 13-(S)-HOTrE(γ) effect, indicating that the greater allosteric effect of 13-(S)-HODE is not due to a tighter binding affinity, but rather a greater kinetic effect. It should be noted that the K_i value of 13-(S)-HODE is greater than our previous estimation with LA as substrate and 15-LOX-2.[48] As mentioned previously, this discrepancy is most likely due to LA being a poor substrate for 15-LOX-2 and the lower activity of the previous SF9 preparations of 15-LOX-2.[41, 47, 48] Interestingly, the 13-(S)-HODE data at pH 8.5 could not be fit using the hyperbolic partial inhibition (Scheme 1), nor a simple non-competitive model, therefore, the change of k_{cat}/K_M was plotted versus 13-(S)-HODE and fit with a saturation curve (**Figure 4.8**). From this data, the K_D was 8.6

± 0.7 µM at pH 7.5, comparable to the K_i of 9.8 ± 0.2 µM found in the hyperbolic partial inhibition fit. However, the K_D at pH 8.5 was increased to 53.2 ± 25.2 µM, considerably greater than that at pH 7.5, indicating a change in the binding affinity with pH. This is an unusual result since the K_i of 13-(S)-HOTrE(γ) is not affected by pH and suggests that the difference in the kinetic effects of the two products could be due to a difference in binding modes. We are currently investigating this further in order to understand the structural requirements for both products binding to the allosteric site.

As described above, preliminary studies of 13-(S)-HODE and 13-(S)-HOTrE (γ) exhibited the opposite effect (**Table 4.3**), with the AA kinetics being activated by both products, while the GLA kinetics were inhibited. In order to investigate this effect further, titration kinetics with 13-(S)-HODE, the stronger activator, were determined with AA at pH 7.5, similar to that done for GLA (**Figures 4.6-4.10**). It was observed that 13-(S)-HODE activates AA kinetics with an α value of 0.2 ± 0.01 and a K_i value of 1.2 ± 0.03 µM **(Figure 4.9),** as seen by the hyperbolic decrease in K_M (app) from 3.5 µM to ~ 0.7 µM. The α value demonstrates a five-fold activation in K_M, which is opposite to that of the GLA kinetic inhibition, but of a similar magnitude (a seven-fold increase in K_M for GLA). Interestingly, the k_{cat} decreased slightly with increasing 13-(S)-HODE, resulting in a β value of 0.76 ± 0.002 and indicating inhibition of product release **(Figure 4.10)**. This is in contrast to the β value for 13-(S)-HODE with GLA (β = 1.6 ± 0.1). Nevertheless, the major allosteric

144

effect is clearly on substrate capture, as seen by the decrease in k_{cat}/K_M. This data is remarkable because 13-(S)-HODE has opposite effects on the rate of substrate capture, activating AA but inhibiting GLA, and 13-(S)-HODE manifests different thresholds of response, with the activation of AA occurring at a lower concentration than the inhibition of GLA (K_i = 1.2 ± 0.03 μM and 9.8 ± 0.02 μM, respectively). This latter fact may indicate two distinct allosteric sites or two distinct binding modes for 13-(S)-HODE. We are currently investigating both of these possibilities.

In summary, competitive substrate capture results indicate that C_{18} and C_{20} fatty acid substrates have distinct responses to pH. This observation is confirmed with steady-state kinetics, where the k_{cat} and k_{cat}/K_M of GLA (C_{18}) are decreased with increasing pH, while the same kinetic parameters of AA, DGLA and EPA (C_{20}) are increased with increasing pH. These data result in a net increase in the C_{20}/C_{18} substrate specificity ratio and indicate that some steps of the molecular mechanism for C_{18} and C_{20} fatty acid substrates are distinct. Addition of C_{18} products, 13-(S)-HODE and 13-(S)-HOTrE(γ), mirror the k_{cat}/K_M pH effect, with an increase in the AA/GLA ratio and are partially additive, with the AA/GLA k_{cat}/K_M ratio increasing from 0.62 (pH 7.5 and no products added) to 6.8 (pH 8.5 and 15 μM product added), an 11-fold increase. This increase is significant, and if it applies to all C_{20}/C_{18} fatty acid pairs, like the AA/LA pair, it could have important ramifications for human health, because of the distinct effects their LOX products, 15-(S)-HETE and 13-(S)-HODE, have on disease progression.[51-55] Finally, the two allosteric effectors, 13-(S)-

145

HODE and 13-(S)-HOTrE(γ), display hyperbolic inhibition kinetics with GLA as substrate and display similar K_i values, 9.8 ± 0.2 μM and 4.9 ± 0.7 μM respectively. However, the K_i of 13-(S)-HODE is pH dependent and the effect of 13-(S)-HODE on the K_M (α value) is 2.1 fold greater that that of 13-(S)- HOTrE(γ). In addition, it is observed that 13-(S)-HODE activates AA substrate capture, but inhibits GLA substrate capture. Considering that the molecular mechanism for AA and GLA are distinct, it is tempting to postulate that the allosteric site exploits this difference to manifest opposite effects on the rate of substrate capture. In total, these data indicate that the differences in unsaturation between these two LOX products, one additional double bond at C_6 for 13-(S)-HODE, affect their binding constraints and their effect on the microscopic rate constants. These data demonstrate the exquisite selectivity of both the active site and the allosteric site to control substrate specificity, which could have broad implications in the regulation of eicosanoid products in the cell. We are currently investigating the structural origins of these effects in order to determine the location of the allosteric site and the molecular mechanism for the pH and product effects.

4.4 Acknowledgements

4.5 Figures

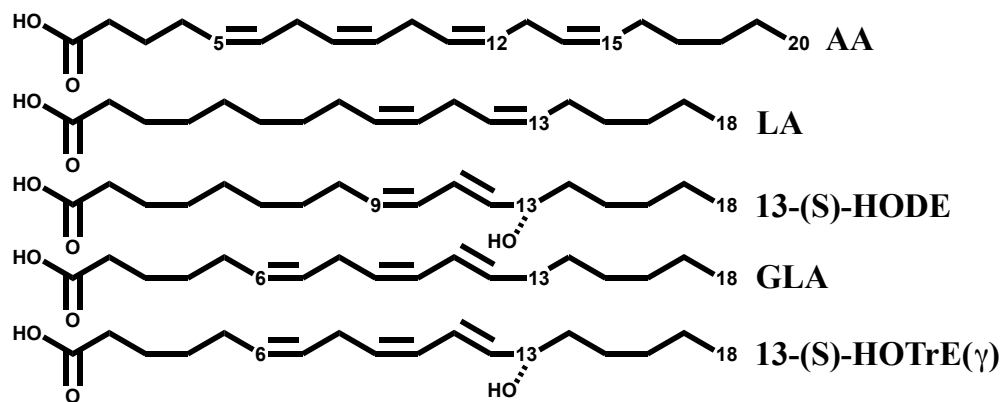**Figure 4.1 Structures of LA, 13-(S)-HODE, GLA and 13-(S)-HOTrE(γ).**

Figure 4.2 Effect of 13(S)-HOTrE (γ) on K_M (app) of 15-LOX-2 with GLA.

(pH 7.5, 25 mM hepes, 1-20 μM GLA at each product point) The curve line is fit to

equation 2 (Scheme 4.1), where K_m= 2.8 μM. α and K_i were determined to be 3.5 ±
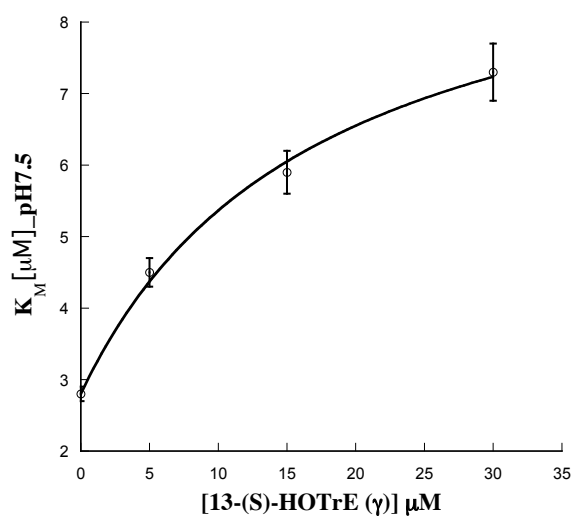
0.2 and 4.9 ± 0.7 respectively.

Figure 4.3 Effect of 13(S)-HOTrE (γ) on K_{cat}/K_M of 15-LOX-2 with GLA.

(pH 7.5, 25 mM hepes, 1-20 μM GLA at each product point) The curve line is fit to equation 3 (Scheme 4.1), where $K_m = 2.8$ μM, $K_{cat} = 0.65$ s^{-1}, $\alpha = 3.5$ and $K_i = 4.9$ μM. β was determined to be 1.2 ± 0.02.
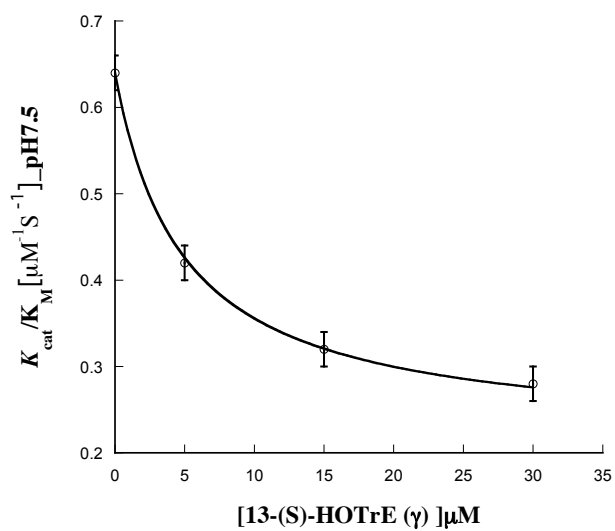
Figure 4.4 Effect of 13(S)-HOTrE (γ) on K_M (app) of 15-LOX-2 with GLA.

(pH 8.5, 25mM hepes, 1-20 μM GLA at each product point) The curve line is fit to equation 2 (Scheme 4.1), where K_m= 3.1 μM. α and K_i were determined to be 2.0 ± 0.1 and 6.1 ± 1.5 respectively.
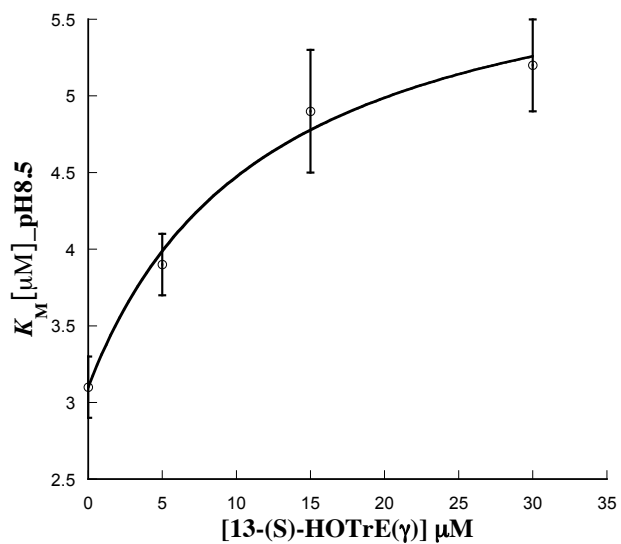
Figure 5: Effect of 13(S)-HOTrE (γ) on K_{cat}/K_M of 15-LOX-2 with GLA

(pH 8.5, 25mM hepes, 1-20 μM GLA at each product point) The curve line is fit to

equation 3 (Scheme 4.1), where K_m = 3.1 μM, K_{cat} =0.37 s^{-1}, α = 2.0 and K_i = 6.1 μM.
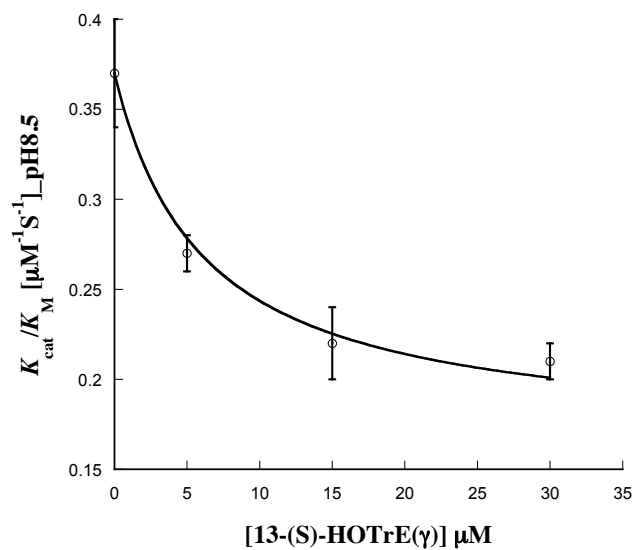
β was determined to be 0.9 ± 0.04.

Figure 4.6 Effect of 13(S)-HODE on K_M (app) of 15-LOX-2 with GLA

(pH 7.5, 25mM hepes, 1-20 μM GLA at each product point) The curve line is fit to equation 2 (Scheme 4.1), where K_m = 2.8 μM. α and K_i were determined to be 7.3 ± 0.06 and 9.8 ± 0.2, respectively.

.

Figure 4.7 Effect of 13(S)-HODE on K_{cat}/K_M of 15-LOX-2 with GLA

(pH 7.5, 25mM hepes, 1-20 μ M GLA at each product point) The curve line is fit to equation 3 (Scheme 4.1), where K_m = 2.8 μ M, K_{cat} =0.65 s^{-1}, α = 7.3 and K_i = 9.8 μ M. β was determined to be 1.6 ± 0.1.
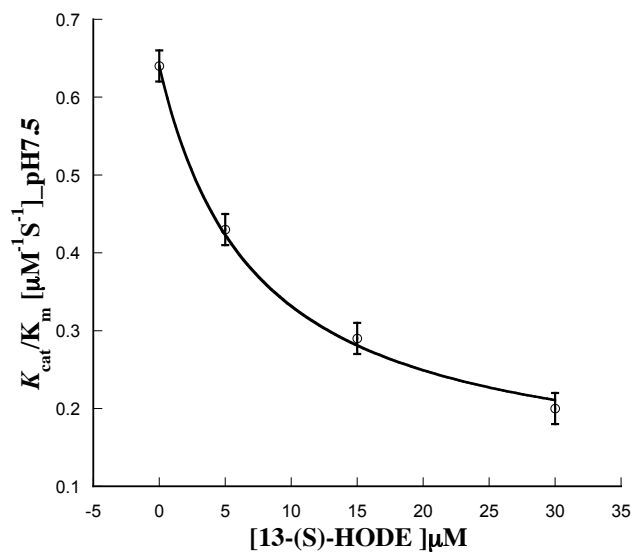
Figure 4.8 Steady-state kinetics titration of 15-LOX-2-GLA with 13-HODE at

both pH values

(closed circles $-$ $\Delta\,(k_{cat}/K_M)^{\,\text{GLA}}$ at pH 7.5; open squares $-\Delta\,(k_{cat}/K_M)^{\,\text{GLA}}$ at pH8.5.

The K_D of 13 (S)-HODE with GLA was calculated to be 8.6 ± 0.7 μ M at pH7.5 and

53.2 ± 25.2 µM at pH8.5)
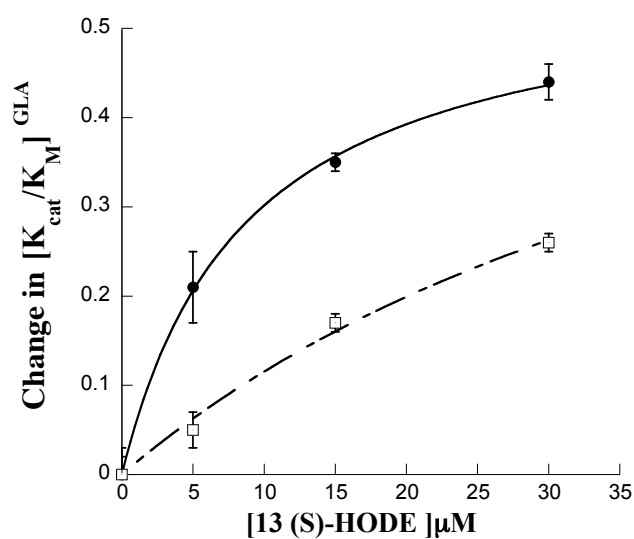
Figure 4.9 Effect of 13(S)-HODE on K_M (app) of 15-LOX-2 with AA

(pH 7.5, 25 mM hepes, 1-20 μ M AA at each product point) The curve line is fit to equation 2 (Scheme 4.1), where K_m = 3.5 μ M. α and K_i were determined to be 0.2± 0.01 and 1.2 ± 0.03, respectively.
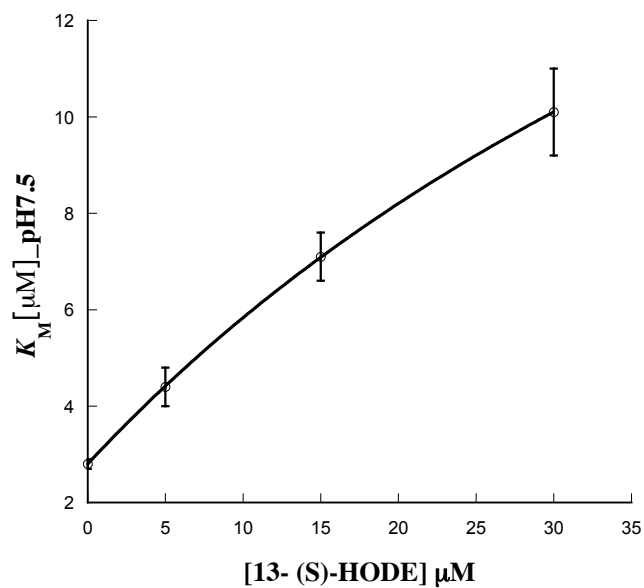
Figure 4.10 Effect of 13(S)-HODE on K_{cat}/K_M of 15-LOX-2 with AA

(pH 7.5, 25 mM hepes, 1-20 μ M AA at each product point) The curve line is fit to equation 3 (Scheme 4.1), where K_m = 3.5 μ M, K_{cat} =1.4 s^{-1}, α = 0.2 and K_i = 1.2 μ M. β was determined to be 0.76 $\pm$ 0.002.
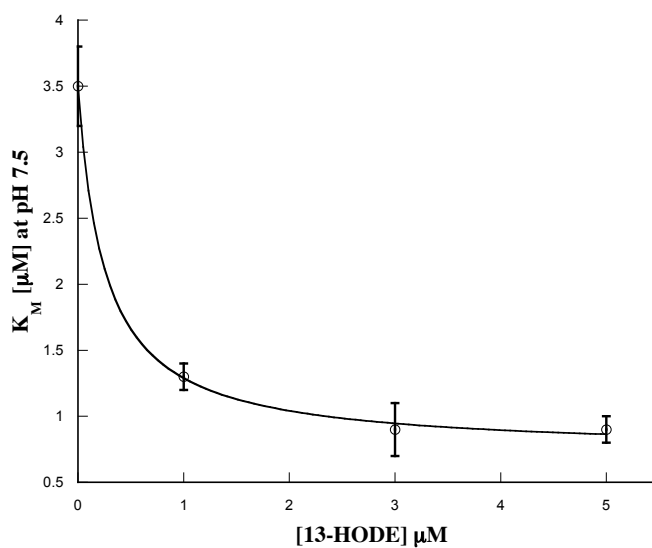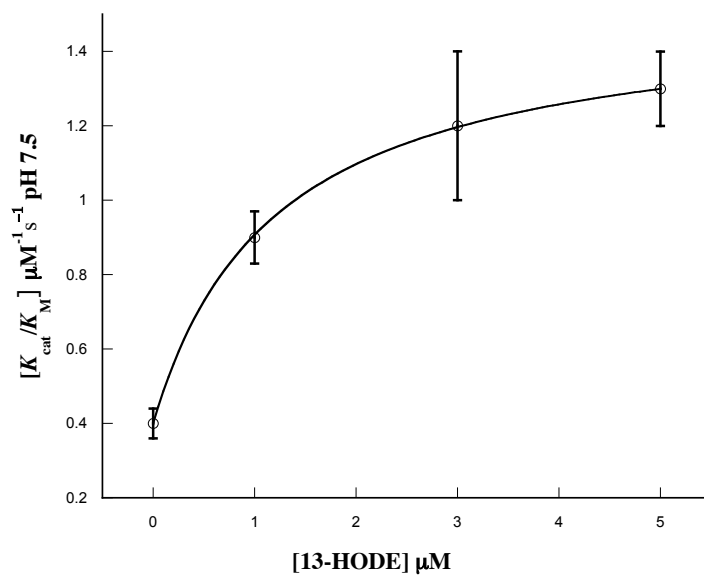
4.6 Tables

Table 4.1 Substrate specificity ratio of 15-LOX-2 with different substrate pairs at both pH values [a]			
Substrate Pair	Differences as compared to AA	Substrate Specificity Ratio with respect to AA	
		pH 7.5	pH 8.5
AA / LA	20:4(ω-6) Vs. 18:2(ω-6)	2.3 ± 0.4	4.9 ± 0.5
AA / ALA	20:4(ω-6) Vs. 18:3(ω-3)	3.6 ± 0.8	6.4 ± 2
AA / GLA	20:4(ω-6) Vs. 18:3(ω-6)	2.5 ± 0.4	4.9 ± 1
AA / EDA	20:4(ω-6) Vs. 20:2(ω-6)	1.1 ± 0.4	1.1 ± 0.4
AA / DGLA	20:4(ω-6) Vs. 20:3(ω-6)	0.6 ± 0.2	0.5 ± 0.1
AA / EPA	20:4(ω-6) Vs. 20:5(ω-3)	2.2 ± 0.4	3.2 ± 1
[a] Enzymatic assays were performed at 5 µM total substrate concentration in 25 mM Hepes at 22°C			

158

	k_{cat}/K_M (µM^{-1}s^{-1})		k_{cat} (s^{-1})	
	pH 7.5	pH 8.5	pH 7.5	pH 8.5
GLA	0.64 ± 0.02	0.37 ± 0.03	1.8 ± 0.03	1.1 ± 0.02
AA	0.40 ± 0.02	0.76 ± 0.06	1.5 ± 0.03	2.0 ± 0.04
DGLA	0.26 ± 0.04	0.49 ± 0.08	1.5 ± 0.08	1.8 ± 0.1
EPA	0.72 ± 0.03	1.4 ± 0.07	2.1 ± 0.02	2.8 ± 0.04
	pH 7.5	pH 8.5	pH 7.5	pH 8.5
AA / GLA	0.63 ± 0.04	2.1 ± 0.03	0.83 ± 0.02	1.8 ± 0.05
AA / DGLA	1.5 ± 0.2	1.6 ± 0.3	0.99 ± 0.06	1.1 ± 0.07
AA / EPA	0.56 ± 0.04	0.54 ± 0.05	0.71 ± 0.02	0.72 ± 0.02

Table 4.2 Comparison of the kinetic parameters of 15-LOX-2 with various substrates at both pH values [a]

[a] Enzymatic assays were performed in 25 mM Hepes at 22°C.

Table 4.3 Comparison of Kinetic parameters of 15-LOX-2 with AA and GLA, with and without different products at pH 7.5[a]

	k_{cat}/K_M ($\mu M^{-1}s^{-1}$)			k_{cat} (s^{-1})		
	AA	GLA	AA /GLA	AA	GLA	AA /GLA
No Product	0.40 ± 0.02	0.64 ± 0.02	0.63 ± 0.04	1.5 ± 0.03	1.8 ± 0.03	0.83 ± 0.02
13-(S)-HODE	0.66 ± 0.07	0.29 ± 0.02	2.3 ± 0.3	1.3 ± 0.02	2.0 ± 0.06	0.65 ± 0.02
13-(S)-HOTrE(γ)	0.45 ± 0.03	0.32 ± 0.02	1.4 ± 0.01	1.4 ± 0.05	1.9 ± 0.04	0.73 ± 0.01

[a] Enzymatic assays were performed in 25 mM Hepes, pH 7.5, at 22°C with and without 15 μM 13-(S)-HODE and 15 μM 13-(S)-HOTrE(γ).

Table 4.4 Product and pH effect on kinetic parameters of 15-LOX-2 with GLA[a]				
	k_{cat}/K_M ($\mu M^{-1}s^{-1}$)		k_{cat} (s^{-1})	
Conditions	pH 7.5	pH 8.5	pH 7.5	pH 8.5
No product	0.64 ± 0.02	0.37 ± 0.03	1.8 ± 0.03	1.1 ± 0.02
13-(S)-HODE	0.29 ± 0.02	0.21 ± 0.02	2.0 ± 0.06	1.1 ± 0.02
13-(S)-HOTrE(γ)	0.32 ± 0.02	0.22 ± 0.03	1.9 ± 0.04	1.1 ± 0.03
[a]Enzymatic assays were performed in 25 mM Hepes, pH 7.5 and pH 8.5 at 22°C with and without 15 μM products.				

Table 4.5 Product and pH effect on kinetic parameters of 15-LOX-2 with AA[a]				
	k_{cat}/K_M ($\mu M^{-1}s^{-1}$)		k_{cat} (s^{-1})	
Conditions	pH 7.5	pH 8.5	pH 7.5	pH 8.5
No product	0.40 ± 0.02	0.76 ± 0.06	1.5 ± 0.03	2.0 ± 0.04
13-(S)-HODE	0.66 ± 0.07	1.4 ± 0.1	1.3 ± 0.02	1.9 ± 0.03
13-(S)-HOTrE(γ)	0.45 ± 0.04	0.87 ± 0.09	1.4 ± 0.05	1.8 ± 0.04

[a] Enzymatic assays were performed in 25 mM Hepes, pH 7.5 and pH 8.5 at 22°C with and without 15 μM products.

Scheme 4.1

$$\text{E} + \text{S} \underset{K_M}{\rightleftharpoons} \text{E}\bullet\text{S} \xrightarrow{k_2} \text{E} + \text{P}$$

$$+ \quad\quad\quad\quad + \text{I}$$
$$\text{I}$$

$$K_i \updownarrow \quad\quad \alpha K_i \updownarrow$$

$$\text{I}\bullet\text{E} \underset{\alpha K_M}{\rightleftharpoons} \text{I}\bullet\text{E}\bullet\text{S} \xrightarrow{\beta k_2} \text{I}\bullet\text{E} + \text{P}$$
$$+ \text{S}$$

163
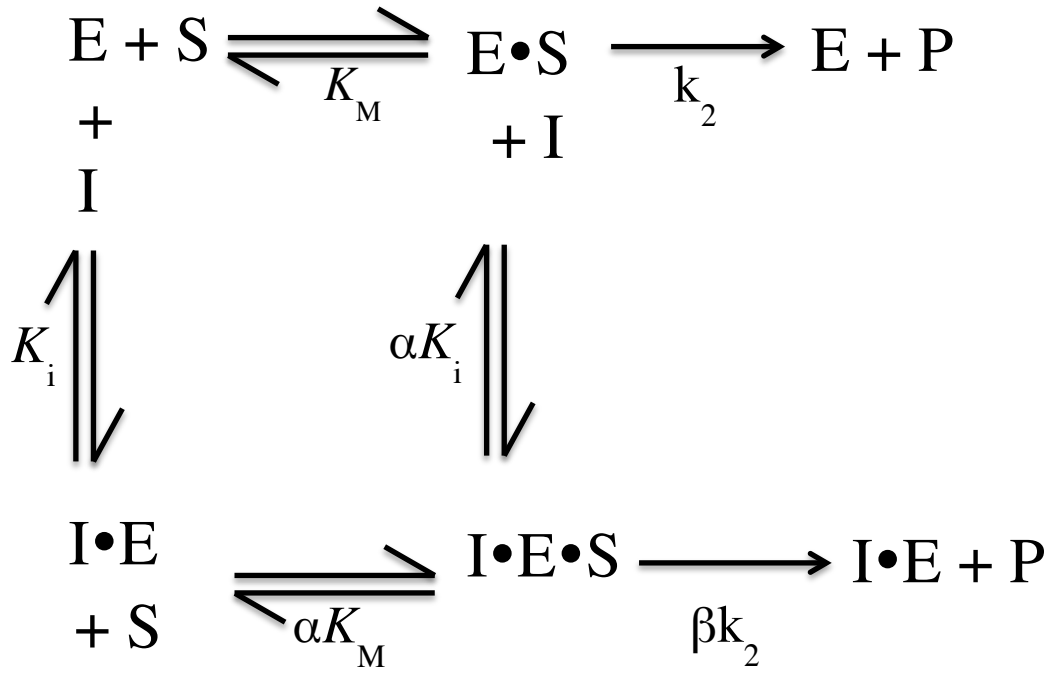
4.7 References

1.   Brash, A. R. (1999) Lipoxygenases: Occurrence, Functions, Catalysis and Acquisition of Substrate, *J. Biol. Chem. 274*, 23679-23682.

2.   Kuhn, H., Saam, J., Eibach, S., Holzhutter, H. G., Ivanov, I., and Walther, M. (2005) Structural biology of mammalian lipoxygenases: enzymatic consequences of targeted alterations of the protein structure, *Biochemical and biophysical research communications 338*, 93-101.

3.   Schneider, C., Pratt, D. A., Porter, N. A., and Brash, A. R. (2007) Control of oxygenation in lipoxygenase and cyclooxygenase catalysis, *Chemistry & biology 14*, 473-488.

4.   Glickman, M. H., and Klinman, J. P. (1995) Nature of Rate-Limiting Steps in the Soybean Lipoxygenase-1 Reaction, *Biochemistry 34*, 14077-14092.

5.   Rickert, K. W., and Klinman, J. P. (1999) Nature of Hydrogen Transfer in Soybean Lipoxygenase-1: Separation of Primary and Secondary Isotope Effects, *Biochemistry 38*, 12218-12228.

6.   Lehnert, N., and Solomon, E. I. (2003) Density-functional investigation on the mechanism of H-atom abstraction by lipoxygenase, *Journal of biological inorganic chemistry : JBIC : a publication of the Society of Biological Inorganic Chemistry 8*, 294-305.

7.   Hatcher, E., Soudackov, A. V., and Hammes-Schiffer, S. (2004) Proton-coupled electron transfer in soybean lipoxygenase, *Journal of the American Chemical Society 126*, 5763-5775.

8.   Yamamoto, S. (1992) Mammalian lipoxygenases: molecular structures and functions, *Biochimica et biophysica acta 1128*, 117-131.

9.   Choi, J., Chon, J. K., Kim, S., and Shin, W. (2008) Conformational flexibility in mammalian 15S-lipoxygenase: Reinterpretation of the crystallographic data, *Proteins 70*, 1023-1032.

10.   Gilbert, N. C., Bartlett, S. G., Waight, M. T., Neau, D. B., Boeglin, W. E., Brash, A. R., and Newcomer, M. E. (2011) The structure of human 5-lipoxygenase, *Science 331*, 217-219.

11.   Minor, W., Steczko, J., Boguslaw, S., Otwinowski, Z., Bolin, J. T., Walter, R., and Axelrod, B. (1996) Crystal Structure of Soybean Lipoxygenase L-1 at 1.4 A Resolution, *Biochemistry 35*, 10687-10701.

12.   Skrzypczak-Jankun, E., Amzel, L. M., Kroa, B. A., and Funk, M. O., Jr. (1997) Structure of soybean lipoxygenase L3 and a comparison with its L1 isoenzyme, *Proteins 29*, 15-31.

13.   Neau, D. B., Gilbert, N. C., Bartlett, S. G., Boeglin, W., Brash, A. R., and Newcomer, M. E. (2009) The 1.85 A structure of an 8R-lipoxygenase suggests a general model for lipoxygenase product specificity, *Biochemistry 48*, 7906-7915.

14.   Gillmor, S. A., Villasenor, A., Fletterick, R., Sigal, E., and Browner, M. (1997) The structure of mammalian 15-lipoxygenase reveals similarity to the lipases and the determinants of substrate specificity., *Nature Struct. Biol. 4*, 1003-1009.

15.   Oldham, M. L., Brash, A. R., and Newcomer, M. E. (2005) Insights from the X-ray crystal structure of coral 8R-lipoxygenase: calcium activation via a C2-like domain and a structural basis of product chirality, *The Journal of biological chemistry 280*, 39545-39552.

16.   Ivanov, I., Heydeck, D., Hofheinz, K., Roffeis, J., O'Donnell, V. B., Kuhn, H., and Walther, M. (2010) Molecular enzymology of lipoxygenases, *Arch Biochem Biophys 503*, 161-174.

17.   Chahinian, H., Sias, B., and Carriere, F. (2000) The C-terminal domain of pancreatic lipase: functional and structural analogies with c2 domains, *Curr Protein Pept Sci 1*, 91-103.

18. May, C., Hohne, M., Gnau, P., Schwennesen, K., and Kindl, H. (2000) The N-terminal beta-barrel structure of lipid body lipoxygenase mediates its binding to liposomes and lipid bodies, *European journal of biochemistry / FEBS 267*, 1100-1109.

19. Tatulian, S. A., Steczko, J., and Minor, W. (1998) Uncovering a calcium-regulated membrane-binding mechanism for soybean lipoxygenase-1, *Biochemistry 37*, 15481-15490.

20. Ziboh, V. A., Cho, Y., Mani, I., and Xi, S. (2002) Biological significance of essential fatty acids/prostanoids/lipoxygenase-derived monohydroxy fatty acids in the skin, *Archives of pharmacal research 25*, 747-758.

21. Calder, P. C. (2006) n-3 polyunsaturated fatty acids, inflammation, and inflammatory diseases, *The American journal of clinical nutrition 83*, 1505S-1519S.

22. Calder, P. C. (2006) Polyunsaturated fatty acids and inflammation, *Prostaglandins, leukotrienes, and essential fatty acids 75*, 197-202.

23. Iversen, L., Fogh, K., and Kragballe, K. (1992) Effect of dihomogammalinolenic acid and its 15-lipoxygenase metabolite on eicosanoid metabolism by human mononuclear leukocytes in vitro: selective inhibition of the 5-lipoxygenase pathway, *Arch Dermatol Res 284*, 222-226.

24. Samuelsson, B., Borgeat, P., Hammarstrom, S., and Murphy, R. C. (1980) Leukotrienes: a new group of biologically active compounds, *Advances in prostaglandin and thromboxane research 6*, 1-18.

25. Jakschik, B. A., and Lee, L. H. (1980) Enzymatic assembly of slow reacting substance, *Nature 287*, 51-52.

26. Funk, C. D. (2001) Prostaglandins and leukotrienes: Advances in eicosanoid biology [Review], *Science 294*, 1871-1875.

166

27. Serhan, C. N., Chiang, N., and Van Dyke, T. E. (2008) Resolving inflammation: dual anti-inflammatory and pro-resolution lipid mediators, *Nat Rev Immunol 8*, 349-361.

28. Serhan, C. N. (2005) Mediator lipidomics, *Prostaglandins & other lipid mediators 77*, 4-14.

29. Serhan, C. N., Arita, M., Hong, S., and Gotlinger, K. (2004) Resolvins, docosatrienes, and neuroprotectins, novel omega-3-derived mediators, and their endogenous aspirin-triggered epimers, *Lipids 39*, 1125-1132.

30. Serhan, C. N., Hamberg, M., and Samuelsson, B. (1984) Lipoxins: novel series of biologically active compounds formed from arachidonic acid in human leukocytes, *Proc Natl Acad Sci U S A 81*, 5335-5339.

31. Ariel, A., Li, P. L., Wang, W., Tang, W. X., Fredman, G., Hong, S., Gotlinger, K. H., and Serhan, C. N. (2005) The docosatriene protectin D1 is produced by TH2 skewing and promotes human T cell apoptosis via lipid raft clustering, *The Journal of biological chemistry 280*, 43079-43086.

32. Schnurr, K., Belkner, J., Ursini, F., Schewe, T., and Kuhn, H. (1996) The selenoenzyme phospholipid hydroperoxide glutathione peroxidase controls the activity of the 15-lipoxygenase with complex substrates and preserves the specificity of the oxygenation products, *J Biol Chem 271*, 4653-4658.

33. Ziboh, V. A., Miller, C. C., and Cho, Y. (2000) Metabolism of polyunsaturated fatty acids by skin epidermal enzymes: generation of antiinflammatory and antiproliferative metabolites, *The American journal of clinical nutrition 71*, 361S-366S.

34. Ziboh, V. A., Miller, C. C., and Cho, Y. (2000) Significance of lipoxygenase-derived monohydroxy fatty acids in cutaneous biology, *Prostaglandins & other lipid mediators 63*, 3-13.

35. Shappell, S. B., Manning, S., Boeglin, W. E., Guan, Y. F., Roberts, R. L., Davis, L., Olson, S. J., Jack, G. S., Coffey, C. S., Wheeler, T. M., Breyer, M.

167

D., and Brash, A. R. (2001) Alterations in lipoxygenase and cyclooxygenase-2 catalytic activity and mRNA expression in prostate carcinoma, *Neoplasia 3*, 287-303.

36.   Butler, R., Mitchell, S. H., Tindall, D. J., and Young, C. Y. (2000) Nonapoptotic cell death associated with S-phase arrest of prostate cancer cells via the peroxisome proliferator-activated receptor gamma ligand, 15-deoxy-delta12,14-prostaglandin J2, *Cell Growth Differ 11*, 49-61.

37.   Serhan, C. N. (1994) Lipoxin biosynthesis and its impact in inflammatory and vascular events, *Biochimica et biophysica acta 1212*, 1-25.

38.   Tang, D. G., Bhatia, B., Tang, S., and Schneider-Broussard, R. (2007) 15-lipoxygenase 2 (15-LOX2) is a functional tumor suppressor that regulates human prostate epithelial cell differentiation, senescence, and growth (size), *Prostaglandins & other lipid mediators 82*, 135-146.

39.   Brash, A. R., Boeglin, W. E., and Chang, M. S. (1997) Discovery of a second 15S-lipoxygenase in humans, *Proceedings of the National Academy of Sciences of the United States of America 94*, 6148-6152.

40.   Jisaka, M., Kim, R. B., Boeglin, W. E., and Brash, A. R. (2000) Identification of amino acid determinants of the positional specificity of mouse 8S-lipoxygenase and human 15S-lipoxygenase-2, *The Journal of biological chemistry 275*, 1287-1293.

41.   Wecksler, A. T., Kenyon, V., Deschamps, J. D., and Holman, T. R. (2008) Substrate specificity changes for human reticulocyte and epithelial 15-lipoxygenases reveal allosteric product regulation, *Biochemistry 47*, 7364-7375.

42.   Reichard, P. (2002) Ribonucleotide reductases: the evolution of allosteric regulation, *Arch Biochem Biophys 397*, 149-155.

43.   Nordlund, P., and Reichard, P. (2006) Ribonucleotide reductases, *Annu Rev Biochem 75*, 681-706.

44.   Blommel, P. G., and Fox, B. G. (2007) A combined approach to improving large-scale production of tobacco etch virus protease, *Protein Expr Purif 55*, 53-68.

45.   Jeon, W. B., Aceti, D. J., Bingman, C. A., Vojtik, F. C., Olson, A. C., Ellefson, J. M., McCombs, J. E., Sreenath, H. K., Blommel, P. G., Seder, K. D., Burns, B. T., Geetha, H. V., Harms, A. C., Sabat, G., Sussman, M. R., Fox, B. G., and Phillips, G. N., Jr. (2005) High-throughput purification and quality assurance of Arabidopsis thaliana proteins for eukaryotic structural genomics, *Journal of structural and functional genomics 6*, 143-147.

46.   Deschamps, J. D., Kenyon, V. A., and Holman, T. R. (2006) Baicalein is a potent in vitro inhibitor against both reticulocyte 15-human and platelet 12-human lipoxygenases, *Bioorg Med Chem 14*, 4295-4301.

47.   Wecksler, A. T., Jacquot, C., van der Donk, W. A., and Holman, T. R. (2009) Mechanistic investigations of human reticulocyte 15- and platelet 12-lipoxygenases with arachidonic acid, *Biochemistry 48*, 6259-6267.

48.   Wecksler, A. T., Kenyon, V., Garcia, N. K., Deschamps, J. D., van der Donk, W. A., and Holman, T. R. (2009) Kinetic and structural investigations of the allosteric site in human epithelial 15-lipoxygenase-2, *Biochemistry 48*, 8721-8730.

49.   Mogul, R., Johansen, E., and Holman, T. R. (2000) Oleyl sulfate reveals allosteric inhibition of Soybean Lipoxygenase-1 and Human 15-Lipoxygenase, *Biochemistry 39*, 4801-4807.

50.   Mogul, R., and Holman, T. R. (2001) Inhibition studies of soybean and human 15-lipoxygenases with long-chain alkenyl sulfate substrates, *Biochemistry 40*, 4391-4397.

51.   Hsi, L. C., Wilson, L. C., and Eling, T. E. (2002) Opposing effects of 15-lipoxygenase-1 and -2 metabolites on MAPK signaling in prostate. Alteration in peroxisome proliferator-activated receptor gamma, *J Biol Chem 277*, 40549-40556.

52. Haas, T. A., Bastida, E., Nakamura, K., Hullin, F., Admirall, L., and Buchanan, M. R. (1988) Binding of 13-HODE and 5-, 12- and 15-HETE to endothelial cells and subsequent platelet, neutrophil and tumor cell adhesion, *Biochimica et biophysica acta 961*, 153-159.

53. Bastida, E., Bertomeu, M. C., Haas, T. A., Almirall, L., Lauri, D., Orr, F. W., and Buchanan, M. R. (1990) Regulation of tumor cell adhesion by intracellular 13-HODE: 15-HETE ratio, *Journal of lipid mediators 2*, 281-293.

54. Buchanan, M. R., Bertomeu, M. C., and Bastida, E. (1990) Fatty acid metabolism and cell/cell interactions, *Agents and actions 29*, 16-20.

55. M.E. Pasqualinia, V. L. H., P. Manzob, A.R. Eynard. (2002) Association between E-cadherin expression by human colon, bladder and breast cancer cells and the 13-HODE:15-HETE ratio. A possible role of their metastatic potential$, *Prostaglandins, Leukotrienes and Essential Fatty Acids 68*, 9–16.